

1-1-2013

Optimization Models for Cost Efficient and Environmentally Friendly Supply Chain Management

Gokce Palak

Follow this and additional works at: <https://scholarsjunction.msstate.edu/td>

Recommended Citation

Palak, Gokce, "Optimization Models for Cost Efficient and Environmentally Friendly Supply Chain Management" (2013). *Theses and Dissertations*. 3397.
<https://scholarsjunction.msstate.edu/td/3397>

This Dissertation - Open Access is brought to you for free and open access by the Theses and Dissertations at Scholars Junction. It has been accepted for inclusion in Theses and Dissertations by an authorized administrator of Scholars Junction. For more information, please contact scholcomm@msstate.libanswers.com.

Optimization models for cost efficient and environmentally friendly
supply chain management

By

Gökçe Palak

A Dissertation
Submitted to the Faculty of
Mississippi State University
in Partial Fulfillment of the Requirements
for the Degree of Doctorate of Philosophy
in Operations Research
in the Department of Industrial and Systems Engineering

Mississippi State, Mississippi

December 2013

Copyright by

Gökçe Palak

2013

Optimization models for cost efficient and environmentally friendly
supply chain management

By

Gökçe Palak

Approved:

Sandra D. Ekşiođlu
(Major Professor)

Burak Ekşiođlu
(Committee Member)

Allen G. Greenwood
(Committee Member)

Joseph Geunes
(Committee Member)

Mingzhou Jin
(Committee Member)

Kari Babski-Reeves
(Graduate Coordinator)

Achille Messac
Dean
James Worth Bagley College of Engineering

Name: Gökçe Palak

Date of Degree: December 14, 2013

Institution: Mississippi State University

Major Field: Operations Research

Major Professor: Dr. Sandra D. Ekşioğlu

Title of Study: Optimization models for cost efficient and environmentally friendly supply chain management

Pages of Study: 146

Candidate for Degree of Doctorate of Philosophy

This dissertation aims to provide models which will help companies make sustainable logistics management and transportation decisions. These models are extensions of the economic lot sizing model with the availability of multiple replenishment modes. The objective of the models is to minimize total replenishment costs and emissions. The study provides applications of these models on contemporary supply chain problems. Initially, the impact of carbon regulatory mechanisms on the replenishment decisions are analyzed for a biomass supply chain under fixed charge replenishment costs. Then, models are extended to consider multiple-setups replenishment costs for age dependent perishable products. For a cost minimization objective, solution algorithms are proposed to solve cases where one, two or multiple replenishment modes are available. Finally, using a bi-objective model, tradeoffs in costs and emissions are analyzed in a perishable product supply chain.

Key words: Economic lot sizing, transportation, carbon emissions, perishable inventory, multi-mode replenishment

DEDICATION

To my four favorite people:

My parents, Halil İbrahim and Şükran, and my sisters, Gizem and Handan.

I love you all..

ACKNOWLEDGEMENTS

I would like to thank the people who supported me in my journey of the graduate school. I express my sincere appreciation to my advisor, Dr. Sandra D. Ekşiođlu, for her continuous support, guidance and patience throughout my studies. Her enthusiasm opened doors for me and she encouraged me to go through them. I am indebted to her for being a great friend and a role model. I would like to extend my gratitude to Dr. Burak Ekşiođlu for initiating my opportunity to study at Mississippi State, being there for me whenever I needed help and being a part of my committee. My sincere thanks go to Dr. Joseph Geunes for his invaluable ideas, feedback and help on my research as a member of my committee. I appreciate his working closely with me at my visit to the University of Florida. I would like to thank Drs. Allen Greenwood and Mingzhou Jin for being a part of my committee and providing their time and valuable comments for my dissertation. I am grateful to department heads Drs. Royce Bowden and John Usher for letting me teach for a long time. Thanks to them I have had the chance to meet great students and gain a teaching experience that not many graduate students get the chance to have.

A heartfelt appreciation is for my sister, Gizem Palak. During her one year stay with me to study at Mississippi State, she did not only give an enormous moral support for my studies but also increased my standards of having fun at graduate school. She amused me and our friends by exploring Starkville in a couple of months more than we did in three

years. Many thanks are also due to all my friends in Starkville. In particular, I would like to thank Dr. Hüseyin Tunç, Dr. Şule Doğan and Burcu Ellidört Tunç for making this town a more enjoyable place for me. I have been fortunate to have great lab-mates. Special thanks to Mohammad Marufuzzaman, Dr. Ambarish Acharya, Daniela Gonzales for their companionship. I also cannot thank Dr. Hüseyin Sarper enough for being a second father to me in the US. I am grateful to him for his unconditional support and faith in me.

Last but certainly not the least, I am forever indebted to my parents, Halil İbrahim and Şükran Palak, and my sisters, Gizem and Handan Palak for their endless love and encouragement. My big cheerful family would be incomplete without my aunt, Nükhet Palak, and my grandmother Fatma Şükran Palak. The eternal support and prayers of my family reach me to give me strength from thousands of miles away. I could not have done it without them.

TABLE OF CONTENTS

DEDICATION	ii
ACKNOWLEDGEMENTS	iii
LIST OF TABLES	viii
LIST OF FIGURES	x
CHAPTER	
1. INTRODUCTION	1
2. LITERATURE REVIEW	8
3. ANALYZING IMPACT OF CARBON REGULATORY MECHANISMS ON SUPPLIER AND MODE SELECTION DECISIONS	14
3.1 Introduction	14
3.2 An Illustrative Replenishment Model	19
3.3 Supplier Selection Problem	22
3.3.1 Problem Description	22
3.3.2 Problem Formulation under Cost Minimization	25
3.3.2.1 Proposition 3.1	27
3.3.2.2 Theorem 3.1	28
3.4 Modeling Supply Chain Emissions Constraints and Costs	29
3.4.1 Problem Description	29
3.4.2 Formulation for Carbon Cap Mechanism	30
3.4.2.1 Theorem 3.2	32
3.4.2.2 Proposition 3.2	33
3.4.3 Formulation for Carbon Tax Mechanism	34
3.4.4 Formulation for Carbon Cap and Trade Mechanism	35
3.4.5 Formulation for Carbon Offset Mechanism	36
3.4.6 Summary of Model Formulations	37
3.5 Data Collection and Analysis	38

3.6	Observations from Experiments	44
3.6.1	Carbon Cap	45
3.6.2	Carbon Tax	51
3.6.3	Carbon Cap and Trade	54
3.6.4	Carbon Offset	60
3.7	Conclusions	65
4.	MODELS FOR REPLENISHMENT DECISIONS OF PERISHABLE PRODUCTS VIA MULTIPLE TRANSPORTATION MODES	67
4.1	Introduction	67
4.2	Model Formulations	69
4.2.1	Formulation (P)	69
4.2.2	Formulation (Q)	74
4.2.3	Comparison of LP Relaxations of (P) and (Q)	77
4.2.3.1	Optimality Gap	77
4.2.3.1.1	Theorem 4.1	78
4.2.3.2	Running times	81
4.3	Properties of an Optimal Solution	83
4.3.1	Property 4.1	83
4.3.2	Property 4.2	84
4.4	Special Case: Single Replenishment Mode	85
4.4.1	Proposition 4.1	85
4.4.2	Property 4.3	88
4.4.3	Property 4.4	89
4.4.4	Dynamic Programming Algorithm for Zero Inventory Ordering Policy	90
4.4.5	Dynamic Programming Algorithm for Multiple Setups Cost Structure	92
4.4.6	Numerical Study	95
4.5	Special Case: Two Replenishment Modes	102
4.5.1	Numerical Study	105
4.6	General Case: Multiple Replenishment Modes	106
4.6.1	The Minimum Cost Knapsack-Based Algorithm	108
4.6.2	A Primal - Dual Algorithm	108
4.6.2.1	Complementary Slackness Conditions	110
4.6.2.1.1	Proposition 4.2	112
4.6.3	Numerical Study	113
4.7	Conclusions	116
5.	BI-OBJECTIVE MODELS FOR GREEN SUPPLY CHAIN MANAGEMENT OF PERISHABLE PRODUCTS	117
5.1	Introduction	117

5.2	Multi Objective Model Formulation	119
5.3	Solution Approaches	120
5.3.1	Weighted sum method	121
5.3.2	ϵ -constraint method	122
5.4	Results	123
5.5	Conclusions	132
6.	CONCLUDING REMARKS	134
	REFERENCES	137

LIST OF TABLES

3.1	Problem Inputs for the EOQ Model	20
3.2	Emissions Due to Transportation	21
3.3	Input Data Generation	39
3.4	Transportation Mode Assignment Scheme	40
3.5	Variable Costs for Truck Transportation	41
4.1	Problem Parameters for LP Relaxations	81
4.2	Problem Characteristics for LP Relaxations	81
4.3	CPU Running times (in sec) for (P) and (Q)	82
4.4	Problem Parameters for Single Mode Problem	95
4.5	Problem Characteristics for Single Mode Problem	96
4.6	Running times (in sec) - Low Demand - $\alpha = 0.01$	97
4.7	Error Gaps (in %) - Low Demand - $\alpha = 0.01$	97
4.8	Running times (in sec) - Med Demand - $\alpha = 0.01$	98
4.9	Running times (in sec) - High Demand - $\alpha = 0.01$	99
4.10	Error Gaps (in %) - Med Demand - $\alpha = 0.01$	99
4.11	Error Gaps (in %) - High Demand - $\alpha = 0.01$	100
4.12	Running times (in sec) - Low Demand - $\alpha = 0.01$	100
4.13	Error Gaps (in %) - Low Demand - $\alpha = 0.01$	101

4.14	Running times wr/t changes in α - Low Demand	101
4.15	Problem Parameters for 2 Mode Problem	105
4.16	Problem Characteristics for Two Mode Problem	106
4.17	CPLEX Running Times (in sec) for Two Mode Problem	107
4.18	Error gap (in %) of the Knapsack algorithm	107
4.19	Problem Parameters for Multiple Mode Problem	114
4.20	Problem Characteristics for Multiple Mode Problem	114
4.21	Running Times (in sec) for Multiple Mode Problem	115
4.22	Error gap (in %) of Algorithms	115
5.1	Problem Parameters	124

LIST OF FIGURES

3.1	EOQ Model	22
3.2	Network representation of a two-period, three-supplier problem	24
3.3	Carbon Cap Mechanism - Total Costs	46
3.4	Carbon Cap Mechanism - Total Emissions	48
3.5	Carbon Cap Mechanism - Tech 1 - Costs and Distances	48
3.6	Carbon Cap Mechanism - Transportation Mode Percentages	49
3.7	Carbon Tax Mechanism - Total Costs	52
3.8	Carbon Tax Mechanism - Total Emissions	53
3.9	Carbon Tax Mechanism - Tech 1 - Costs and Distances	54
3.10	Carbon Tax Mechanism - Transportation Mode Percentages	55
3.11	Carbon Cap and Trade Mechanism - Total Costs	56
3.12	Carbon Cap and Trade Mechanism - Total Emissions	57
3.13	Carbon Cap and Trade Mechanism - Average Carbon Bought and Sold	58
3.14	Carbon Cap and Trade Mechanism - Transportation Mode Percentages	59
3.15	Carbon Offset Mechanism - Total Costs	61
3.16	Carbon Offset Mechanism - Total Emissions	62
3.17	Carbon Offset Mechanism - Average Carbon Bought	63
3.18	Carbon Offset Mechanism - Transportation Mode Percentages	64

4.1	Multiple-Setups Cost Structure	70
4.2	Network Representation for a 2-mode, 3-period Problem (P)	74
4.3	Network Representation for a 2-mode, 3-period Problem (Q)	75
4.4	Network Representation for Dynamic Programming Algorithm ($T = 4$)	91
4.5	Dual Algorithm	111
4.6	Primal Algorithm	111
5.1	Transportation Mode Selection	126
5.2	Total Cost Distribution	127
5.3	Total Unit Costs	128
5.4	Emissions versus Costs	129
5.5	Total Emissions versus λ_2	130
5.6	Lead Time Costs	131
5.7	Lead Time Emissions	131

CHAPTER 1

INTRODUCTION

For decades, the main objective of models developed for supply chain optimization, logistics management and transportation systems analysis has focused on minimizing costs. These models have been driven by the needs of different industries to improve cost efficiency and performance. Primary costs in supply chain result from activities such as purchasing, inventory holding, and transportation. Thus, the coordination of decisions related to material procurement, inventory management and transportation management have so far been the major concern in the traditional supply chain management problems.

More recently, the need for long term sustainability has been recognized with the public awareness on environmental issues. Scientists raise their concerns about the increased levels of greenhouse gas concentrations and their impacts on the global climate change. To regulate the carbon emissions, an increasing number of efforts have been initiated worldwide, such as Kyoto Protocol [97] and European Climate Change Programme [34]. These policies require the companies to reduce their carbon footprint by revising their operations and updating their technologies. Companies in the US are not yet subject to any federal carbon regulations. However, a number of states have joined forces to launch regional emission-trading programs, such as the Regional Greenhouse Gas Initiative (RGGI), the

Western Climate Initiative (WCI), and the Midwest Greenhouse Gas Reduction Accord (MGGRA). Therefore, we believe that the day when federal carbon regulatory policies are in place, at least to some degree, is not far off.

Many large companies such as Walmart, Tesco, UPS and Hewlett Packard are readily committed to going green [45]. They reorganize their shipment schedules and use fuel efficient vehicles to minimize their carbon emissions. These companies realize that by implementing the green initiatives, they do not only protect the environment, but also gain competitive advantage by increasing customer goodwill and loyalty. The expectation is that other companies will join this trend to strengthen their brand image and strive to reduce their carbon footprint.

Emissions within the supply chain of a product may result from production, inventory and transportation activities. According to the International Energy Agency (IEA)[53], a quarter of the energy-related CO₂ emissions worldwide currently result from transportation. IEA also estimates that transportation emissions will double by 2050. Recent studies show that transportation emissions can be reduced by improvements in the energy efficiency, using alternative energy sources, and modifying supply chain operations [24, 54, 55, 70, 71]. For example, shifting to less energy intensive transportation modes can potentially decrease the emissions. However, the total system costs and lead times are also affected with transportation mode selection decisions. The challenge lies in identifying the appropriate modes of transportation while minimizing the total system costs and emissions and satisfying the demand of the customer on time.

The objective of this research is to develop models for designing and managing cost efficient and environmentally friendly supply chains. The goal is to provide insights and direction to guide companies on making sustainable logistics management and transportation decisions. For that purpose, this study develops mathematical models which represent the relationships that exist between costs and emissions in a two-stage supply chain. These mathematical models will minimize total transportation and inventory holding costs in the supply chain, while accounting for carbon emissions due to transportation and other logistics and supply chain-related activities. Most of the studies in the supply chain literature with a “green” perspective propose mathematical models that consider objectives such as remanufacturing and disposal. Minimizing the carbon footprint of the supply chain is relatively new in the literature. Two main streams of research related to carbon emissions can be put into the categories of measuring [13, 75, 81, 92] and minimizing [1, 9, 10, 44, 41, 79] the level of carbon emissions in the supply chains. This study falls into the latter stream of research, which identifies operational policy changes that impact costs and emissions in the supply chain. It specifically contributes to the literature by improving transportation-related costs and emissions in the supply chain, and consequently achieving the long-term sustainability of transportation systems. The models proposed have the potential to help companies improve transportation and logistics-related costs and emissions, and therefore, become competitive while mitigating environmental impacts.

The mathematical models developed are extensions of the classical Economic Lot Sizing (ELS) model introduced by Wagner and Whitin [104]. The classical ELS model identifies an inventory replenishment schedule for a fixed planning horizon with time-varying

demand. This model assumes that one supplier and one transportation mode are available to replenish inventories. A number of studies have generalized this classical model to account for emissions. Benjaafar et al. [10] extend the ELS model to handle carbon cap, carbon tax, carbon cap-and-trade and carbon offset mechanisms. These mechanisms work as described in the following: Under a carbon cap mechanism, the amount of carbon emitted due to transportation, production and inventory activities cannot surpass a predetermined cap. Under a carbon tax mechanism, a facility pays a tax per ton of carbon emitted due to its operations. Under a carbon cap-and-trade mechanism, a carbon cap is imposed on the facility, where a carbon market also exists which allows the facility to sell unused carbon credits at a profit, or to purchase carbon credits if needed. Under a carbon offset mechanism, a carbon cap is imposed on the facility. A carbon market also exists which allows the facility to purchase carbon credits if needed, but the facility cannot sell back unused carbon credits. Helmrich et al. [41], Mooij [73], Ty [95] develop solution algorithms for the models proposed by Benjaafar et al. [10]. This research extends the ELS models with multiple modes of replenishment and analyze the impacts of carbon regulatory mechanisms on replenishment decisions. Multiple replenishment modes have been considered by Absi et al. [1] for different variations of the carbon cap policy. Hoen et al. [44] focus on measuring and analyzing carbon emissions due to transportation. The methodology developed by Hoen et al. [44] is used in the numerical analysis.

Chapter 3 explains models with multiple replenishment modes with carbon emission considerations and provides insights on the impact of carbon regulatory mechanisms on supply chain performance. This chapter also analyzes the complexity of the models as

models with carbon emission considerations are new in the literature. Models considering carbon cap and carbon offset mechanisms are shown to be NP-hard. The models with carbon tax and carbon cap-and-trade mechanisms are easier problems and they can be solved by an $O(IT^2)$ algorithm. A two-tier supply chain consisting of a number of suppliers and one facility is considered. The facility faces a time varying and deterministic demand. In order to satisfy customer demand, a facility may replenish its inventories using one or more suppliers. The facility may correspond to a manufacturer or a retailer who makes inventory replacement decisions every period within a fixed planning horizon of length T. A supplier in this model is defined by the combination of a physical supplier and the corresponding transportation mode used. A facility may replenish its inventories using local suppliers or using suppliers located further way. A fixed charge transportation cost structure is assumed. A fixed cost is charged for initiating a shipment, and a variable cost is charged per unit delivered. For example, the fixed charge for rail transportation is higher than truck, but the variable cost is smaller. In addition to costs, the models consider emissions due to transportation and inventory holding in this two-tier supply chain. The structure of the emission functions also contains a fixed plus linear structure. A fixed amount of carbon is emitted every time we initiate a shipment due to loading and unloading activities. Variable emissions depend on the quantity shipped and distance traveled. Thus, the fixed and variable emissions depend on the transportation mode used. For example, more effort is typically required to load and unload a rail car and barge than a truck. Thus, fixed emissions are higher for rail and barge than truck. Gas usage per ton and per mile for trucks is higher than rail and barge; consequently, unit variable emissions for trucks are higher.

However, depending on the transportation distance, total emissions for long hauls using rail and barge may be higher. In the numerical analysis the study specifically considers a biofuel supply chain. As logistics costs of biomass are high, transportation mode and supplier selection decisions are especially important in this contemporary supply chain problem. Observations from the experiments show that a significant decrease in emissions can be achieved through supply chain operations with a low cost. Counter intuitively, local suppliers with truck transportation are preferred as the carbon cap levels decrease.

With the motivation of obtaining valuable insights about the impact of carbon regulatory mechanisms on supply chain performance, the study in Chapter 3 is extended to consider more realistic and complex scenarios in Chapter 4 and 5. For these chapters, a multiple setups cost structure is assumed which includes a fixed order cost, a unit variable cost charged for each unit shipped, and a fixed cargo container cost which is charged for each container used. There also exists a unit variable emission and fixed emissions resulting from loading and unloading of each cargo container. This cost structure allows a more accurately representation of costs and emissions associated with a given mode as a function of quantity shipped. These chapters consider age-dependent perishable inventories. These inventories deteriorate with respect to their age and lose a percentage of their value at every time period. They are eventually discarded due to spoilage. Examples include agricultural and dairy products. These products are of particular interest because of emissions resulting from the required refrigeration to transport and hold the products. The tradeoffs do not only exist between costs and emissions, replenishment and inventory holding costs, but also lead time and the remaining shelf life of the perishable products.

Chapter 4 is dedicated to analyzing models with age-dependent perishable inventories and multiple setups replenishment costs with the single objective of cost minimization. The properties of an optimal solution are defined. The chapter considers special cases where only a single mode or two modes of replenishment are available. Algorithms are proposed to solve both general and special cases that provide good quality solutions in short running times. In Chapter 5, the research extends the model proposed in Chapter 4 to minimize the environmental impacts using a multi-objective approach. Some studies in the literature incorporate carbon emissions into multi-objective models [15, 62, 107]. This study constructs a bi-objective model with the minimization of total costs and total emissions objectives. It provides insights about supplier selection and the tradeoffs between costs and emissions in the supply chain using weighted sum and ϵ -constraint methods. The analyses show how the results of these two solution approaches would explain the performance of the supply chain under carbon tax and carbon cap policies respectively.

Overall, this research analyzes extensions of the economic lot sizing models to deal with contemporary issues in the supply chains. Supply chains with biomass and perishable products are of interest which require an emphasis on the product characteristics. Additionally this research provides insights on the replenishment decisions such as transportation mode selection and transportation schedules which would minimize the costs as well as the environmental impacts.

CHAPTER 2

LITERATURE REVIEW

The supply chain management (SCM) literature mostly focuses on improving the profitability and efficiency of the chain [17], where cost is an all-important measure of efficiency. Major contributors to total system costs include purchasing, inventory holding, and transportation costs. As noted by Simchi-Levi et al. [87], the coordination of decisions related to material procurement, inventory management, and transportation management can greatly impact overall system costs and service levels. More recently, because of increased public awareness of environmental issues, SCM research has considered the “green” perspective. As a consequence, SCM literature is expanding in a new direction which aims to limit the environmental impact of supply chain activities. Thus far, the literature on “green” supply chain management (GSCM) has concentrated on topics involving product recycling, reuse, and disposal. We refer interested readers to Srivastava [90] and Dekker et al. [23] for a thorough literature review on GSCM.

A new stream of literature within GSCM analyzes the carbon footprint of a product’s supply chain. A number of studies propose methods to measure and quantify carbon emissions in the supply chain due to processes such as transportation [13, 75, 81, 92]. Other studies propose optimization models to minimize the carbon footprint of a supply chain

through changes in supply chain design and operations [10]. The work presented in this paper falls in this latter stream of research, which identifies operational policy changes (e.g., in inventory replenishment schedules, transportation modes and supplier selection) that impact costs and emissions in the supply chain.

Production of fuels using renewable sources of energy (such as biomass) is experiencing growth in the US. The existing literature on biofuel supply chains has concentrated on identifying supply chain designs and management practices which optimize the system performance. A number of research articles utilize cost minimization models to determine optimal locations and capacities for biorefineries given the distribution of biomass and the location of final customers [4, 26, 27, 30, 40, 49, 94, 112]. Other studies use models which identify supply chain management practices that maximize profits [61, 67, 69, 80] and/or minimize risk associated with investments [20]. Stochastic programming and simulation models have been used to capture the uncertainties in biomass supply and costs in the supply chain [22, 52, 65, 88, 83, 93]. This literature features a number of studies emphasizing the importance of minimizing transportation costs in biofuel supply chains [31, 74, 110]. Please see An et al. [5] and Iakovou et al. [51] for a thorough review of the literature on biofuel and biomass supply chain design and management tools.

Traditional inventory management models in the SCM literature, such as the EOQ model and the dynamic economic lot sizing model, identify inventory replenishment schedules for a single facility facing deterministic demand for a single item. These models take into account the tradeoffs that exist between fixed ordering costs and inventory holding costs in a supply chain. A number of studies in the area of GSCM have extended these

basic inventory models to account for carbon emissions due to production and inventory in the supply chain. For example, the EOQ model has been extended by Chen et al. [16], Hua et al. [48], Arslan and Turkay [6] and Wahab et al. [105] to address carbon cap, carbon tax, carbon cap and trade, and carbon offset mechanisms. Benjaafar et al. [10] extend the ELS model to handle these carbon regulatory mechanisms. Helmrich et al. [41], Mooij [73] and Ty [95] develop solution algorithms for the models proposed by Benjaafar et al. [10]. These extensions of the ELS model are inspired by current logistics practices that also serve as a motivation for our work. We contribute to these efforts by extending the ELS models to consider the impact of carbon regulatory mechanisms on replenishment decisions when a company has the option of using multiple suppliers and modes to replenish inventories. The models we develop can be used as sub-modules in MRP systems to help environmentally conscious companies with requirements planning when multi-mode and multi-supplier replenishment options are available. These tools enable companies to determine whether they should employ a single supplier and a single replenishment mode, or a combination of different suppliers and modes. We refer readers to Bonney and Jaber [12] for a wide range of extensions to traditional inventory models.

A number of prior studies have focused on analyzing emissions from transportation activities in the supply chain. For example, Bauer et al. [9] propose an integer programming model to identify a transportation network design that minimizes total emissions due to transportation. Winebrake et al. [109] present an energy and environmental network analysis model that explores the tradeoffs between costs, time and emissions resulting from freight transportation. Pan et al. [79] discuss how shipment consolidation in supply chains

impacts emissions from freight transportation. Absi et al. [1] extend the formulation of an inventory replenishment model under a carbon cap mechanism proposed by Benjaafar et al. [10] to capture the impact that the multiple mode availability in transportation has on emissions. They model different variations of a carbon cap mechanism (such as a time-cumulative cap, a period-by-period cap, a rolling cap, and a global cap) and analyze the complexity of these models. The work by Hoen et al. [44] focuses on measuring and analyzing carbon emissions due to transportation. Rosič [86] integrates environmental regulations (such as emissions limits, emissions taxes and emissions trading) into a basic dual-sourcing model within a supply chain. This work demonstrates the way in which transportation related decisions may be influenced by carbon regulations.

Several additional studies have addressed supply chain network design decisions with carbon emission considerations. These studies take different approaches to incorporate carbon emissions into multi-objective optimization models [15, 62, 107] and game theoretic models [25] for supply chain network design.

Within the aforementioned literature, our research is most closely related to the work by Hoen et al. [44]. Hoen et al. [44] develop a methodology that can be used to quantify transportation carbon emissions. They use this methodology to compare emissions levels when shipping via different modes of transportation. Their results show that product characteristics, such as volume and density, impact transportation mode selection, and modal shifts can result in large emission reductions. The methodology developed by Hoen et al. [44] generates data for our study's numerical experiments, and, as a consequence, derives

meaningful and realistic representations of the relationship between different transportation modes and consequent emissions levels.

Our research is closely related to a study by Benjaafar et al. [10] and Helmrich et al. [41] that assume that a single supplier is used to replenish inventories. Our work adds an important dimension to this problem, by accounting for supplier and transportation mode selection decisions. As a consequence, our models capture not only the tradeoffs that exist between costs and emissions due to inventory and transportation, but they also capture the tradeoffs between cost and emissions resulting from the use of different suppliers and transportation modes.

Our research is also related to the multi-objective modeling for cost and emissions minimization. There is an extensive existing literature in the field of multi-objective programming (MOP) [91]. The purpose of MOP models is to optimize systematically and simultaneously a collection of conflicting objectives. Solving an MOP problem means identifying the set of Pareto optimal solutions which are solutions that are nondominated in the sense that no subset of objectives can be improved without making at least one objective worse. MOP models have been used to optimize green supply chains. For example, Wang et al. [106] uses a bi-optimization model to design a supply chain network which optimizes costs and emissions. This paper extends the classical facility location model to consider transportation-related costs and emissions when making facility location decisions. Neto et al. [77] propose an algorithm to solve an MOP model with three objectives: minimize costs, cumulative energy demand and waste in a reverse logistics network. This

paper is consistent with this work since it uses an MOP to optimize costs and emissions in a supply chain.

Our research considers the replenishment of special characteristic products, such as perishable products. Different from the literature, our models identify tradeoffs that exist between lead time, remaining shelf life and product perishability in the supply chain. Nahmias [76], and Goyal and Giri [38] present extensive reviews of inventory replenishment models for perishable products. Nahmias distinguishes between perishable products with fixed versus random lifetime. Our article considers perishable products that deteriorate with time and therefore have a random lifetime. The literature discusses deterministic inventory replenishment models for perishable products with random lifetime. These are extensions of the Economic Order Quantity (EOQ) model [37, 19], and Economic Lot Sizing model [47]. For inventory replenishment models for perishable products with fixed lifetime see Eksioglu and Jin [29], Ahuja et al. [3], Zhang and Eksioglu [113], and Onal [78].

Our research provides extensions of models studied by Hwang [50], Jaruphongsa et al. [59], Lee [64], and Hsu [46]. Hwang [50], Lee [64] and Jaruphongsa et al. [59] consider multiple setups replenishment costs in their studies. Hwang [50] provides an extensive study that presents algorithms for a set of different cost structures. Jaruphongsa et al. [59] propose a dynamic programming algorithm for the special case of dual transportation modes. Hsu [46] provides an efficient algorithm for age-dependent products under a fixed setup cost structure using a single replenishment mode.

CHAPTER 3

ANALYZING IMPACT OF CARBON REGULATORY MECHANISMS ON SUPPLIER AND MODE SELECTION DECISIONS

3.1 Introduction

Global climate change is an important contemporary issue that is being investigated from numerous perspectives. Many prominent world leaders and scientists have raised concerns in recent years regarding increased levels of greenhouse gas (GHG) emissions and the impacts these emissions have on climate change. The Intergovernmental Panel on Climate Change (IPCC) estimates an increase of 1.8° to 4° Celsius in Earth's temperature by the end of this century because of increased GHGs, such as carbon dioxide (CO₂), methane and nitrous oxide [89]. Of major concern is the burning of fossil fuels, since their extensive usage in areas ranging from power generation to transportation yields significant GHG emissions levels.

These concerns have inspired a worldwide debate about GHG emission reduction targets and regulations. A study by McKinsey & Company [71] indicates that a delay of action in the next 10 years will have a great impact on the environment. Rogner et al. [85] argue that in order to prevent global warming and climate change, GHG emissions should be reduced by 50% of their 1990 levels by 2050. Many countries and governments have accepted the premise that an urgent need exists to put policies into action, and as a result

have already set reduction targets. For example, through its European Climate Change Programme, the European Union aims to reduce its GHG emissions by at least 20% by 2020 compared to 1990 levels [34]. While the media has chronicled a fair amount of controversy regarding GHGs and climate change, our study does not to weigh in on this debate; instead our research assumes that reducing fossil fuel consumption will provide economic benefits and improve quality of life.

Transportation and other supply chain related activities are a major contributor to GHG emissions [57]. According to the International Transport Forum, global CO₂ emissions from fossil fuel combustion will increase by 45% from 2006 to 2030 [56]. The International Energy Agency (IEA) [53] states that 19% of the energy consumption, and almost a quarter of the energy-related CO₂ emissions worldwide result from transportation. In the US, transportation comprises 28% of the total energy consumption [21]. The US Environmental Protection Agency (EPA) estimates that during the period from 1990 to 2010, transportation-related emissions rose by 18% [33]. This is mainly due to the increased demand for travel, and the US vehicle fleet's stagnant fuel efficiency. Considering current worldwide trends in transportation mode usage, the IEA estimates that transportation will experience the largest growth in energy demand in the next 40 years. Transportation demand is expected to increase by 50% by 2030 and 80% by 2050. As a consequence, transportation related emissions are projected to nearly double, going from 7.5 Gigatonnes (Gt) in 2006 to about 14 Gt in 2050 [53]. Given these trends, achieving the target of a 50% reduction in total carbon emissions by 2050 will be almost impossible, unless transportation-related emissions are reduced significantly.

Road transportation is the largest contributor to transportation-related emissions. Private automobiles and light truck vehicles contribute over 60% of these emissions. Other modes of transportation contribute to transportation-related emissions in the following order: air transport, marine, rail, and pipelines [39]. Air transportation-related emissions are expected to increase by 60% in 2025, compared to 2001 levels because of the increased usage [96]. Increased emissions from rail transportation will depend, to a large extent, on the development of adequate infrastructure as a result of capital investments.

In order to reduce transportation emissions, several studies advise modal shifts from energy intensive modes, such as road and air to rail, barge, and ship [24, 54, 55, 70]. However, in the context of supply chain management, shifting from one transportation mode to another will impact costs and delivery lead times. Additionally, firms may not have access to a mode with lower emissions, such as rail or marine transportation, due to infrastructure and geographic limitations. Therefore, managers must identify the appropriate transportation mode(s) in a supply chain in order to address the tradeoffs between inventory and transportation costs, customer satisfaction (via on-time product delivery), and the carbon footprint of the product delivered.

The opportunities for reducing carbon emissions are multi-fold. A recent study by McKinsey & Company [70] shows that improvements in energy efficiency, using alternative fuels (e.g., biofuels), and using alternative energy sources (e.g. wind and nuclear) can potentially reduce carbon emissions. In addition to developing new technologies, additional measures to reduce carbon emissions include how shifts in the operational policies within a product's supply chain can serve to reduce transportation-related carbon emis-

sions. This study investigates how decisions regarding which suppliers and transportation mode(s) are used and the degree of transportation vehicle utilization can greatly reduce energy usage without significantly impacting costs. We propose several optimization models, each of which is an extension of the classical economic lot-sizing (ELS) model to allow for constraints and/or costs on carbon emissions. We demonstrate through our numerical study that operations policy modifications can address tradeoffs between inventory-related costs and carbon emissions.

We contribute to the existing literature by providing model-based insights on the impacts that potential carbon regulatory policies, such as carbon cap, tax, cap-and-trade and offset have on supplier and transportation mode selection decisions. The economic lot-sizing models with multiple replenishment modes and carbon constraints this study presents offer some interesting observations with respect to the tradeoffs between costs and emissions. As models with carbon emission considerations are new in the literature, we also find it useful to provide insights about the complexity of the proposed models. We show that the models for carbon cap and carbon offset mechanisms are NP-hard, while the models for carbon tax and cap-and-trade mechanisms are easier problems and can be solved by a polynomial time algorithm. The main contribution of this paper, however, lies in applying the proposed models to a contemporary supply chain problem (biofuel supply chain) and deriving meaningful numerical results and insights.

In the numerical analysis we consider inventory replenishment decisions at a biorefinery which uses woody biomass for production of cellulosic ethanol. It is estimated that the US annually supplies 327 million tons (MT) of woody biomass for production of biofu-

els. This amount constitutes 20% of the total 1.6 billion tons/year of biomass available for production of biofuels [99]. Based on the Renewable Fuel Standard (RFS), the minimum level of renewable fuels used in the US transportation industry is expected to increase from 9.0 billion gallons per year (BGY) in 2008 to 36 BGY in 2022 [84]. We expect that, due to these requirements, the production of cellulosic ethanol will increase.

Inventory replenishment decisions at the biorefinery are very important because of the high in-bound logistics-related costs that occur as a result of the characteristics of the raw material (in this case, woody biomass) which: (a) is bulky and difficult to transport, (b) has low energy density, and (c) is widely dispersed geographically. Assuming a conversion rate of 60 gallons per dry ton, a medium-sized biorefinery which produces 60 million gallons per year (MGY) of ethanol would typically receive 1 MT per year of biomass. Assuming 260 working days per year, 128 truck loads of biomass would be shipped daily. Biorefineries consider receiving shipments by using different modes of transportation such as barge or unit rail, high capacity transportation modes that have historically been used for transportation of wood and other bulky products. Using these modes of transportation has the potential to reduce transportation costs, decrease road traffic and improve road safety in the surrounding communities, and increase the pool of suppliers available. Increased biomass availability enables the establishment of large capacity plants, and consequently allows for economies of scale in production. We have identified at least two biorefineries in Mississippi which are located near to an in-land port and also have access to rail: KiOR Inc.'s facility in Columbus and Bluefire Renewables in Fulton. KiOR's plant has started operating in early 2013 [63] and has a capacity of 11 MGY. This plant is located by the

Tennessee-Tombigbee Waterway port of Columbus and has access to Burlington Northern Santa Fe (BNSF) Railway, Norfolk Southern and Canadian National/Illinois Central railways. Bluefire Renewables' plan features a capacity of 19 MGY [100], and will have access to the Mississippi River, port of Itawamba and be served by the Mississippian Railway.

In our numerical experiments, we use a methodology for estimating emissions from transportation developed by Hoen et al. [43]. This methodology calculates emissions as a function of distance traveled, load weight, and the transportation mode used. We use publicly available data to derive transportation cost functions for rail, barge, and truck. As a consequence, our numerical results are meaningful and give a realistic representation of emissions levels and costs when using different transportation modes.

The rest of this chapter is organized as follows. In Section 3.2, we use a simple Economic Order Quantity (EOQ) model to illustrate the tradeoffs between costs and emissions. Section 3.3 presents the formulation for the supplier selection problem. Section 3.4 presents models that capture carbon constraints and costs. In Sections 3.5 and 3.6, we discuss the data collection and analyze the results of our numerical experiments. We conclude with the observations from our study in Section 3.7.

3.2 An Illustrative Replenishment Model

We use an illustrative example of the EOQ model in order to show how transportation mode selection decisions are affected by carbon regulatory mechanisms. The goal

is to provide some insights about the impact of carbon emission limitations on inventory replenishment decisions.

Table 3.1 summarizes the data used in this example. Consider a facility that uses three different suppliers to replenish inventories. The annual requirements at the facility are 3,000 tons. Suppliers are located 50, 150, and 400 miles away from the plant. Depending on transportation distance, and the availability of transportation infrastructures, these suppliers have access to different transportation modes. Table 3.1 lists the available transportation mode, unit variable cost (c), fixed order cost (K), and unit inventory holding cost (h) for each supplier.

Table 3.1

Problem Inputs for the EOQ Model

Notation	Supplier #	Transp. Mode	Distance (miles)	Var. Costs (\$/(mile*ton))	Fixed Costs (\$/Order)	Inv. Hold. Costs (\$/(ton*year))
S1 M1	1	Truck	50	10	20	0.005
S2 M2	2	Rail	150	5	400	0.005
S3 M3	3	Barge	400	1	2,000	0.005

Table 3.2 provides the unit emissions due to transportation (in kilograms (kg) of CO₂ per ton and per mile shipped) for each supplier. Total transportation-related emissions are a function of the distance traveled and transportation mode used. Emissions due to storage are considered to be fixed at 0.1 tons of CO₂ per year. Details about the methodology used for generating costs and emissions-related data are provided in Section 3.5.

Table 3.2

Emissions Due to Transportation

Supplier	Distance (miles)	Mode Capacity (tons)	Emissions (kg CO ₂ /(mile*ton))	Emissions (kg CO ₂ /ton)
S1 M1	50	30	0.06	1.8
S2 M2	150	100	0.03	3.0
S2 M3	400	1,000	0.01	10.0

Suppose that a carbon cap mechanism is used to control emissions in the supply chain. Such a mechanism forces total emissions (over some time horizon) to be less than the cap. Figures 3.1(a) and 3.1(b) present the total cost and total emission curves for different order quantities. If emissions were not considered in this problem setting, then replenishment of inventory from the 3rd supplier using barge provides the minimum costs (see Figure 3.1(a)). Consider the case when a carbon cap of 10 tons per year exists. In this case, only shipments from supplier 1 can meet the emissions requirement (see Figure 3.1(b)). Supplier 1 is located nearby the facility, and therefore, this supplier's total emissions are the smallest. The EOQ for this supplier is 4,899 and corresponding total costs are \$31,225. Consider the scenario when the carbon cap is increased to 13 tons per year. Under such a scenario, shipments from suppliers 1 and 3 are considered due to their emission levels. Inventories are replenished through Supplier 2 which has lower total emissions than the cap.

The results from this numerical example indicate that transportation mode selection decisions are not only impacted by the tradeoffs that exist between inventory and transportation costs, but also by the tradeoffs that exist between costs and carbon emissions

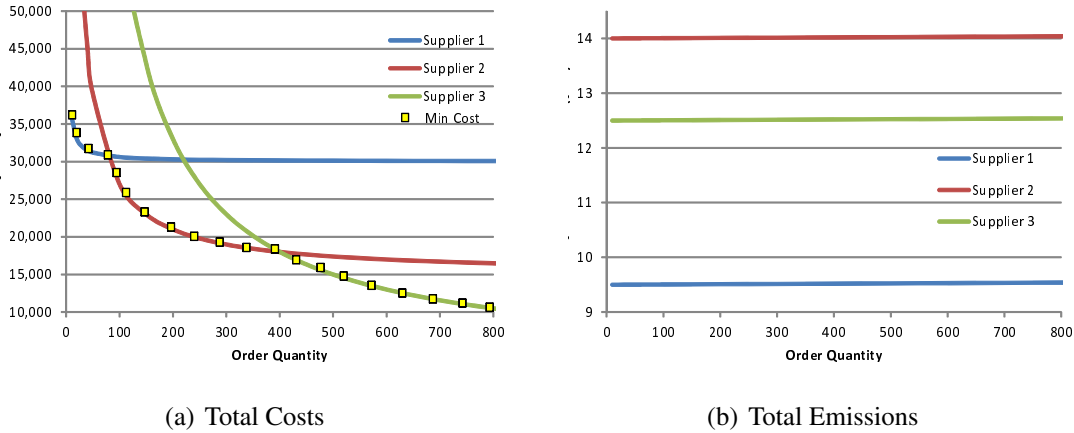


Figure 3.1

EOQ Model

in the supply chain. For example, emission per ton and per mile traveled are highest for truck transportation as compared to barge and rail. However, emissions per ton shipped are smallest for supplier 1 who uses truck and is located 50 miles away from the plant. Consequently, total emissions are minimized when using supplier 1.

3.3 Supplier Selection Problem

This section discusses the mathematical model we propose in order to identify a replenishment schedule that minimizes total supply chain costs. In the following sections we define and formulate the problem; then we describe an algorithm that solves the problem in polynomial time.

3.3.1 Problem Description

Our supply chain consists of a single facility and its suppliers. The facility could be a manufacturing facility, or a retailer making inventory replacement decisions every period

within a fixed planning horizon of length T . A “supplier” in our model corresponds to a unique combination of a supply firm and a particular transportation mode. Thus, there may be multiple “suppliers” for a given supply firm- but one for each transportation mode.

A facility can replenish its inventories using local or distant suppliers. Typically, if shipment delivery time is not a concern, a facility can increase the supplier pool size by considering suppliers located further away, which increases the likelihood that the facility will be able to identify suppliers (e.g., wholesalers) that can provide products at a competitive price. Depending on the distance traveled and transportation mode accessibility, barge, rail, or truck can be used to replenish inventories. The facility may, alternatively, replenish inventories using nearby suppliers who can respond in a timely manner. Because of short travel distances, these suppliers tend to use truck shipments. Shipments are initiated depending on the size of a shipment, e.g., full truck load (FTL) or less-than-full truck load (LTL). Somewhat paradoxically, replenishment costs from local suppliers are often higher compared to more distant suppliers, mainly due to frequent LTL shipments, as opposed to the FTL shipments from more distant suppliers. Our goal is to identify suppliers and a replenishment schedule that minimizes total replenishment (purchase and transportation) and inventory holding costs.

In this problem, operations costs consist of replenishment and inventory holding costs. Replenishment costs from supplier i ($i = 1, \dots, I$) in period t consist of a fixed order cost (f_{it}) and a variable cost (c_{it}). Recall that a supplier in our model is defined by the combination of a physical supplier and specific transportation mode. Thus, the fixed order cost consists of the costs necessary to process an order as well as to load or unload a shipment.

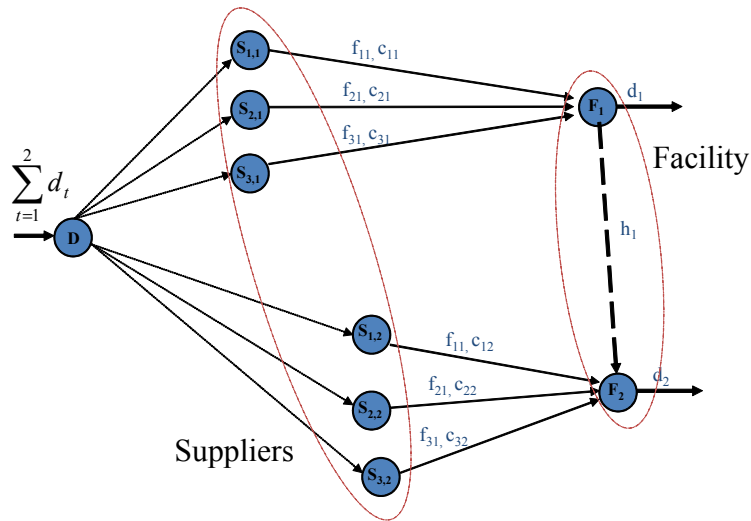


Figure 3.2

Network representation of a two-period, three-supplier problem

The variable cost consists of the purchasing cost and distance-dependent transportation costs. These costs are a function of quantity shipped. A unit inventory holding cost is charged per unit of inventory held at the facility at the end of each time period (h_t).

Figure 3.2 provides a network representation of a two-tier supply chain problem with three suppliers and one facility. The time horizon consists of two time periods.

This network contains one dummy node, a total of T facility nodes (one node per time period), and $I * T$ supplier nodes. The dummy node has a supply equal to the total demand over the planning horizon. A facility nodes t has a demand equal to d_t , which denotes demand in period t ($t = 1, \dots, T$). The supplier nodes correspond to each supplier in every time period. The network has $I * T$ replenishment arcs, $T - 1$ inventory arcs and $I * T$ dummy arcs. Replenishment arcs connect suppliers with the facility in each time period. The cost per unit flow on a replenishment arc is c_{it} ($i = 1, \dots, I; t = 1, \dots, T$). There is

also a fixed cost for using supplier i in period t equal to f_{it} ($i = 1, \dots, I; t = 1, \dots, T$) which is incurred when using a replenishment arc. Inventory arcs connect the facility nodes in consecutive time periods. The cost per unit of flow on an inventory arc is h_t ($t = 1, \dots, T$).

An optimal solution for this problem consists of a set of paths, with each path originating at the dummy node and ending at a facility node. These paths identify the suppliers and transportation modes used to satisfy demand at minimum cost. We refer to such a solution structure as a *tree solution*. Note that we will assume that demand must be satisfied in every time period, i.e., backorders are not allowed.

3.3.2 Problem Formulation under Cost Minimization

We define decision variables for our models as follows. y_{it} is a binary variable, which is equal to 1 if a shipment is received from mode i in period t and 0 otherwise. q_{it} represents the amount received from mode i in period t . H_t denotes the amount of inventory carried from period t to $t + 1$.

The following is a mixed integer programming formulation of the cost minimization model. We refer to this as model (P).

$$\text{minimize } \sum_{i=1}^I \sum_{t=1}^T \{f_{it}y_{it} + c_{it}q_{it} + h_t H_t\} \quad (3.1)$$

$$\text{Subject to } \sum_{i=1}^I q_{it} + H_{t-1} - d_t = H_t \quad t = 1, \dots, T \quad (3.2)$$

$$H_0 = 0 \quad (3.3)$$

$$q_{it} \leq \left(\sum_{\tau=t}^T d_{\tau} \right) y_{it} \quad i = 1, \dots, I; t = 1, \dots, T \quad (3.4)$$

$$y_{it} \in \{0, 1\} \quad i = 1, \dots, I; t = 1, \dots, T \quad (3.5)$$

$$q_{it}, H_t \geq 0 \quad i = 1, \dots, I; t = 1, \dots, T \quad (3.6)$$

The objective function of (P) minimizes total costs. Constraints (3.2) are the inventory balance constraints. Constraints (3.3) set the initial inventory to zero. Constraints (3.4) connect continuous and binary variables, and ensure that no flow is shipped from supplier i in period t , unless $y_{it} = 1$. The remaining constraints are the binary and the nonnegativity constraints, respectively.

Jaruphongsra et al. [59] have studied the ELS problem with two-mode replenishment options. Their replenishment cost function is different from model (P) since it possesses a multiple-setup structure to account for cargo capacities. Eksioglu [28] studied the ELS problem with multi-mode replenishment costs and cargo capacity constraints. Thus, model (P) is a special case of the problem discussed by Eksioglu [28].

Problem (P) is an extension of the traditional ELS problem introduced by Wagner and Whitin [104]. An optimal solution to both problems has the Zero Inventory and Single Source properties, as shown in Proposition 3.1. Therefore, one can extend existing algorithms for ELS ([35, 104, 103]) in order to solve (P). Eksioglu [28] proposes an extension of the dynamic programming algorithm of Wagner and Whitin [104] that solves the ELS model with multi-mode replenishment and fixed-charge cost function, model (P). We present this algorithm in Theorem 3.1. Problem (P) is also a special case of the lot sizing

problem with substitutions with a single end-product and multiple substitutable components [7].

Note that the classical ELS problem assumes that a single supplier and a single transportation mode are used to replenish inventories. A number of studies have generalized the classical ELS model with various considerations. These extensions include finite production capacity models [11, 36], multi-echelon models [60] and multi-item models [8, 66]. The general purpose of these extensions is to replicate real problems faced by manufacturing companies. However, because of current pressures on logistics activities to ensure sustainable practices, additional extensions of this problem class are practical and relevant. This is one of the motivations for this research, in addition to the need to develop replenishment planning decision models and policies that account for the carbon footprint of transportation modes.

3.3.2.1 Proposition 3.1

There exists an optimal solution to (P) such that:

$$q_{it}^* q_{lt}^* = 0 \quad i, l = 1, \dots, I; i \neq l; t = 1, 2, \dots, T \quad (3.7)$$

$$q_{it}^* H_{t-1}^* = 0 \quad i = 1, \dots, I; t = 1, \dots, T \quad (3.8)$$

$$H_{t-1}^* \left(\sum_{i=1}^I q_{it}^* \right) = 0 \quad t = 1, \dots, T \quad (3.9)$$

Problem (P) minimizes a concave (fixed charge) cost function over a polyhedron. Therefore, optimizing (P) results in an extreme point solution. The extreme points of problem (P), which is an uncapacitated network flow model, correspond to tree solutions in the network model described above (Figure 3.2). The tree structure of an optimal solution im-

plies that demand is satisfied either by using existing inventories or receiving a shipment (*Zero Inventory Property*), but not both. The tree structure of the optimal solution also implies that inventories are replenished using a single supplier and a single transportation mode (*Single Source Property*).

3.3.2.2 Theorem 3.1

There exists a dynamic programming algorithm that solves problem (P) in $O(IT^2)$.

By the *Zero Inventory Property* of (P), an optimal replenishment schedule exists such that if period t is a replenishment period, the corresponding replenishment quantity equals $\sum_{\tau=t}^{t'-1} d_{\tau}$ for some $t \leq t' \leq T + 1$ (where t' is the next replenishment period after period t , and we use the dummy period $T + 1$ as a final replenishment period in any solution by convention). By the *Single Source Property* of (P), the minimum cost associated with periods t through $t' - 1$ equals

$$g_{t,t'} = \left\{ \min_{i=1,\dots,I} (f_{it} + c_{it}d_{t,t'-1}) \right\} + \sum_{\tau=t}^{t'-1} h_{\tau}d_{\tau+1,t'-1}, \quad (3.10)$$

where, $d_{k,j} = \sum_{\tau=k}^j d_{\tau}$ and $k = 1, \dots, T$ and $0 < k \leq j \leq T$. Because any solution contains a sequence of setup periods, we can solve problem (P) by solving a shortest path problem in an acyclic network. That is, we create a graph G , where the total number of nodes in G is $T + 1$, with one node per time period plus a dummy node ($T + 1$). Traversing arc $(t, t') \in G$ represents the choice of satisfying demand for periods $t, \dots, t' - 1$ using a replenishment in period t . The cost of arc (t, t') is $g_{t,t'}$, and the supplier used for replenishment in period t is the one that gives the minimum in (3.10). The goal is to find the shortest path from node 1 to $T + 1$ in G .

For any given supplier, we can determine all arc costs associated with the supplier in $O(T^2)$ time. Thus, computing all arc costs for every supplier takes a total of $O(IT^2)$ time. Then, for each of the $O(T^2)$ arcs, we can determine the minimum cost supplier associated with the arc in $O(I)$ time for a total of $O(IT^2)$ time. Finally, we can solve the shortest path problem in $O(T^2)$. The total worst-case complexity is therefore $O(IT^2 + IT^2 + T^2)$ which implies a worst-case complexity of $O(IT^2)$.

3.4 Modeling Supply Chain Emissions Constraints and Costs

In this section we describe the supplier and transportation mode selection problem under a number of carbon regulatory mechanisms, including carbon cap, carbon tax, carbon cap-and-trade, and carbon offset. These models explore the tradeoffs between costs and emissions in this two-level supply chain.

3.4.1 Problem Description

Consider the two-tier supply chain described above which consists of a facility and a number of suppliers (Figure 3.2). The facility has the option to use nearby suppliers to replenish its inventories, or use suppliers located further away. In addition to costs, concerns about emissions now impact replenishment decisions made by the facility. Transportation-related emissions for shipments from local suppliers are typically low due to shorter distances traveled. Emissions per ton and per mile for barge and rail are smaller than those from trucks. However, depending on the transportation distance, the total emissions for long hauls using rail and barge may be higher. The objective of the models we propose is

to identify a replenishment schedule that minimizes the total system costs and the carbon footprint of this supply chain.

We assume that carbon emissions in this supply chain result from transportation activities and holding inventory. We separate transportation related emissions into fixed (\hat{f}_i) and variable (\hat{c}_i) emissions. Fixed emissions are mainly due to loading and unloading of a shipment. These emissions depend on the transportation mode used since the equipment required to load and unload a barge, rail car, or truck, is different. Variable emissions also depend on the transportation mode used since the amount of carbon emitted per ton and per mile traveled by truck is different from that of rail or barge. Our model also considers emissions that may result from holding inventories. For example, the emissions per unit of inventory held in a time period (\hat{h}_t) depend on the heating/cooling system at the facility (note that we do not consider perishable products, however).

3.4.2 Formulation for Carbon Cap Mechanism

We now discuss a first extension of model (P) that applies a carbon cap mechanism over the finite horizon. As a result, the total carbon emitted into the horizon due to transportation and inventory activities cannot surpass this cap. To represent the existence of such a mechanism mathematically, we add a constraint to our model. Constraint (3.12) limits the total emissions in the supply chain to C , the carbon cap level over the horizon. We refer to this as model (P_CC).

$$\text{minimize } \sum_{i=1}^I \sum_{t=1}^T \{f_{it}y_{it} + c_{it}q_{it} + h_t H_t\} \quad (3.11)$$

Subject to (3.2) – (3.6)

$$\sum_{i=1}^I \sum_{t=1}^T (\hat{f}_i y_{it} + \hat{c}_i q_{it} + \hat{h}_t H_t) \leq C \quad (3.12)$$

The objective function of (P_CC) minimizes total costs, subject to flow conservation constraints, setup forcing constraints and a carbon emission constraint (3.12). This model, in addition to cost, keeps track of emissions from inventory holding, transportation and loading/unloading activities. While the firm still minimizes supply chain related costs, it must ensure that the carbon constraint is not violated. This additional constraint can potentially increase total costs and impact supplier and transportation mode selection decisions.

In Theorem 3.2, we show that the problem is NP-hard even for a special case of model (P_CC) with a single supplier. Work by van den Heuvel et al. [102] demonstrates that a special case of model (P_CC) with a single replenishment mode (single supplier), and non-speculative cost structure, is NP-complete. Work by Helmrich et al. [41] shows yet another special case of (P_CC) with two replenishment modes, and time-invariant costs and emissions, is NP-hard. Since these special cases of (P_CC) are NP-hard, we conclude that problem (P_CC) is NP-hard. In Proposition 3.2 we show that whether problem (P_CC) has a feasible solution or not can be identified in $O(IT^2)$.

Work by Helmrich et al. [41], Mooij [73], and Ty [95] proposes solution approaches for the single-supplier version of (P). These approaches rely on Lagrangian relaxation, variable neighborhood search, and other pseudo-polynomial time algorithms. Absi et al. [1] proposes models and analyzes the complexity for variations of the emissions constraint, such as, time-cumulative emission cap, period-by-period cap, rolling cap, and global cap.

3.4.2.1 Theorem 3.2

Problem (P_CC) is NP-hard.

We show that the problem is NP-hard even for a special case of model (P_CC) with a single supplier. Consider the problem

$$\text{minimize } \sum_{t=1}^T \{f_t y_t + c_t q_t + h_t H_t\} \quad (3.13)$$

$$\text{Subject to } q_t + H_{t-1} - d_t = H_t \quad t = 1, \dots, T \quad (3.14)$$

$$H_0 = 0 \quad (3.15)$$

$$q_t \leq d_{t,T} y_{it} \quad t = 1, \dots, T \quad (3.16)$$

$$\sum_{t=1}^T (\hat{f}_t y_t + \hat{c}_t q_t + \hat{h}_t H_t) \leq C \quad (3.17)$$

$$y_t \in \{0, 1\} \quad t = 1, \dots, T \quad (3.18)$$

$$q_t, H_t \geq 0 \quad t = 1, \dots, T \quad (3.19)$$

We begin with an instance of the knapsack problem (KP) in which we have n items, where item j has value r_j and weight w_j for $j = 1, \dots, n$ (assume without loss of generality that all r_j and w_j are positive). The knapsack problem determines a subset of items $S \subset N = \{1, \dots, n\}$ such that $\sum_{j \in S} w_j \leq C$ (for some positive real number C) with a maximum value of $\sum_{j \in S} r_j$.

Given an instance of KP we create an instance of (P) that equivalently solves KP. We create the instance of (P) as follows.

1. For each item j , create two periods $t_j = 2j - 1$ and $t_{j+1} = 2j$ (thus $T = 2n$).
2. For $j = 1, \dots, n$ set $d_{t_j} = 0$ and $d_{t_{j+1}} = 1$ so we have alternating demands of 0 and 1 in each pair of periods.

3. For $j = 1, \dots, n$ set $f_{t_j} = r_j + K$ for some positive constant K and let $f_{t_{j+1}} = K$ (note that $f_{t_{j+1}} = f_{t_j} - r_j$).
4. For $j = 1, \dots, n$ set $h_{t_j} = 0$ and $h_{t_{j+1}} = M$ for some large positive number M .
5. For $j = 1, \dots, n$ set $\hat{f}_{t_j} = 0$ and $\hat{f}_{t_{j+1}} = w_j$.
6. For $t = 1, \dots, 2n$ set $c_t = \hat{c}_t = \hat{h}_t = 0$.

Items 2 through 4 above imply that an optimal solution will never set both y_{t_j} and $y_{t_{j+1}}$ both equal to one, and the requirement that we meet all demands in problem (P) thus implies that for any j we must have $y_{t_j} + y_{t_{j+1}} = 1$ in an optimal solution. Our assumptions on cost and demands imply that for each j we must therefore produce the demand in period t_{j+1} in either period t_j or t_{j+1} in an optimal solution. We can write our objective function value as $\sum_{j=1}^n \{f_{t_j}y_{t_j} + f_{t_{j+1}}y_{t_{j+1}}\} = \sum_{j=1}^n \{f_{t_j}y_{t_j} + (f_{t_j} - r_j)y_{t_{j+1}}\} = \sum_{j=1}^n \{f_{t_j}(y_{t_j} + y_{t_{j+1}}) - r_jy_{t_{j+1}}\} = \sum_{j=1}^n f_{t_j} - \sum_{j=1}^n r_jy_{t_{j+1}}$.

Thus, this special case of (P) is equivalent to

$$\text{maximize } \sum_{j=1}^n r_j y_{t_{j+1}} \quad (3.20)$$

$$\text{Subject to } \sum_{j=1}^n \hat{f}_{t_{j+1}} y_{t_{j+1}} \leq C \quad (3.21)$$

$$y_{t_{j+1}} \in \{0, 1\} \quad j = 1, \dots, n \quad (3.22)$$

Because $\hat{f}_{t_{j+1}} = w_j$ for $j = 1, \dots, n$, the above is equivalent to our knapsack problem.

3.4.2.2 Proposition 3.2

One can identify whether problem (P-CC) has a feasible solution or not in $O(IT^2)$.

If carbon emissions were minimized instead of costs, the model would reduce to problem (P) and the optimal solution would thus be a tree solution. This is because the emis-

sions function E_{it} for supply mode i in period t (defined below) is concave, and the sum of concave functions $(\sum_{i=1}^I \sum_{t=1}^T E_{it})$ is concave.

$$E_{it}(q_{it}, H_t) = \begin{cases} \hat{f}_i + \hat{c}_{it}q_{it} + \hat{h}_t H_t & \text{if supplier } i \text{ is used in period } t \\ 0 & \text{otherwise} \end{cases} \quad (3.23)$$

As is the case with problem (P), an optimal solution to this problem will satisfy the Zero Inventory and Single Source properties. This problem can be solved to optimality using the dynamic programming algorithm in $O(IT^2)$. Therefore, identifying whether problem (P_CC) has a feasible solution takes $O(IT^2)$. In this case, one would solve the variation of problem (P) which minimizes emissions rather than costs. If the corresponding minimum function value is less than the cap C , the problem at hand has a feasible solution.

3.4.3 Formulation for Carbon Tax Mechanism

Under a carbon tax mechanism, a facility is charged a fee for each unit of CO_2 emitted. Let α denote the tax charged per unit of CO_2 emitted. The corresponding model formulation is called model (P_CT).

$$\text{minimize } \sum_{i=1}^I \sum_{t=1}^T \{(f_{it} + \alpha \hat{f}_i)y_{it} + (c_{it} + \alpha \hat{c}_i)q_{it} + (h_t + \alpha \hat{h}_t)H_t\} \quad (3.24)$$

Subject to (3.2) – (3.6)

The objective function minimizes the total replenishment costs, inventory costs, and emission taxes. Formulations (P_CT) and (P) have the same feasible region, but slightly different cost functions. However, both functions contain the same mathematical structure. Therefore, an optimal solution to (P_CT) (as discussed above for (P)) will satisfy the Zero

Inventory and Single Source properties. The same dynamic programming algorithm can thus be used to solve this problem in $O(IT^2)$ time in the worst case.

3.4.4 Formulation for Carbon Cap and Trade Mechanism

A carbon cap is imposed on the facility under a carbon cap-and-trade mechanism. However, a carbon market also exists, which allows the facility to sell unused carbon credits at a profit, or to purchase carbon credits if needed to satisfy customer demand (the European Union Emissions Trading system was the first large emission trading scheme in the world). Let e_t^+ (e_t^-) denote the amount of carbon credit purchased (sold) in period t . We denote the market price per unit of carbon by p . The following model minimizes total system costs under a carbon cap-and-trade mechanism. We refer to this as model (P_CCT).

$$\text{minimize } \sum_{i=1}^I \sum_{t=1}^T \{f_{it}y_{it} + c_{it}q_{it} + h_t H_t\} + p \sum_{t=1}^T (e_t^+ - e_t^-) \quad (3.25)$$

Subject to (3.2) – (3.6)

$$\sum_{i=1}^I \sum_{t=1}^T (\hat{f}_i y_{it} + \hat{c}_i q_{it} + \hat{h}_t H_t) + \sum_{t=1}^T e_t^- \leq C + \sum_{t=1}^T e_t^+ \quad (3.26)$$

$$e_t^+, e_t^- \geq 0 \quad \forall t \quad (3.27)$$

Note that in an optimal solution of (P_CCT), constraints (3.26) are necessarily binding. For any solution such that the left-hand side is less than the right-hand side, we can decrease the objective (assuming $p > 0$) by increasing the value of one or more e_t^- variables. We can thus re-write constraint (3.26) as follows: $\sum_{i=1}^I \sum_{t=1}^T (\hat{f}_i y_{it} + \hat{c}_i q_{it} + \hat{h}_t H_t) - C = \sum_{t=1}^T (e_t^+ - e_t^-)$. We can then substitute $\sum_{t=1}^T (e_t^+ - e_t^-)$ out of the objective function of (P_CCT) as follows:

$$\min \sum_{i=1}^I \sum_{t=1}^T \{f_{it}y_{it} + c_{it}q_{it} + h_t H_t\} + p \left\{ \sum_{i=1}^I \sum_{t=1}^T (\hat{f}_i y_{it} + \hat{c}_i q_{it} + \hat{h}_t H_t) - C \right\} \quad (3.28)$$

Next, we set $\tilde{f}_{it} = f_{it} + p\hat{f}_i$, $\tilde{c}_i = c_{it} + p\hat{c}_i$, and $\tilde{h}_t = h_t + p\hat{h}_t$ for all $i = 1, \dots, I$ and $t = 1, \dots, T$. We can re-arrange the terms in the objective function to obtain:

$$\text{minimize } \sum_{i=1}^I \sum_{t=1}^T \{\tilde{f}_{it}y_{it} + \tilde{c}_{it}q_{it} + \tilde{h}_t H_t\} - pC \quad (3.29)$$

Note that in this objective function, pC is a constant, and so we can remove it from the objective without loss of optimality. After this transformation, the feasible regions of (P) and (P_CCT) are identical, as is the mathematical structure of the objective function in both cases. Therefore, we can use the dynamic programming approach to solve this problem in $O(IT^2)$ time.

3.4.5 Formulation for Carbon Offset Mechanism

A carbon cap is imposed on the facility under a carbon offset mechanism, and a carbon market also exists that allows the facility to purchase carbon credits. However, under a carbon offset mechanism, a facility cannot sell unused carbon credits. The resulting problem formulation, which we denote by (P_CO), is as follows.

$$\text{minimize } \sum_{i=1}^I \sum_{t=1}^T \{f_{it}y_{it} + c_{it}q_{it} + h_t H_t\} + \sum_{t=1}^T p e_t^+ \quad (3.30)$$

Subject to (3.2) – (3.6)

$$\sum_{i=1}^I \sum_{t=1}^T (\hat{f}_i y_{it} + \hat{c}_i q_{it} + \hat{h}_t H_t) \leq C + \sum_{t=1}^T e_t^+ \quad (3.31)$$

$$e_t^+ \geq 0 \quad \forall t \quad (3.32)$$

The objective function minimizes total costs, including the cost of purchasing offsets. A voluntarily carbon offset market exists in the US, wherein a variety of consumers buy offsets, including individuals, businesses, nonprofit organizations, governments, universities, etc. Major motivations for purchasing offsets are corporate responsibility and public relations [101]. Observe that (P_CC) corresponds to the special case of (P_CO) in which p is a very large number. Because (P_CC) is NP-hard, the same therefore holds for (P_CO).

3.4.6 Summary of Model Formulations

We propose four extensions of Model (P) which capture the impact of carbon regulatory mechanisms on supplier and transportation mode selection decisions in the supply chain. The mechanisms we investigate are carbon cap, carbon tax, carbon cap-and-trade and carbon offset. The models for carbon tax and carbon cap-and-trade mechanisms are easily solvable. We present a dynamic programming algorithm in the Appendix which solves these problems in polynomial time. The models for carbon cap and carbon offset mechanisms are NP-hard. In our numerical analysis, we use CPLEX to solve small instances of these problems. The two NP-hard models imply that solution times, when the problems are solved using standard MILP solvers, will be impractical as the problem sizes grow. Both models include a single carbon cap constraint. In the absence of this constraint, the problems are shown to be polynomially solvable. Thus, relaxation of this constraint leads to easily solvable subproblems. Considering this fact, one can develop Lagrangian relaxation-based algorithms to generate good lower and upper bounds for these difficult problems. It is also possible to generate upper bounds for these models by remov-

ing the carbon cap constraint, and changing the objective to minimizing the total carbon emissions. However, we do not provide details for these algorithms since this is beyond the scope of this paper, which focuses on demonstrating how carbon regulatory mechanisms influence costs and emissions in a biofuel supply chain.

3.5 Data Collection and Analysis

In this section we discuss our data collection and analysis. The models discussed above consider inventory replenishment decisions for a single commodity. The product on which we focus in this analysis is forest residue. Due to its physical characteristics of bulkiness, barge, rail, and truck may be used for shipping. The choice of the transportation mode depends on the travel distance and the associated level of carbon emissions. Forest residues are raw materials that can be used by biorefineries to produce cellulosic ethanol. We assume that such a biorefinery can meet its demand for forest residues using suppliers located nearby, or other suppliers around the nation. Canada is rich in forest, and therefore Canadian companies can be potential suppliers of forest residues. These suppliers may use rail or barge to ship their products to the US.

Table 3.3 summarizes some of the parameters our study used to generate data related to suppliers. We use uniform distributions to randomly generate transportation distances and variable replenishment costs. The selection of purchasing costs (at the roadside) is motivated by the following fact. The US Department of Energy (US DOE) estimates that for a price ranging from \$20 to \$80 per dry ton at the roadside, quantities of forest biomass currently available for production of biofuels would vary (at the national level) from 33

to 119 million dry tons (MDT) annually. However, for the biofuels industry to thrive, high levels of biomass should be available at lower prices. The US DOE is investigating a number of technology improvements, such as pre-processing of biomass, that would reduce these prices in the near future [42]. The data in the table indicates a decrease in purchasing costs as we consider suppliers located further away. This is mainly because the pool of available suppliers increases as we consider suppliers located further away. A larger supplier pool provides the facility with more competitive prices.

Table 3.3

Input Data Generation

Distance (in miles)	Number of Suppliers	Purchasing Costs (in \$)
U[5-25]	5	U[40-42]
U[25-100]	5	U[38-40]
U[100-500]	5	U[36-38]
U[500-1,000]	15	U[34-36]
U[1,000-1,500]	15	U[30-35]

Table 3.4 presents the scheme we use to assign transportation modes to suppliers. We assume that suppliers located within 25 miles of the facility will use truck shipments only. The suppliers located between 25 and 100 miles have access only to truck shipments with a 50% chance, or both truck and rail by the remaining 50% chance. Thus, if both truck and rail are available for a supplier, it represents two different replenishment modes for our models. The percentage of usage between these two replenishment modes is determined as a result of the models. Similarly by a 50% chance, the suppliers located between 100 and

500 miles have access to both truck and rail; or all modes of truck, rail and barge by the remaining 50% chance. As distance increases, the percentage of suppliers that have access to all modes of transportation increases. We use this scheme to also capture the reality that some suppliers may not have access to barge or rail due to the limited rail and barge infrastructure.

Table 3.4

Transportation Mode Assignment Scheme

Distance (in miles)	Truck (in %)	Truck&Rail (in %)	Truck&Rail &Barge (in %)
U[5-25]	100	0	0
U[25-100]	50	50	0
U[100-500]	0	50	50
U[500-1,000]	0	30	70
U[1,000-1,500]	0	0	100

Table 3.5 presents the scheme we use to generate variable costs for truck transportation. Variable transportation costs depend on the distances traveled and the quantities shipped; therefore, the unit costs presented in the table are charged per mile and per ton traveled. The intervals that we use to calculate costs were generated by analyzing data made available by the Agricultural Marketing Service (AMS) of the US Department of Agriculture. The AMS publishes quarterly reports which present truck transportation trends for agricultural products in different regions of the US [2]. The data in the table presents the average national rates charged during the last six quarters, beginning in January 2011.

Table 3.5

Variable Costs for Truck Transportation

Distance (in miles)	Unit cost (\$/(mile * ton))
[0 – 25]	U[0.0801-0.2401]
[25 – 100]	U[0.0457-0.1857]
> 100	U[0.0346-0.1746]

We randomly generated the fixed cost and variable costs for rail shipments. To identify these costs, we investigated the web-sites of Class I railway companies, such as CSX Transportation and BNSF Railway. These companies provide quotes (in \$ per rail car) for different products and different origin-destination pairs. We used the data provided for forest products to derive regression equations. The independent variable in these equations is the distance traveled, and the dependent variable is the price charged per rail car. The value of R^2 for these equations was 70% and the p-values of all independent variables were smaller than 0.1%. These values indicate that transportation distance has a great impact on the price charged. Based on these results, we decided to generate the fixed transportation cost using the following uniform distribution $U[\$2,500, \$3,500]$ (in\$/shipment), and the unit variable cost using the following uniform distribution $U[\$0.008, \$0.2]$ (in \$/(mile*ton)).

We also use data from AMS publications to derive transportation costs for barge. Based on this data, we generated the variable transportation cost using the following uniform distribution $U[\$0.100, \$0.112]$ (in \$/(mile*ton)).

Our case study also considers the in-transit inventory costs. This is very important as the travel time differs substantially in different transportation modes. To calculate these

costs, we first identify the travel time (in number of days) per shipment using information about travel distance and the average speed of the transportation vehicle. We assume the average speed for a truck is 65 mph, for rail 18 mph, and for barge 6.25 mph; vehicles operate for a total of 16 hours per day, and vehicles operate for 350 days per year. The annual unit inventory holding cost (in \$ /ton) is set equal to 20% of the unit purchase cost. We then use trip duration and unit inventory holding costs to calculate the inventory holding costs per ton shipped.

In our optimization model (P), the total unit replenishment cost for supplier i , c_i (in \$/ton), is the sum of the unit purchasing, transportation and in-transit inventory holding costs. The unit purchasing cost for supplier i is charged per ton of product replenished. Since variable transportation costs are provided in \$(/mile*ton), we multiply a supplier's transportation distance by the variable transportation cost in order to calculate a variable transportation cost per ton shipped from supplier i .

We consider a time horizon of $T = 12$ months, with $t = 1, \dots, 12$. We assume that demand for forest residues in each month is uniformly distributed between 80,000 and 100,000 tons. The conversion rate is estimated to be 60 gallons of ethanol per ton of residues [14]. Thus, the production capacity of the facility ranges between 57.6 and 72 MG. Thus, the production capacity of the facility ranges between 57.6 and 72 MG.

Let us now discuss the approach we used to collect emissions related data. In order to calculate emissions from material handling, we assume that loading and unloading of trucks, rail cars and barge are completed using loaders. The maximum allowable load for trucks (30 tons) is much smaller than rail (100 tons) or barge (1,500 tons) [58]. For a 30

ton truck, the loading time of forest residue bundles takes about 45 to 50 minutes, and unloading takes about 50 to 55 minutes [82]. We assume that a loader with horsepower of 140 and fuel consumption of 0.0217 gals/(hp*hr) is used [72]. It is estimated that the consumption of one gallon of diesel fuel emits 9,922 grams of CO₂ [32]. We assume that all modes of transportation use the same loading and unloading equipment, and therefore, we calculate the fixed emissions in tons of CO₂ per ton loaded and unloaded as follows: (duration of loading and unloading activities) * 0.0217 * 140 * 9,922 * 10⁻⁶ / 30. Loading and unloading times are given in hours.

We also consider emissions due to storage of forest residues. A study by Wihersaari [108] indicates that greenhouse gas emissions from storage can be much greater than emissions from the transportation of forest residues. The study indicates that “Greenhouse gas emissions are probably methane, when the temperature in the fuel stack is above the ambient temperature, and nitrous oxide, when the temperature is falling and the decaying process is slowing down.” Following this study, we consider emissions due to storage and inventory to be uniformly distributed between 5 and 10 kg per ton of forest residues held in inventory every month.

We use the method developed by Hoen et al. [43] to calculate emissions from transportation. Hoen et al. [43] provide the following equations to calculate emissions for transportation via truck, rail and barge. In these equations, transportation distance D is in kilometers, the load weight w is in kilograms, v denotes volume, and ρ denotes density.

$$e_{truck} = v * \max(250, \rho) * (0.0002089 + 0.00003143D) \quad (3.33)$$

$$e_{rail} = 2.223 * 10^{-5} * D * w \quad (3.34)$$

$$e_{barge} = 1.3904 * 10^{-5} * D * w \quad (3.35)$$

3.6 Observations from Experiments

In this section, we discuss important observations related to the impact that different carbon regulatory mechanisms have on costs, emissions, and transportation mode decisions in this supply chain.

Below, we summarize the results from solving a wide variety of problems we generated using our data. Note that each point in any of the graphs represents the average results from solving 10 different randomly generated problem instances corresponding to the settings described for that particular problem.

Through our experiments we are also interested in investigating the impact that technological improvements may have on reducing carbon emissions in the supply chain. Technology improvements, for the purposes of this paper, correspond to improvements in fuel efficiency for transportation vehicles. These tests are motivated by a recent announcement from the US Department of Energy to fund nine projects (for a total of \$187 million) that propose improvements in the fuel efficiency of heavy duty trucks and passenger vehicles [98].

We define Technology 1 to be the base case scenario (i.e., business as usual). Due to improvements in fuel efficiency for Technologies 2, 3, and 4, carbon emissions are

reduced by 10%, 20%, and 30%, respectively, as compared to Technology 1. Improving the fuel efficiency of transportation vehicles doubtlessly does not come free and will require investments. However, identifying these costs is not easy and not relevant to this paper, so we do not apply an arbitrary cost. Thus, our sensitivity analysis (and cost savings estimated) to identify the maximum investments in these technologies in order to break even.

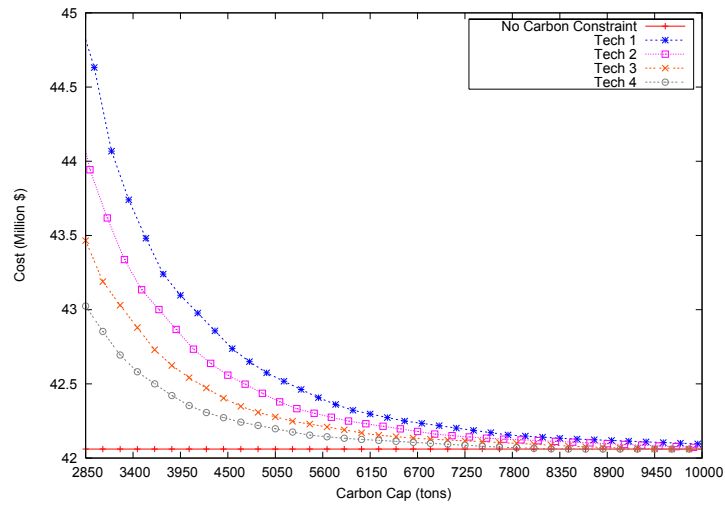
We solved all associated mixed integer programming models using the ILOG/ CPLEX commercial solver.

3.6.1 Carbon Cap

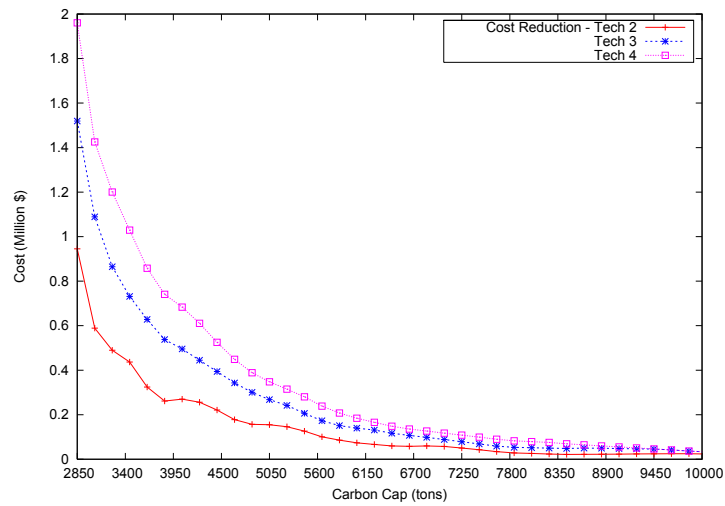
Figure 3.3(a) illustrates the relationship between costs and emissions under a carbon cap mechanism. We consider an annual carbon cap which varies from 2,850 tons to 10,000 tons. We did not investigate smaller cap values because these led to infeasible problem instances for model (P_CC).

Five curves appear in Figure 3.3(a). The straight line at the bottom shows the total costs if no carbon cap exists. The total emissions in this case equal 7,145 tons. The top curve (Technology 1) represents the cost-carbon relationship when the supplier replenishes inventories using existing transportation vehicles with a relatively low fuel efficiency. The remaining curves correspond to the technological improvements in vehicle fuel efficiency as described above.

Figure 3.3(a) indicates a decrease in total system costs as the carbon cap increases. The decrease in cost is steeper when the carbon cap is tighter. As the carbon cap increases, the



(a) Total Costs



(b) Savings compared to Tech 1

Figure 3.3

Carbon Cap Mechanism - Total Costs

curves become flatter and converge to the no-cap solution. At low levels of the carbon cap, the cost of maintaining operations (in order to satisfy demand) is higher compared to high levels of the carbon cap. The difference in costs between these technologies increases as the carbon cap decreases. This indicates that the benefits from technology improvements become more evident as the carbon cap gets tighter.

Figure 3.3(b) displays the amount of cost savings achieved by using better technologies instead of the base-case technology. This graph provides insights about the value that each technology generates for the facility, at different levels of the carbon cap. One can use these cost savings to identify when (under what cap) it becomes worth investing in any technology improvements. Note that, the optimization models used find a minimum cost solution. Such a solution identifies changes in the operational decisions, such as supplier and transportation mode selection. Thus, the cost savings presented in these graphs result from the deployment of new technologies as well as due to operational changes.

Figure 3.4 shows that, under a carbon cap mechanism, the amount of carbon emitted closely follows the carbon cap. As the carbon cap increases, the curves become flatter. The reason for the linear increase in emissions for tight caps is that there is no motivation for a facility to use less carbon than what is allowed by the cap. Technology improvements allow the facility to perform the same operations at a lower level of emissions. However, the facility can further reduce costs by exploring a larger pool of suppliers who are not necessarily located nearby (see Figure 3.5). Therefore, total emissions remain the same, and total supply chain costs decrease with technology improvements.

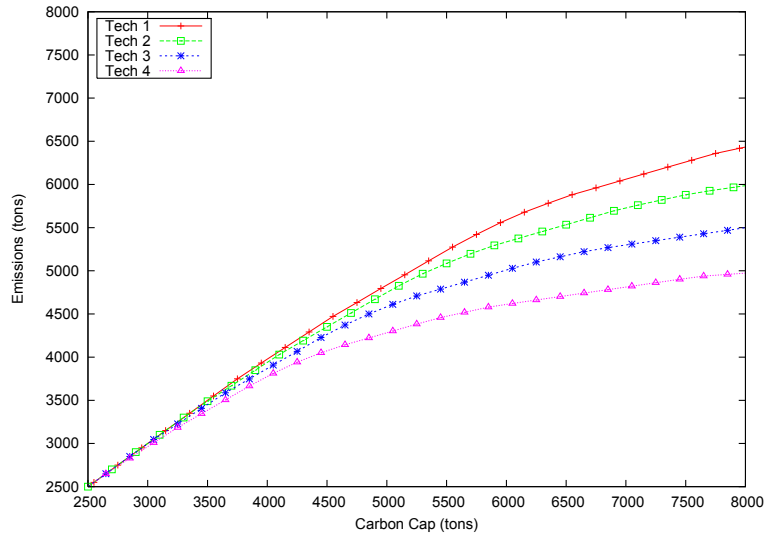


Figure 3.4

Carbon Cap Mechanism - Total Emissions

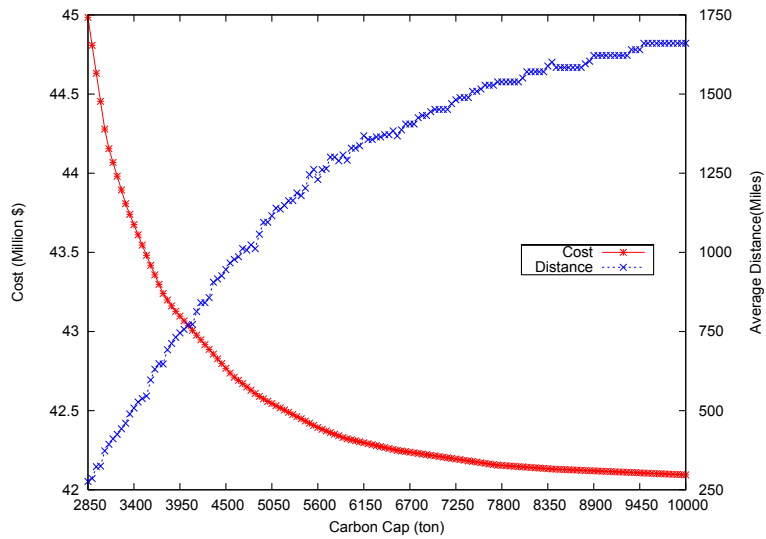
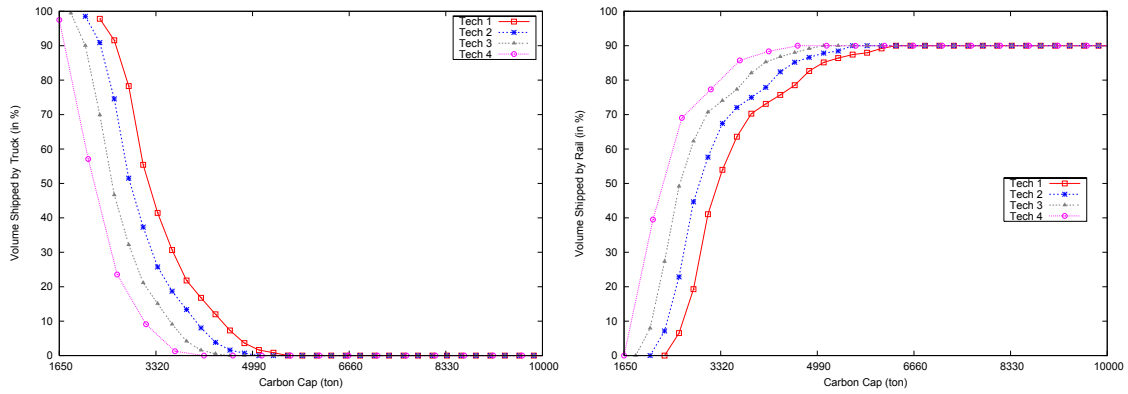


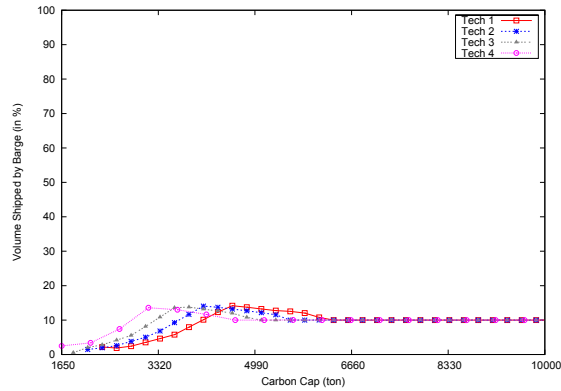
Figure 3.5

Carbon Cap Mechanism - Tech 1 - Costs and Distances



(a) Road

(b) Rail



(c) Barge

Figure 3.6

Carbon Cap Mechanism - Transportation Mode Percentages

A carbon cap mechanism impacts transportation mode selection decisions. Figure 3.6 shows the percentage use of each transportation mode under each technology. Intuitively, selection of truck transportation is not anticipated at low levels of the carbon cap because trucks have higher emissions per mile and per ton compared to rail and barge. However, Figure 3.6(a) indicates that when the carbon cap is small, inventories are primarily replenished using truck shipments from local suppliers. A company minimizes emissions by minimizing traveled distance. As the carbon cap increases, other modes of transportation are explored (see Figure 3.6(b) and Figure 3.6(c)). The volume shipped using rail transportation increases at a faster rate than the volume shipped by barge because only a small number of suppliers have access to barge.

We highlight a few additional observations from comparing the graphs in Figure 3.6. First, technology improvements clearly impact transportation mode selection decisions and related costs. As the technology improves, the volume shipped using cost efficient transportation modes increases for tight carbon caps. For example, under Technology 1, at a carbon cap of 3,350 tons, the volume shipped using road is 41%, rail 54%, and barge 5% of the total. At the same level of carbon cap, under Technology 3, the volume shipped by road decreases to 15%, rail increases to 75% and barge increases to 10% of the total. These modal shifts result in lower transportation costs.

Second, all the curves in these figures are steeper at low levels of the carbon cap. These curves become flat and overlap when the cap is over 5,000 tons. This behavior indicates that the system is very sensitive and reacts fast to changes in the carbon cap when the cap is

tight. At high levels of the carbon cap, the system stabilizes where 90% of the total volume is shipped using rail, and 10% using barge transportation.

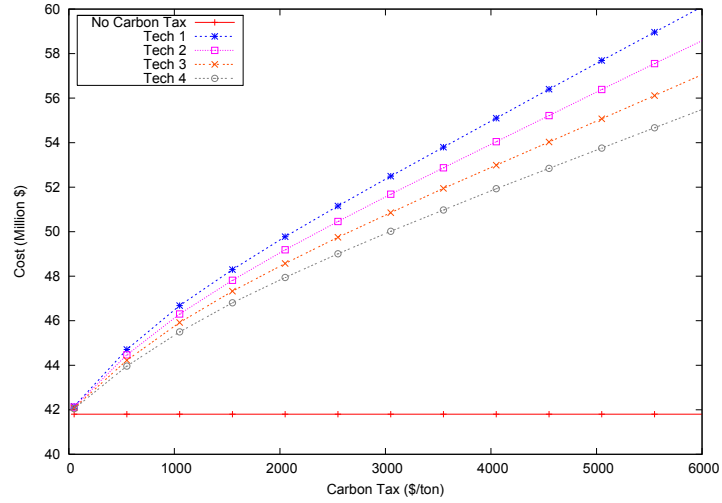
In summary, a carbon cap is an effective tool to reduce emissions from transportation activities in the supply chain. Improvements in fuel efficiency of transportation vehicles give companies room to make better transportation-related decisions. These improvements have an impact on operational costs, but do not necessarily lead to reductions in emissions (below what is required) under a carbon cap policy.

3.6.2 Carbon Tax

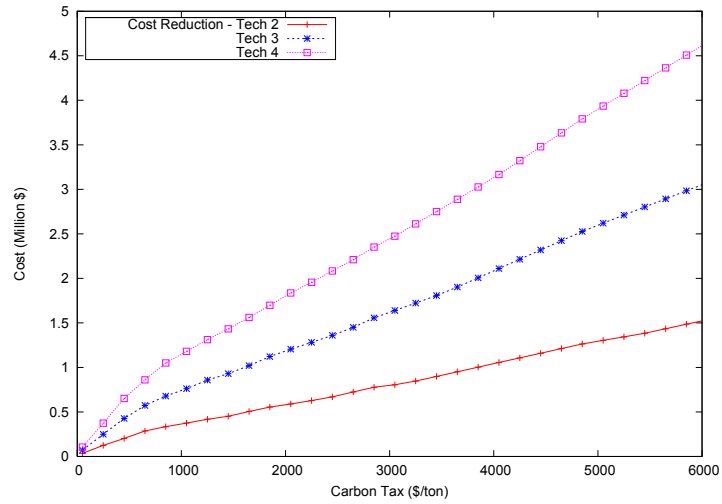
Figure 3.7(a) shows the relationship between costs and the carbon tax rate (in \$/ton). We use tax rate which vary from \$0 to \$6,000 per ton of CO₂ emitted. The \$6,000 per ton tax is a very high value, as related studies discuss tax rates which are not higher than \$70 per ton [18]. However, the goal here is to analyze the behavior of the systems and identify trends which in fact do become apparent at high levels of tax.

Figure 3.7(a) shows that the relationship between tax and carbon cap is almost linear since we consider a fixed tax rate for every unit of carbon emitted. The gap between the lines which represent different technologies widens as the tax rate increases indicating that cost savings by using fuel efficient technologies increase with the tax rate. Figure 3.7(b) presents cost savings achieved by switching from technology 1 to fuel-efficient technologies.

Figure 3.8 shows the relationship between total emissions and carbon tax rate. As the tax rate increases, we initially see a drastic decrease in total emissions. This reflects the fact



(a) Total Costs



(b) Savings compared to Tech 1

Figure 3.7

Carbon Tax Mechanism - Total Costs

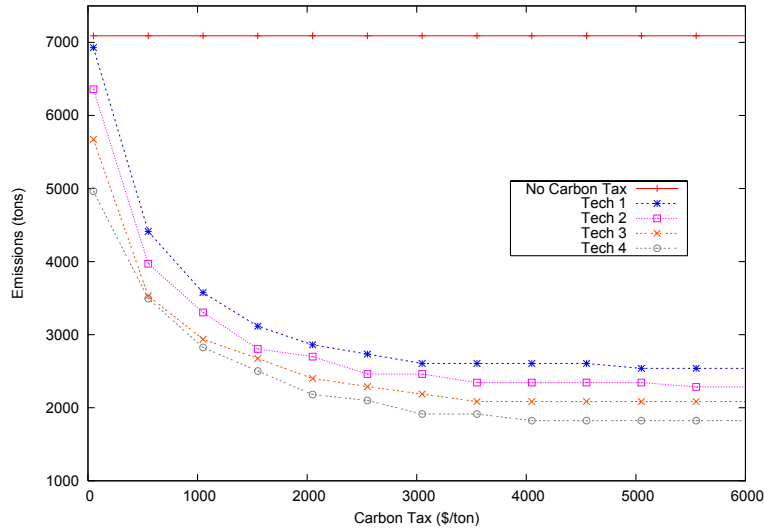


Figure 3.8

Carbon Tax Mechanism - Total Emissions

that the company seeks operational changes to reduce emissions and consequently costs. However, the curve eventually flattens since, given the supply chain structure, there exist no more operational changes which impact emissions.

The results in Figure 3.9 indicate that the average distance traveled decreases as the carbon tax increases. However, this change does not occur linearly with the increase in taxes. We observe that small tax rates will not force firms to change their behavior. Long travel distances and high emissions prevail for tax rates smaller than \$100. Figure 3.10 illustrates the shifts in transportation mode selection decisions as the carbon tax increases, and as the fuel efficiency of transportation vehicles improves. When the carbon tax is relatively small, rail and barge transportation are used to replenish inventories with suppliers located further away. As the tax increases, road shipments from local suppliers increase. The shape of the curves for different technologies is somewhat similar to the shapes in Fig-

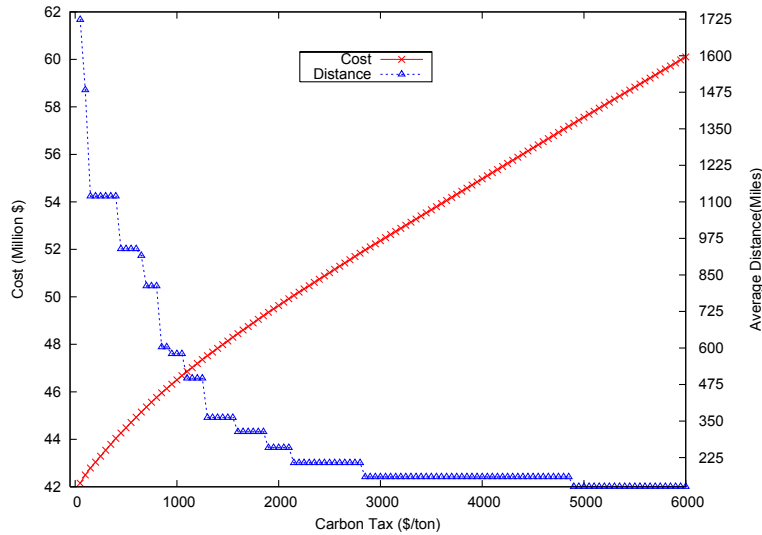


Figure 3.9

Carbon Tax Mechanism - Tech 1 - Costs and Distances

Figure 3.6. However, the curves in Figure 3.10 are step functions, which indicate that mode changes occur at discrete points in the tax rate. The graphs in Figure 3.6, on the other hand, indicate a continuous reaction to changes in the carbon cap level. This continuous reaction is mainly due to the carbon cap constraint which forces the supply chain to identify operational changes (such as supplier selection) that result in lower emissions at each level of the cap.

3.6.3 Carbon Cap and Trade

In this section we present results from experimenting with the carbon cap and trade mechanism. We assume that the company trades emission credits at the market price we determine, and there is no limit on the amount of carbon traded at any of the market prices.

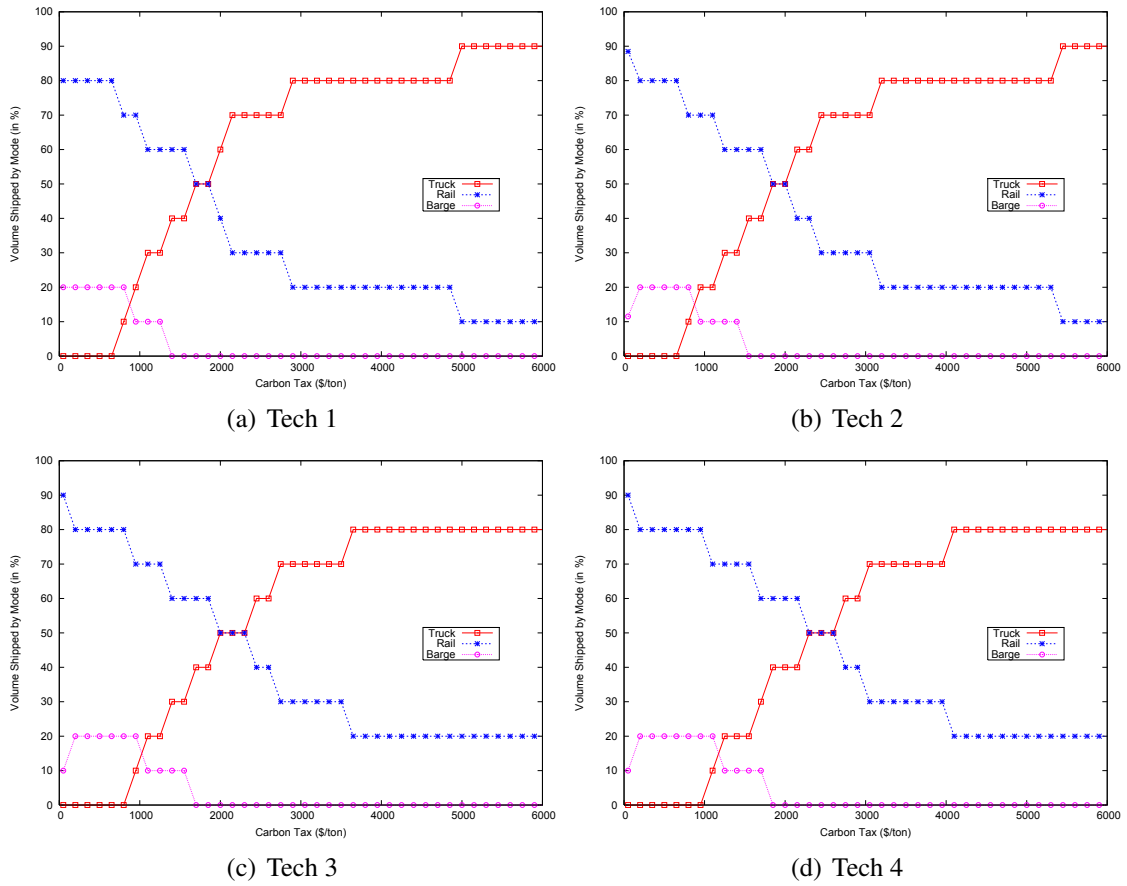


Figure 3.10

Carbon Tax Mechanism - Transportation Mode Percentages

Figure 3.11 shows the effect that a carbon cap and trade mechanism has on total costs at different values of the carbon credit market price. As the market price of carbon increases, the curves become steeper, indicating that changes in the carbon price have a greater impact on total system costs.

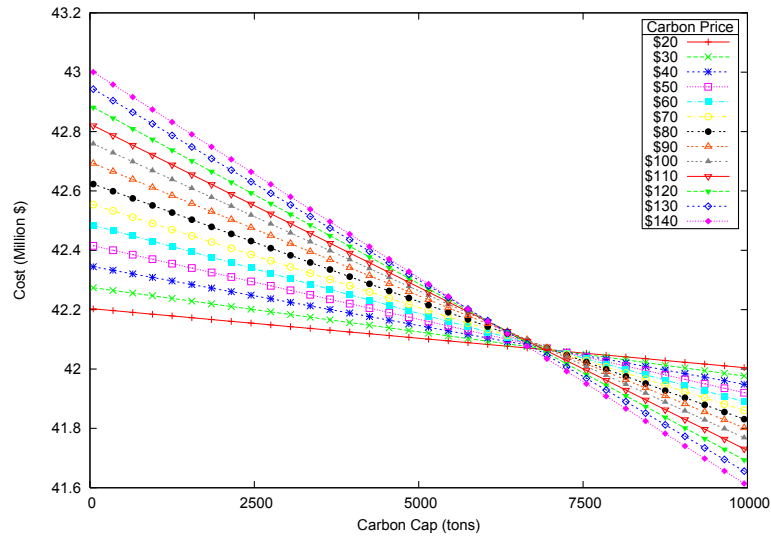


Figure 3.11

Carbon Cap and Trade Mechanism - Total Costs

Comparing the results in Figure 3.4 and Figure 3.12 shows the relationship between the emissions and carbon cap levels in two different systems. Under a carbon cap mechanism, emissions initially increase linearly with the carbon cap. Emissions do not further increase beyond a certain level of the carbon cap. However, under a carbon cap and trade mechanism, the emissions level is constant, in spite of changes in the carbon cap level. This is because, as the carbon cap increases, the facility can make a profit by selling carbon credits to the market. The existence of a carbon market is a motivation for the firm to

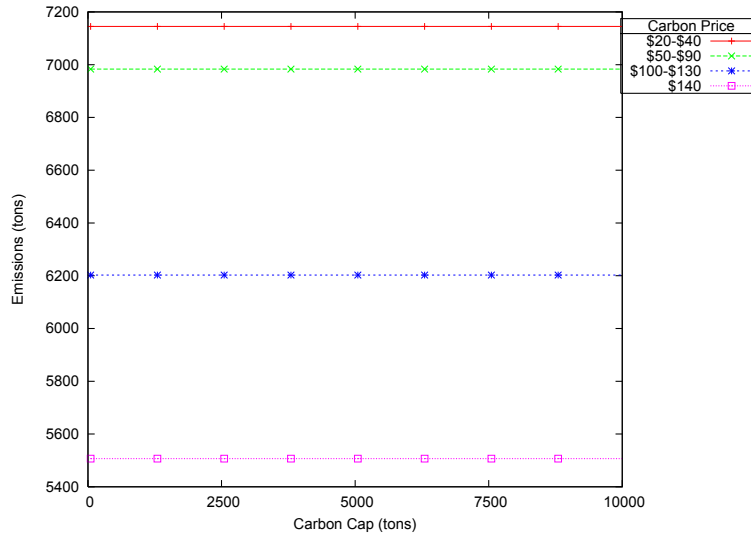
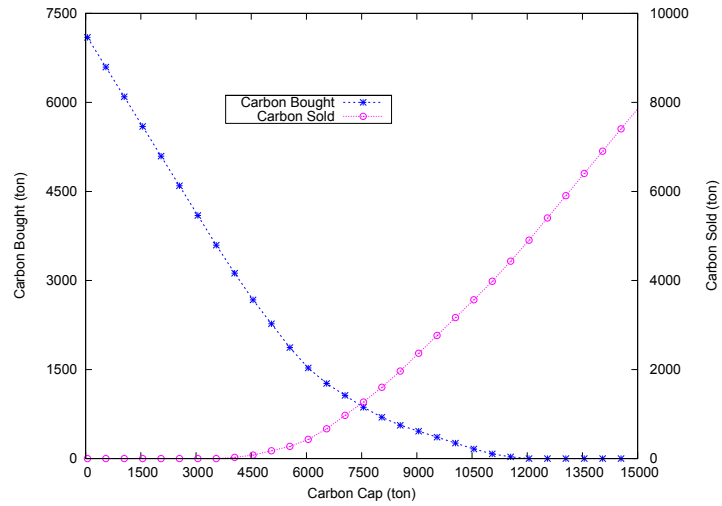


Figure 3.12

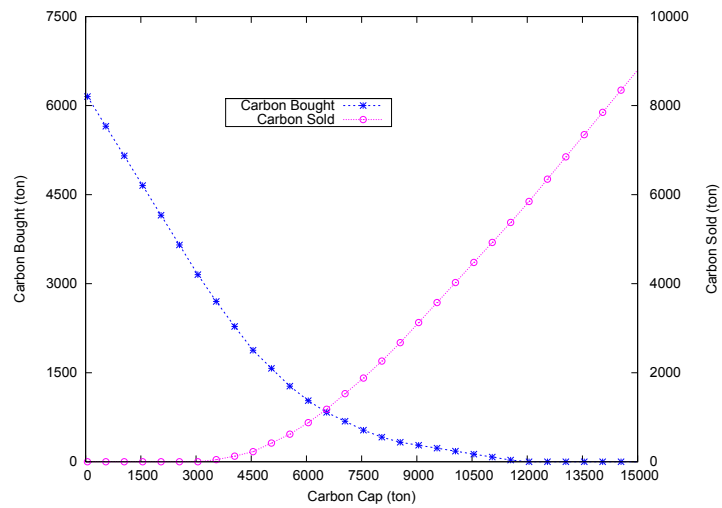
Carbon Cap and Trade Mechanism - Total Emissions

improve emissions performance. Obviously, the goal is to minimize the costs of replenishment and emissions. Therefore, the facility makes supplier selection decisions by looking at the tradeoffs between emission-related costs/benefits and transportation costs.

The market price of carbon effects emission levels. The straight lines in Figure 3.12 indicate that emissions are smaller at higher levels of the carbon market price. Increasing market prices provide strong motivation for the facility to reduce emission levels, and as a result, reduce system costs either by selling unused carbon credits or by reducing the amount of carbon purchased in order to maintain operations. Figure 3.13 shows the amount of carbon purchased and sold at different levels of carbon cap. Figure 3.13(a) shows this relationship when the market price is \$40 per ton, while Figure 3.13(b) does it for a market price of \$100 per ton.



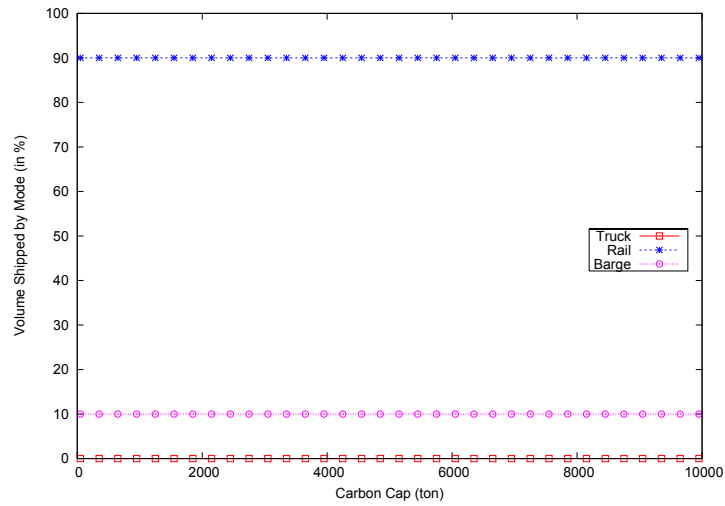
(a) \$40



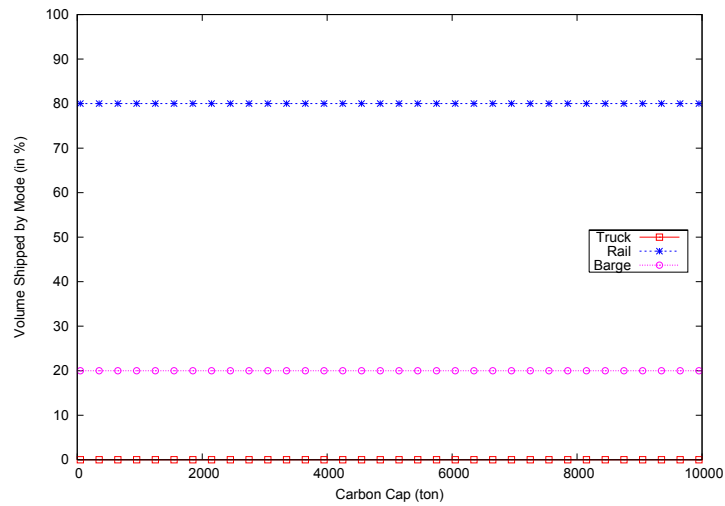
(b) \$100

Figure 3.13

Carbon Cap and Trade Mechanism - Average Carbon Bought and Sold



(a) \$20-\$40



(b) \$50-\$140

Figure 3.14

Carbon Cap and Trade Mechanism - Transportation Mode Percentages

At a higher market price, the firm will sell more and purchase less carbon to satisfy customer demand. We assume that the firm is able to emit less carbon by changing its operations decisions (e.g., by using local suppliers). At a higher carbon price, increased replenishment costs are offset by the benefit of selling carbon credits saved to the market. The slope of the line corresponding to the carbon credits sold is different under the two different market prices. The line is steeper when market price is \$40 per ton, indicating that changes in the carbon cap will have a greater impact on the amount of carbon credits purchased when the market price is lower. At higher market prices, the line that represents carbon sales is steeper, indicating that a small change in the carbon cap will have a greater impact on the amount of carbon sold. Note that above a certain carbon cap level (3,800 tons for carbon price of \$40) the facility purchases carbon in certain periods and sells carbon in other periods in order to balance its operations while minimizing system-wide costs.

Under a carbon cap and trade mechanism, transportation mode selection is only determined by the carbon price (Figure 3.14). For a fixed carbon price, the percent of volume shipped using each transportation mode is not affected by the level of the carbon cap. For example, between \$20 and \$40 per ton, 90% of the volume is received by rail, and 10% by barge. As the market price becomes more than \$50 per ton, the volume shipped by barge increases to 20%.

3.6.4 Carbon Offset

Figure 3.15 displays the relationship between the carbon cap and total system cost at different levels of the market offset price. The carbon offset amount and corresponding

prices impact total system costs. At low levels of carbon cap, the facility offsets the excess carbon used in order to maintain operations. As the offset price increases, the facility faces higher carbon offset costs. The curves belonging to different offset prices approach one another as the carbon cap increases and eventually (when the cap is loose) converge to the same total system cost (which corresponds to the total cost when there is no carbon cap). These lines are also steeper for smaller carbon cap levels indicating that system costs are more sensitive to changes in the offset price at smaller levels of carbon cap.

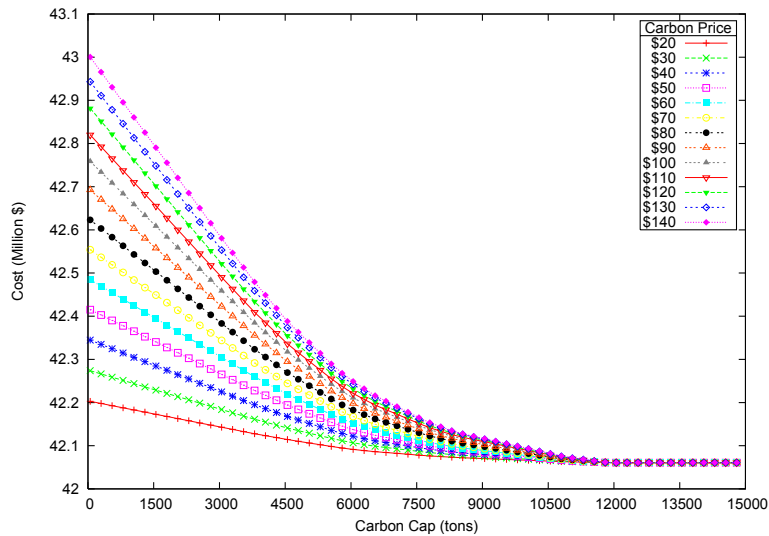


Figure 3.15

Carbon Offset Mechanism - Total Costs

It is interesting to compare the curves in Figure 3.4, Figure 3.12, and Figure 3.16. The shape of the emissions curves differ according to the carbon regulatory mechanisms. At a low carbon offset price (such as \$20-\$40), the level of emissions under the carbon offset mechanism is constant. This is similar to the behavior of the supply chain in a carbon cap

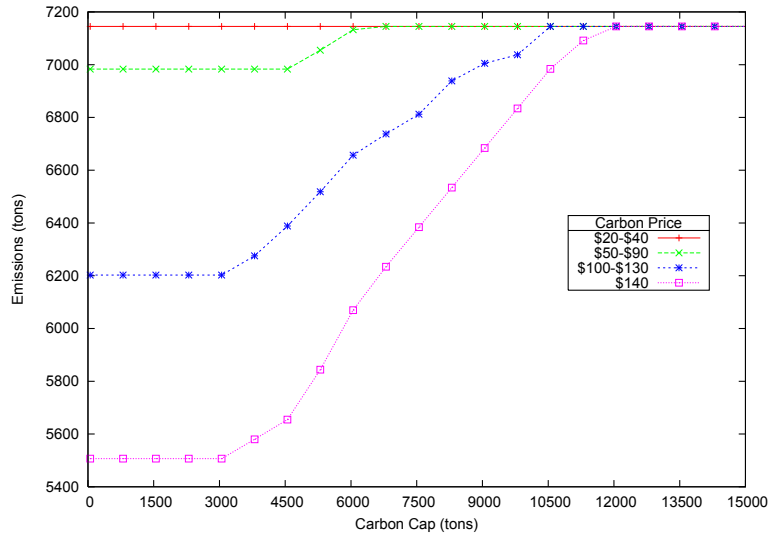


Figure 3.16

Carbon Offset Mechanism - Total Emissions

and trade mechanism. However, as the carbon offset price increases, the level of emissions decreases, especially when the carbon cap is tight. For example, when the offset price is between \$50 and \$90 per ton, emissions are constant up to a carbon cap level of 4,650 tons (similar to Figure 3.12). As the carbon cap increases, emissions also increase. Since the facility cannot sell unused carbon credits, there is no motivation to reduce carbon emission below the requirements set by the cap. Therefore, emission amounts gradually climb to the levels with no carbon cap. The graphs in Figure 3.17 show the amount of carbon offset as the carbon cap increases at two different levels of offset prices.

Figure 3.18 shows the volume shipped by each transportation mode as a function of the carbon cap, and for different levels of carbon offset price. When the offset price is between \$20 and \$40 per ton, rail ships 90%, and barge ships 10% of the total volume. Although the level of carbon cap increases, the volume shipped using each transportation mode does not

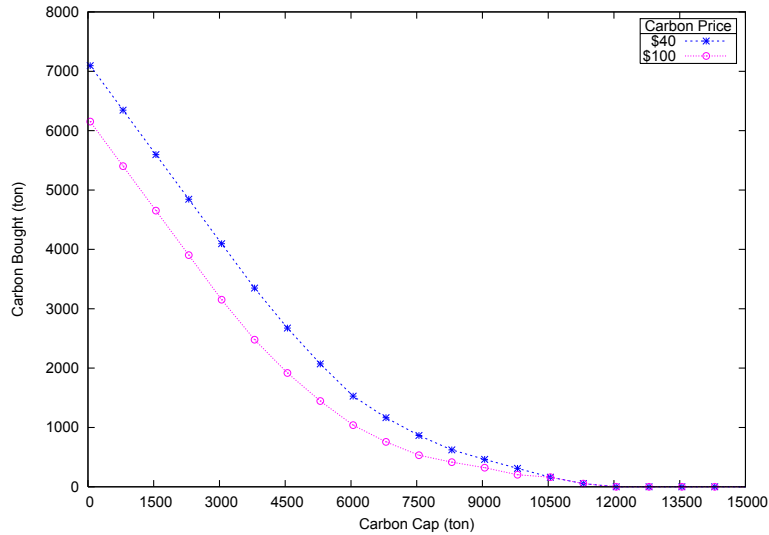
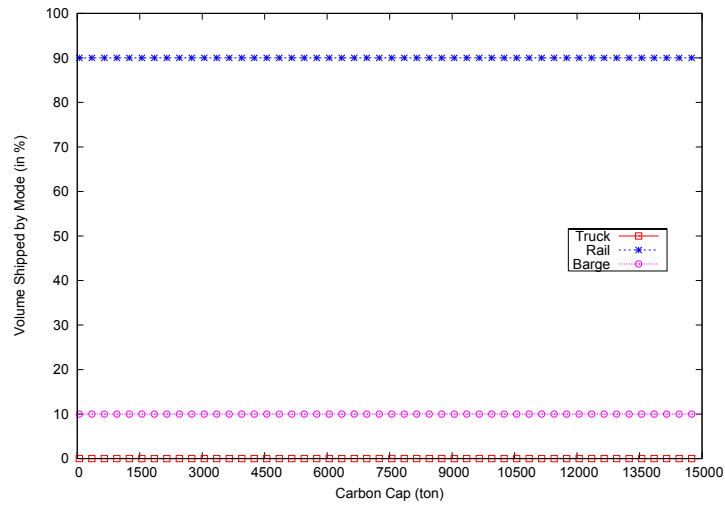


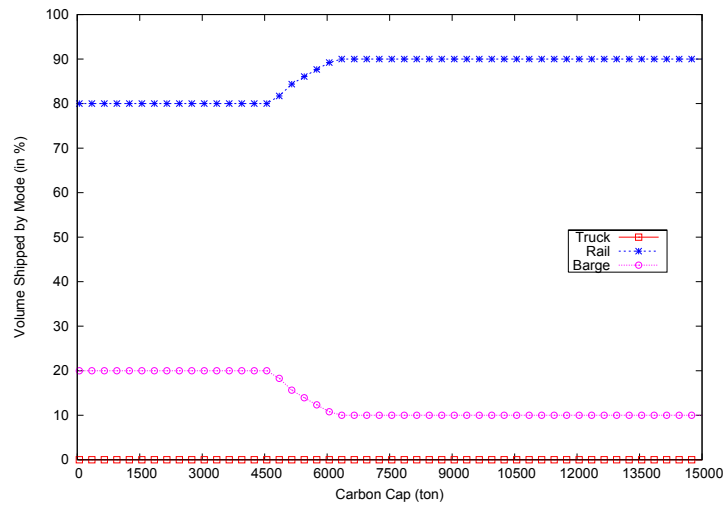
Figure 3.17

Carbon Offset Mechanism - Average Carbon Bought

change. This is similar to the carbon cap and trade mechanism. When the offset price is greater than \$50 per ton, barge accounts for a constant 20% of the total volume shipped and rail accounts for 80% (for low carbon cap levels). When the cap becomes 4,650 tons, the volume shipped by barge decreases to 10%, allowing the remaining shipments be received by rail. This is a point in the system where the facility does not have to make major operational changes to cope with the carbon cap. Since the facility cannot sell unused carbon credits on the market, there is no motivation to limit emissions. We observe that the distribution of volume shipped across different transportation modes (for high carbon caps) has the same pattern as in a carbon cap mechanism. In summary, for small carbon caps, this system behaves as it would under a carbon cap and trade mechanism; and for high carbon caps, the system behaves as it would under a carbon cap mechanism.



(a) \$20-\$40



(b) \$50-\$140

Figure 3.18

Carbon Offset Mechanism - Transportation Mode Percentages

3.7 Conclusions

This paper proposes models that capture the impact of carbon regulatory mechanisms such as carbon cap, carbon tax, carbon cap-and-trade, and carbon offset, on inventory replenishment decisions in a biomass supply chain. In particular, we investigate the impact of these mechanisms on supplier selection and transportation mode selection decisions. The models proposed are extensions of the classical economic lot sizing model. We modified the classical model to allow for multiple suppliers and transportation modes for replenishing inventories. The model selects the suppliers and transportation modes based on costs and emissions levels. Through our experimental results, we observed how existing carbon regulatory mechanisms affect the system's behavior. Below we summarize our key observations:

Observation 1: Carbon regulatory mechanisms have an impact on supplier and transportation mode selection decisions. As the carbon cap decreases, the carbon tax increases, or the market price of carbon increases, the firm tends to use local suppliers to minimize emissions related costs. Local suppliers in such cases rely on truck transportation.

Observation 2: Under a carbon cap mechanism, we can achieve a significant decrease in emissions through supply chain operations changes that come at a low cost. Note the shape of the curves in Figure 3.3(a) for caps between 6,000 tons and 10,000 tons. These curves are almost flat, indicating that changes in the carbon cap level have a small impact on costs.

Observation 3: A carbon cap mechanism is more efficient on the supply chain operations than a carbon tax mechanism. Supply chain operations are less responsive to an

increase in tax versus an increase in the carbon cap (see Figure 3.6 and Figure 3.10). The smoothness of the lines in Figure 3.6 indicate a higher level of responsiveness to changes in carbon cap level.

Observation 4: A carbon cap and trade mechanism is more efficient than a carbon offset mechanism. The supply chain behaves similarly under the two mechanisms when the carbon cap is tight. However, the supply chain behaves differently under the two mechanisms when the cap is loose. Under loose carbon caps, in a cap and trade mechanism, the unused carbon units can be sold in the market at a profit. This is not the case under a carbon offset mechanism, which punishes companies for going over the cap, but does not reward for emissions below the cap. The shapes of the graphs in Figure 3.12 and Figure 3.16 support this observation.

Observation 5: Improvements in the fuel efficiency of transportation vehicles impact emissions levels. Therefore, investments in improving fuel efficiency are important in reducing both supply chain costs and emissions. The impacts of these improvements on emissions and total supply chain costs are more obvious when the carbon caps are tight (Figure 3.3), and/or the carbon tax is high (Figure 3.7). However, these improvements should be accompanied by changes in supply chain operations. Otherwise, the increased demand for transportation will outweigh the positive effects of technological improvements.

CHAPTER 4

MODELS FOR REPLENISHMENT DECISIONS OF PERISHABLE PRODUCTS VIA MULTIPLE TRANSPORTATION MODES

4.1 Introduction

In this chapter we propose a mathematical model that aids inventory replenishment decisions for deteriorating products, such as agricultural and dairy products, human blood, photographic film, etc. Deterioration refers to spoilage, dryness, vaporization, etc., which results in value lost during the storage period. These products are known as age-dependent perishable products. Inventory replenishment decisions for perishable products are more challenging as compared to non-perishable products. This is due to the fact that these products lose value with time, and consequently have a limited shelf life. Therefore, inventory replenishment decisions are impacted not only by the tradeoffs that exist between replenishment and inventory holding costs, but also by the lead time and remaining shelf life of perishable products.

The objective of our model is to minimize total system costs associated with replenishment - related decisions. The model captures the tradeoffs that exist between transportation lead time, time in the storage and remaining shelf-life of products; and transportation and inventory costs. Shorter transportation lead times increase the remaining shelf life for perishable products. This provides companies with more flexibility when making inventory

replenishment decisions. For example, if the shelf life of a product is short, such as one day, then the inventories should be replenished daily. If the shelf life of a product is longer, then a company can reduce replenishment costs by ordering less frequently. A company can reduce transportation lead time for perishable products by using local suppliers, or by using transportation modes such as refrigerated trucks and refrigerated rail cars, or airplanes. However, using suppliers located nearby could result on higher replenishment costs, mainly due to a limited pool of suppliers than can be reached and, therefore, less competitive prices. Using refrigerated trucks, refrigerated rail cars and airplanes results in higher transportation costs as compared to using trucks and rail cars.

The model we propose is an extension of the classical economic lot sizing (ELS) model with the availability of multiple suppliers and/or transportation modes for replenishment of age-dependent perishable products. In Section 4.2, we present our network-flow based cost minimization model (P). We also extend another network-flow based model in the literature, by Hsu [46], to consider multiple replenishment modes. We show that the LP relaxation of our model provides tighter lower bounds. In Section 4.3, we discuss the properties of an optimal solution. Section 4.4 considers the problem with a single replenishment mode, and compares the performance of a dynamic programming algorithm works with a zero inventory ordering policy to an optimal algorithm. Section 4.5 discusses a minimum knapsack problem based dynamic programming algorithm for two available replenishment modes. Section 4.6 presents a primal-dual based algorithm that provides tight upper and lower bounds for the general case with multiple replenishment modes.

4.2 Model Formulations

In this section, we formulate the economic lot sizing model with multiple replenishment modes for perishable products with an objective of total cost minimization.

4.2.1 Formulation (P)

The objective of this problem is to minimize the total inventory and replenishment costs required by a facility in order to satisfy demand for a perishable item during a planning horizon of length T . Let b_t denote demand in period t ($t = 1, \dots, T$).

There are I ($i = 1, \dots, I$) different modes that can be used to replenish inventories. The amount of inventory replenished in period t using replenishment mode i is denoted by q_{it} . A replenishment mode in this model is characterized by a particular transportation mode and a supplier. For example, if there are S suppliers with F number of transportation modes each, then the number of total replenishment modes will be $I = S * F$. The corresponding replenishment costs are represented using a *multiple-setups* cost structure as follows:

$$Q_i(q_{it}) = \begin{cases} s_i + A_i \left\lceil \frac{q_{it}}{C_i} \right\rceil + p_i q_{it} & \text{if } q_{it} > 0 \text{ for } i = 1, \dots, I; t = 1, \dots, T. \\ 0 & \text{otherwise} \end{cases} \quad (4.1)$$

$\lceil a \rceil$ represents the smallest integer that is greater than or equal to a . Different from most of the literature that uses a linear or fixed-charge cost structure, we use a non-linear, step-wise function in order to better represent the structure of the replenishment costs as illustrated in Figure 4.1. In Equation (4.1), p_i denotes the unit replenishment cost. This cost includes the unit procurement cost and unit transportation costs for replenishment mode i . A fixed cost, denoted by s_i , is charged to setup an order from replenishment mode i . The number

of cargo containers used depends on the size of the order, denoted by q_{it} , and the capacity of the container, denoted by C_i . For each unit of cargo shipped, a fixed cost is charged, denoted by A_i , to account for loading/unloading activities.

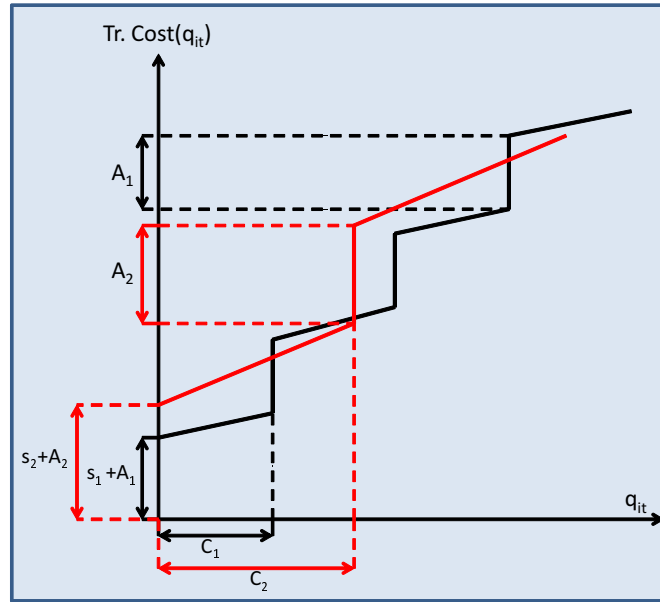


Figure 4.1

Multiple-Setups Cost Structure

We use two decision variables in order to model the step-wise replenishment cost function. These include y_{it} , a binary variable that takes the value 1 if replenishment mode i is used in period t and 0 otherwise; and z_{it} , an integer variable that represents the number of cargo containers used by replenishment mode i in period t .

In our formulation, we further divide variables q_{it} into $q_{it\tau}$ so that we can keep track of the time periods that a replenishment aims to satisfy. Thus, $q_{it\tau}$ represents the amount replenished by mode i which arrives in period t to satisfy demand in period τ . Using

$q_{it\tau}$ allows us to calculate the age of a product and corresponding inventory replenishment costs. Plugging in these new variables, multiple setups cost structure in Equation (4.1) becomes:

$$Q_{it}(q_{it\tau}) = \begin{cases} s_i + A_i \left[\frac{\sum_{\tau=t}^T q_{it\tau}}{C_i} \right] + p_i \sum_{\tau=t}^T q_{it\tau} & \text{if } q_{it\tau} > 0 \text{ for } \forall i, \forall t \\ 0 & \text{otherwise} \end{cases} \quad (4.2)$$

We assume that the product replenished deteriorates during transportation lead time and storage at the facility. We assume that the product is shipped as soon as it is produced. The transportation lead time for replenishment mode i , denoted by L_i , depends on the location and transportation mode used. We denote the deterioration rate for a replenishment using mode i from period t that it enters the inventory to period τ by $\alpha_{it\tau}$. The deterioration rate is not constant; instead, it depends on the duration of product storage. Typically, deterioration rate increases with time, and thus, $\alpha_{it\tau} \leq \alpha_{itj}$ for $1 \leq t \leq \tau \leq j \leq T$.

Let k_{itl} represent the percentage of inventory from replenishment mode i that arrives in period t that has not perished until it is used in period l . The order of this replenishment is made at time $t - L_i$ to count for the transportation lead time. If transportation lead time is assumed to be zero, a replenishment in time period t for the same time period is received without a loss. This means that $\alpha_{itt} = 0$ and 100% of the replenishment is delivered. Thus, we define $k_{itt} = 1$. The remaining k_{itl} for $1 \leq t \leq l \leq T$ are calculated as: $k_{itl} = \prod_{j=t}^{l-1} (1 - \alpha_{itj})$. Based on the assumption stated above, we can see that $k_{itl} \leq k_{i\tau l}$ for $1 \leq t \leq \tau \leq l \leq T$.

When transportation lead time is greater than zero, k_{itt} is not necessarily equal to 1. The replenishment starts deteriorating from time period $t - L_i$ in which it is ordered. This

value can be negative in terms of our notation as t starts from 1, and L_i can be any positive number. So we adjust it as $t - L_i = 1$, which implies that time period t will be the $(L_i + 1)^{th}$ time period. The replenishment arrives at time period t will already be L_i periods old. In this case, $k_{i1(L_i+1)}$ denotes the remaining percentage after the transportation lead time, i.e.

$$k_{itt} = k_{i1(L_i+1)} = \prod_{j=1}^{L_i} (1 - \alpha_{i1j}).$$

The remaining k_{itl} values will depend on the value of $k_{i1(L_i+1)}$ (equivalently k_{itt}) as follows:

$$k_{itl} = k_{i1(L_i+1)} \prod_{j=L_i+1}^{l-t+L_i} (1 - \alpha_{i1j}) \quad (4.3)$$

Thus, in our formulation, any k_{itl} value already contains the information for the deterioration during both the transportation lead time and storage in the facility.

Inventory holding costs are due to using the storage area, and using refrigerated storage. It also captures the lost opportunity of using the money invested in the inventory. Let h_t denote the unit inventory holding cost, and H_t denote the amount of inventory in the end of period t . We expect inventory holding costs to change with time due to, among others, fluctuations in the price and consumption of electricity. Letting $H_t(q_{it\tau})$ denote the inventory holding cost function in period t , then $H_t(q_{it\tau}) = h_t \sum_{i=1}^I \sum_{s=1}^t \sum_{\tau=t+1}^T k_{ist} q_{is\tau}$. The cost associated with each $q_{it\tau}$ is denoted by $c_{it\tau}$. This parameter includes the replenishment cost at period t , in-transit inventory holding cost for the lead time of L_i and the total inventory holding until period τ . It is defined as $c_{it\tau} = p_i + \sum_{s=t}^{\tau-1} h_s k_{its}$.

The formulation of the lot-sizing problem with multi-mode replenishment and age-dependent perishable inventories is the following:

$$\text{minimize } z = \sum_{i=1}^I \sum_{t=1}^T \left[\sum_{\tau=t}^T c_{it\tau} q_{it\tau} + s_i y_{it} + A_i z_{it} \right] \quad (4.4)$$

$$\text{Subject to } \sum_{i=1}^I \sum_{t=1}^{\tau} k_{it\tau} q_{it\tau} = b_{\tau} \quad 1 \leq \tau \leq T \quad (4.5)$$

$$q_{it\tau} - \frac{b_{\tau}}{k_{it\tau}} y_{it} \leq 0 \quad i = 1, 2, \dots, I; 1 \leq t \leq \tau \leq T \quad (4.6)$$

$$\sum_{\tau=t}^T q_{it\tau} - C_i z_{it} \leq 0 \quad i = 1, 2, \dots, I; t = 1, 2, \dots, T \quad (4.7)$$

$$y_{it} \in \{0, 1\} \quad i = 1, 2, \dots, I; t = 1, 2, \dots, T \quad (4.8)$$

$$z_{it} \in Z^+ \quad i = 1, 2, \dots, I; t = 1, 2, \dots, T \quad (4.9)$$

$$q_{it\tau} \geq 0 \quad i = 1, 2, \dots, I; 1 \leq t \leq \tau \leq T \quad (4.10)$$

Constraints (4.5) ensure that demand in period τ ($\tau = 1, \dots, T$) is satisfied. In this constraint the term $k_{it\tau}$ captures product deterioration during both transportation lead time and storage. Constraints (4.6) relate the continuous variables $q_{it\tau}$ to the binary variables y_{it} . When $y_{it} = 0$, this implies no replenishment of inventories in period t , as a consequence $q_{it\tau} = 0$ for $\tau = t, \dots, T$. Constraints (4.5) and (4.6) indicate that replenishment amounts should be larger than the actual demand to compensate for the loss of inventory due to deterioration. Constraints (4.7) identify the number of units of cargo required to replenish inventories from replenishment mode i in period t . Constraints (4.8), (4.9) and (4.10) are, respectively, the binary, integrality and non-negativity constraints.

Figure 4.2 gives a network representation of Formulation (P) with 2 replenishment modes and 3 periods. This network contains one dummy node for total supply, T nodes

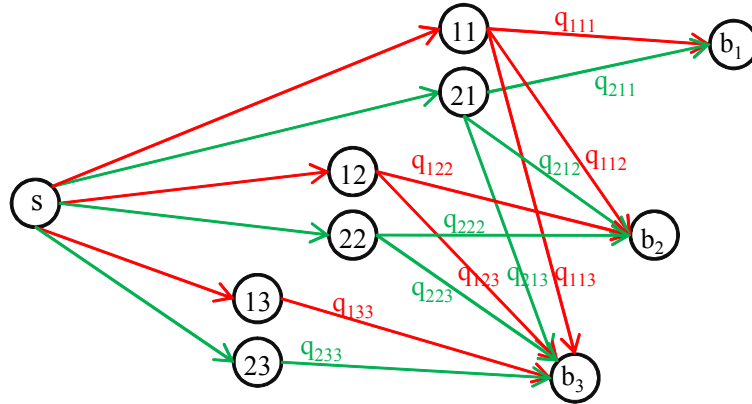


Figure 4.2

Network Representation for a 2-mode, 3-period Problem (P)

for the facility at each time period, and a total of $I * T$ replenishment nodes each of which represent a replenishment mode i in every time period t . In each time period t , the facility has a demand equal to b_t . Replenishment arcs connect replenishment nodes with the facility in each time period. The amount of flow on these arcs ($q_{it\tau}$) represent the amount shipped using replenishment mode i that arrives in time period t for time period τ .

4.2.2 Formulation (Q)

Hsu [46] provides the ELS model with age dependent perishable inventories and a single mode of transportation. Different from our model, Hsu [46]'s model assumes a fixed charge cost function and another network structure. In this section, we show how our problem with multiple replenishment modes and a multiple setups costs structure would be represented using the network model proposed by Hsu [46]. We refer to this as Formulation (Q). In this formulation, we assume that $L_i = 0$. Figure 4.3 gives a network representation of Formulation (Q) with 2 replenishment modes and 3 time periods.

The decision variables used in formulation (Q) are: q_{it} represents the amount replenished in period t using mode i ; $r_{it\tau}$ represents the amount of demand in period τ satisfied from a replenishment made in period t using mode i ; $H_{it\tau}$ represents the amount of inventory in the end of period τ from a replenishment received in period t using mode i ; y_{it} is a binary variable that takes the value 1 if replenishment mode i is used in period t and 0 otherwise; z_{it} represents the number of cargo containers used by replenishment mode i in period t . We use the same parameters that have been defined for Formulation (P).

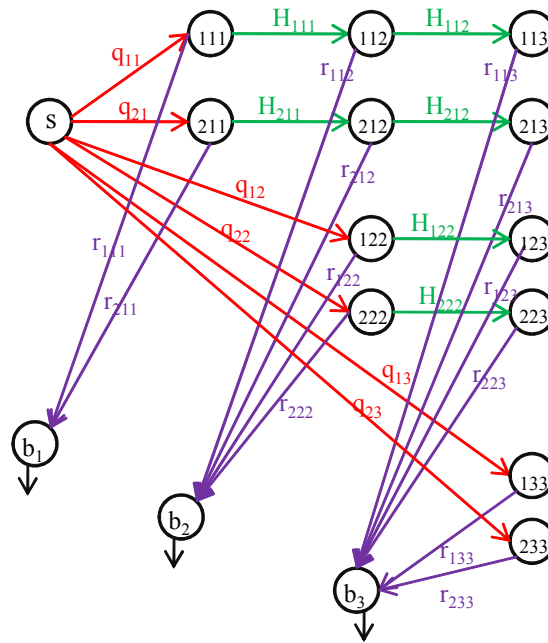


Figure 4.3

Network Representation for a 2-mode, 3-period Problem (Q)

$$\text{minimize } z = \sum_{i=1}^I \sum_{t=1}^T \left[p_i q_{it} + s_i y_{it} + A_i z_{it} + \sum_{\tau=t}^T h_{\tau} H_{it\tau} \right] \quad (4.11)$$

$$\text{Subject to } q_{it} - r_{itt} = H_{itt} \quad i = 1, 2, \dots, I; t = 1, 2, \dots, T. \quad (4.12)$$

$$(1 - \alpha_{it, \tau-1}) H_{it, \tau-1} = H_{it\tau} + r_{it\tau} \quad i = 1, 2, \dots, I; 1 \leq t \leq \tau \leq T. \quad (4.13)$$

$$\sum_{i=1}^I \sum_{t=1}^{\tau} r_{it\tau} = b_{\tau} \quad \tau = 1, 2, \dots, T. \quad (4.14)$$

$$q_{it} - \left(\sum_{\tau=t}^T \frac{b_{\tau}}{k_{it\tau}} \right) y_{it} \leq 0 \quad i = 1, 2, \dots, I; t = 1, 2, \dots, T. \quad (4.15)$$

$$q_{it} - C_i z_{it} \leq 0 \quad i = 1, 2, \dots, I; t = 1, 2, \dots, T. \quad (4.16)$$

$$y_{it} \in \{0, 1\} \quad i = 1, 2, \dots, I; t = 1, 2, \dots, T. \quad (4.17)$$

$$z_{it} \in Z^+ \quad i = 1, 2, \dots, I; t = 1, 2, \dots, T. \quad (4.18)$$

$$q_{it}, r_{it\tau}, H_{it\tau} \geq 0 \quad i = 1, 2, \dots, I; 1 \leq t \leq \tau \leq T. \quad (4.19)$$

In this formulation, constraints (4.12), (4.13), (4.14) and (4.15) are the flow conservation constraints. Constraints (4.16) show that the replenished amount cannot be larger than cargo capacity. Constraints (4.17), (4.18) and (4.19) are respectively the binary, integrity and non-negativity constraints.

Formulation (P) and Formulation (Q) are two different models that represent the same problem with two different network structures. We selected the network structure proposed by Hsu [46] as their study has provided high quality solutions for a special case of Formulation (Q). Hsu [46] considers a fixed charge cost structure and a single replenishment mode and proposes a dynamic programming algorithm that runs in $O(T^4)$. For this reason, we also use a fixed charge cost structure in both formulations for a fair comparison. Thus, this

special case corresponds to using multiple modes of replenishment with no capacity limits under a fixed charge cost structure.

We take the LP relaxations of both models for this special case. We show that the LP relaxation of Formulation (P) provides solutions with zero integrality gap. Therefore it is a tighter formulation than Formulation (Q). The LP relaxation of Formulation (Q) is not very tight due to constraints (4.15). In the LP relaxation of (Q), y_{it} variables represents the fraction of demand from period t to T that is satisfied by a replenishment mode i at time period t . So the sum of all demands from period t to T ($\sum_{\tau=t}^T \frac{b_{\tau}}{k_{it\tau}}$) is a very high upper bound. In Formulation (P), this upper bound is only the demand for a single time period, i.e. $\frac{b_{\tau}}{k_{it\tau}}$ in constraints (4.7). Using a numerical analysis, we also compare the performance of both formulations in terms of their running times.

4.2.3 Comparison of LP Relaxations of (P) and (Q)

4.2.3.1 Optimality Gap

In this section, we compare the performance of Formulations (P) and (Q) in terms of the lower bounds obtained by their LP relaxations and their running times in CPLEX. In particular, we show in Theorem 4.1 that under a fixed charge cost structure, LP relaxation of Formulation (P) is solved to zero integrality gap. In our numerical analysis, our experiments showed that the LP relaxation of Formulation (Q) does not provide a zero optimality gap. Using the data in the following example for comparison of running times, LP relaxation of Formulation (Q) provided us solutions within at least 5% of the optimal solution. Thus, our test results also demonstrated the value of the tighter formulation (P).

4.2.3.1.1 Theorem 4.1

Assuming no cargo capacities and fixed charge replenishment costs, the LP relaxation of Formulation (P) provides solutions with zero integrality gap.

For this special case, we obtain Formulation (P'):

$$\text{minimize } z = \sum_{i=1}^I \sum_{t=1}^T \left[\sum_{\tau=t}^T c_{it\tau} q_{it\tau} + s_i y_{it} \right] \quad (4.20)$$

$$\text{Subject to } \sum_{i=1}^I \sum_{t=1}^{\tau} k_{it\tau} q_{it\tau} = b_{\tau} \quad 1 \leq \tau \leq T \quad (4.5)$$

$$q_{it\tau} - \frac{b_{\tau}}{k_{it\tau}} y_{it} \leq 0 \quad \forall i; 1 \leq t \leq \tau \leq T \quad (4.6)$$

$$y_{it} \in \{0, 1\} \quad \forall i; t = 1, 2, \dots, T \quad (4.8)$$

$$q_{it\tau} \geq 0 \quad \forall i; 1 \leq t \leq \tau \leq T \quad (4.10)$$

Defining $x_{it\tau} = q_{it\tau}/b_{\tau}$ and $\tilde{c}_{it\tau} = c_{it\tau} b_{\tau}$ for all $i, t = 1, \dots, T, \tau = t, \dots, T$, we can write Formulation (P') as

$$\text{minimize } z = \sum_{i=1}^I \sum_{t=1}^T \left[\sum_{\tau=t}^T \tilde{c}_{it\tau} x_{it\tau} + s_i y_{it} \right] \quad (4.21)$$

$$\text{Subject to } \sum_{i=1}^I \sum_{t=1}^{\tau} k_{it\tau} x_{it\tau} = 1 \quad 1 \leq \tau \leq T \quad (4.22)$$

$$x_{it\tau} - \frac{1}{k_{it\tau}} y_{it} \leq 0 \quad \forall i; 1 \leq t \leq \tau \leq T \quad (4.23)$$

$$y_{it} \in \{0, 1\} \quad \forall i; t = 1, 2, \dots, T \quad (4.8)$$

$$x_{it\tau} \geq 0 \quad \forall i; 1 \leq t \leq \tau \leq T \quad (4.10)$$

Let $\lambda_{it\tau}$ denote a Lagrangian multiplier associated with (4.23) and consider the Lagrangian relaxation in which each of these constraints is relaxed. This Lagrangian relaxation can be written as

$$LR(\lambda) = \min \sum_{i=1}^I \sum_{t=1}^T \left[\sum_{\tau=t}^T (\tilde{c}_{it\tau} + \lambda_{it\tau}) x_{it\tau} + \left(s_i - \sum_{\tau=t}^T \frac{\lambda_{it\tau}}{k_{it\tau}} \right) y_{it} \right] \quad (4.24)$$

$$\text{Subject to } \sum_{i=1}^I \sum_{t=1}^{\tau} k_{it\tau} x_{it\tau} = 1 \quad 1 \leq \tau \leq T \quad (4.22)$$

$$y_{it} \in \{0, 1\} \quad \forall i; t = 1, 2, \dots, T \quad (4.8)$$

$$x_{it\tau} \geq 0 \quad \forall i; 1 \leq t \leq \tau \leq T \quad (4.10)$$

For a given vector λ , we can solve the above relaxation as follows. For each i, t pair, if $s_i - \sum_{\tau=t}^T \frac{\lambda_{it\tau}}{k_{it\tau}} \leq 0$, set $y_{it} = 1$; otherwise set $y_{it} = 0$. Let $IT(\lambda)$ denote the set of all i, t pairs such that $y_{it} = 1$. For $\tau = 1, \dots, T$, let $\Phi(\tau, \lambda)$ denote the set of all i, t pairs with $t \leq \tau$ such that $\frac{\tilde{c}_{it\tau} + \lambda_{it\tau}}{k_{it\tau}}$ is minimized. If some i, t pair exists such that $(i, t) \in \{IT(\lambda) \cap \Phi(\tau, \lambda)\}$, then for the element in this set with the biggest value of t , set $x_{it\tau} = 1/k_{it\tau}$. For the given value of τ , set $x_{it\tau} = 0$ for all other (i, t) pairs. If no element exists in $\{IT(\lambda) \cap \Phi(\tau, \lambda)\}$, then choose any $(i, t) \in \Phi(\tau, \lambda)$ and set $x_{it\tau} = 1/k_{it\tau}$. Again for the given value of τ , then set $x_{it\tau} = 0$ for all other (i, t) pairs. Note that this solution is optimal for $LR(\lambda)$.

Since Lagrangian relaxation value satisfies the integrality property, the optimal Lagrangian dual value will equal the LP relaxation of the original formulation. Let λ^* denote the vector that maximizes the Lagrangian dual objective, and let $x(\lambda^*)$ and $y(\lambda^*)$ denote the corresponding solution in the x and y vectors for the Lagrangian relaxation problem at

λ^* as constructed above. If $x(\lambda^*)$ and $y(\lambda^*)$ are feasible for the original problem, this solution is optimal for the original problem. This is because the Lagrangian relaxation problem provides a lower bound on the optimal solution for the original problem. In particular, this implies we have found an integer feasible solution whose objective function value equals the optimal objective function value for the LP relaxation of the original problem.

Next suppose that $x(\lambda^*)$ and $y(\lambda^*)$ are not feasible for the original problem. Then by construction of the solution, this implies that there exists a triplet $(\tilde{i}, \tilde{t}, \tilde{\tau})$ such that $x_{\tilde{i}\tilde{t}\tilde{\tau}} = 1/k_{\tilde{i}\tilde{t}\tilde{\tau}}$ and $y_{\tilde{i}\tilde{t}} = 0$. We also know by construction that $y_{it} = 0$ for all $(i, t) \in \Phi(\tilde{\tau}, \lambda^*)$. This implies that $s_i - \sum_{\tau=t}^T \frac{\lambda_{it\tau}^*}{k_{it\tau}} > 0$ for all $(i, t) \in \Phi(\tilde{\tau}, \lambda^*)$. We can obtain a new vector $\tilde{\lambda}$ by increasing $\lambda_{it\tau}$ by some $\epsilon > 0$ for each $(i, t) \in \Phi(\tilde{\tau}, \lambda^*)$ and leaving all other λ values unchanged. For a sufficiently small $\epsilon > 0$, the coefficient of y_{it} in $LR(\lambda)$, i.e. $s_i - \sum_{\tau=t}^T \frac{\lambda_{it\tau}}{k_{it\tau}}$, remains positive for all (i, t) pairs for which this sign was positive in our original solution (thus $y(\lambda^*) = y(\tilde{\lambda})$). In addition, for sufficiently small ϵ we have $\Phi(\tilde{\tau}, \tilde{\lambda}) = \Phi(\tilde{\tau}, \lambda^*)$ and, therefore, $x(\tilde{\lambda}) = x(\lambda^*)$. However, because of the increase in the value of $\lambda_{it\tau}$ for all $(i, t) \in \Phi(\tilde{\tau}, \lambda^*)$, this implies that the Lagrangian dual solution at $\tilde{\lambda}$ is strictly greater than the Lagrangian dual objective at λ^* , which contradicts the optimality of λ^* for the dual objective. Thus, if we have an optimal dual solution λ^* , there does not exist any triplet $(\tilde{i}, \tilde{t}, \tilde{\tau})$ such that $x_{\tilde{i}\tilde{t}\tilde{\tau}} = 1/k_{\tilde{i}\tilde{t}\tilde{\tau}}$ and $y_{\tilde{i}\tilde{t}} = 0$, and the Lagrangian relaxation solution at the optimal value of λ must be feasible for the original problem.

4.2.3.2 Running times

In the following example, we compare both formulations in terms of their running times.

Table 4.1

Problem Parameters for LP Relaxations

Tr.Mode	s_i	p_i
1	U[100,200]	U[30,40]
2	U[200,300]	U[25,35]
3	U[300,400]	U[20,25]

Table 4.1 presents the input data for comparison. We consider 12 problems with the number of replenishment modes (I) and time periods (T) as shown in Table 4.2. For each problem, we assume equal numbers of different transportation modes. For example, $I = 3$ contains one from each type of transportation modes whereas $I = 15$ contains five of each.

Table 4.2

Problem Characteristics for LP Relaxations

Prob	I	T	Prob	I	T	Prob	I	T
1	3	25	5	6	25	9	15	25
2	3	50	6	6	50	10	15	50
3	3	75	7	6	75	11	15	75
4	3	100	8	6	100	12	15	100

We generate demand per time period following a uniform distribution $U[100, 200]$. Holding cost is assumed to be $h = \$1/(\text{unit} \cdot \text{time period})$. For each problem, we also create 10 cases for different deterioration rates per time period. We analyze deterioration rates between 0.01 to 0.10 per time period in increments of 0.01. For each problem and deterioration rate, we generate 10 test instances and report on the average running times and error gaps. Table 4.3 shows the running times of both formulations in CPLEX for three different deterioration rates per time period ($\alpha = 0.01, 0.05, 0.10$). For all of the problems using different deterioration rates, Formulation (Q) has longer running times compared to Formulation (P).

Table 4.3

CPU Running times (in sec) for (P) and (Q)

$\alpha = 0.01$			$\alpha = 0.05$			$\alpha = 0.10$		
Prob	Q	P	Prob	Q	P	Prob	Q	P
1	0.072	0.012	1	0.088	0.013	1	0.053	0.012
2	0.278	0.039	2	0.278	0.123	2	0.288	0.106
3	0.708	0.245	3	0.553	0.175	3	0.451	0.175
4	1.153	0.322	4	1.113	0.280	4	1.353	0.280
5	0.150	0.063	5	0.153	0.083	5	0.147	0.075
6	0.564	0.178	6	0.494	0.158	6	0.451	0.158
7	1.446	0.322	7	1.094	0.319	7	0.772	0.336
8	2.725	0.570	8	2.289	0.602	8	1.672	0.559
9	0.202	0.141	9	0.205	0.103	9	0.189	0.134
10	0.953	0.363	10	0.855	0.392	10	0.886	0.372
11	2.572	0.786	11	2.276	0.810	11	2.030	1.027
12	6.757	1.808	12	5.280	1.975	12	4.230	1.858

4.3 Properties of an Optimal Solution

We make use of the following definitions that are also used commonly in the literature when we demonstrate the properties of the optimal solution. Period t is an *order period* if $q_t > 0$. In (P), $q_t = \sum_{i=1}^I \sum_{\tau=t}^T q_{it\tau}$. Period t is a *regeneration period* if $I_t = 0$. The interval between two consecutive regeneration points, τ and γ is a *regeneration interval*. In (P), $I_{t-1} = \sum_{i=1}^I \sum_{s=1}^{t-1} k_{ist} q_{ist}$. We define q_{it} as a *Full-Truck-Load (FTL)* shipment if $q_{it} = nC_i$ for some positive integer n ; otherwise, it is a *Less-than-Truck Load (LTL)* shipment. $q_t > 0$ is called a *full order* if q_{it} is either zero or an FTL shipment for all $i = 1, \dots, I$; otherwise it is called a *partial order*.

The following properties have been proposed for the ELS problem with multi-mode replenishments for non-perishable products. We show that they hold for our problem with perishable products.

4.3.1 Property 4.1

If periods $\tau - 1$ and γ are two consecutive regeneration points, there exists an optimal solution such that there is at most one partial order between periods τ and γ . (Adapted from Jaruphongsa et al. [59])

Let an optimal solution contain two partial order periods, x and y ($x < y$) between two consecutive regeneration periods $\tau - 1$ and γ . The quantities shipped at these time periods are q_{mx} and q_{ny} using modes m and n respectively. Let p_i denote the total of the unit replenishment cost and unit cost for in-transit inventory for a replenishment mode i .

There are two possible cases to consider:

1. If $p_m + \sum_{s=x}^{y-1} h_s k_{ixs} < p_n$, then we can increase q_{mx} by $\min\{[q_{mx}/C_m] C_m - q_{mx}, q_{ny} k_{nyy}/k_{mxy}\}$ and decrease q_{ny} by this minimum amount times k_{mxy}/k_{nyy} . After this change, either $q_{ny} = 0$ or q_{mx} is an FTL replenishment. Since $p_m + \sum_{s=x}^{y-1} h_s k_{ixs} < p_n$, and the number of cargo containers do not increase, total costs will not increase. Thus, we obtain a solution whose cost is less than the cost of the optimal solution. This is a contradiction.
2. If $p_m + \sum_{s=x}^{y-1} h_s k_{ixs} > p_n$, then we can increase q_{ny} by $\min\{[q_{ny}/C_n] C_n - q_{ny}, q_{mx} k_{mxy}/k_{nyy}, I_x k_{m(x+1)y}/k_{nyy}, I_{x+1} k_{m(x+2)y}/k_{nyy}, \dots, I_{y-1} k_{myy}/k_{nyy}\}$ and decrease q_{mx} by this minimum amount times $\frac{k_{nyy}}{k_{mxy}}$. After this change, there are three possible cases: $q_{mx} = 0$; q_{ny} is an FTL replenishment; or a regeneration point is created between x and y , and as a result q_{mx} and q_{ny} become LTL shipments that belong to two different regeneration intervals. In all of the cases, replenishment costs will not increase as $p_m + \sum_{s=x}^{y-1} h_s k_{ixs} > p_n$. Number of cargo containers will either stay the same or decrease. Therefore, total costs will decrease and we obtain an optimal solution with lower costs, which creates a contradiction.

Thus, it is not possible for any two periods between two consecutive regeneration points to carry partial orders.

4.3.2 Property 4.2

There exists an optimal solution such that $q_t > 0$ ($t = 1, \dots, T$) if and only if $\sum_{i=1}^I \sum_{s=\tau}^{t-1} k_{ist} q_{ist} < b_t$ where $\tau - 1$ ($0 \leq \tau < t \leq T$) is the latest regeneration point.

This property states that inventories are replenished in period t if the inventory in the beginning of this period, I_{t-1} , is not enough to satisfy demand. Constraints (4.5) state that $\sum_{i=1}^I \sum_{s=1}^t k_{ist} q_{ist} = b_t$. We can rearrange this constraint separating the current period's replenishment from the inventory: $\sum_{i=1}^I \sum_{s=1}^{t-1} k_{ist} q_{ist} + \sum_{i=1}^I k_{itt} q_{itt} = b_t$. Let $\tau_1, \tau_2, \dots, \tau_n$, ($0 \leq \tau_1 \leq \dots \leq \tau_n < t$) be n regeneration points prior to time t . That implies $\sum_{i=1}^I (\sum_{s=0}^{\tau_1-1} k_{ist} q_{ist} + \sum_{s=\tau_1}^{\tau_2-1} k_{ist} q_{ist} + \dots + \sum_{s=\tau_n}^{t-1} k_{ist} q_{ist}) + \sum_{i=1}^I k_{itt} q_{itt} = b_t$. Thus, we obtain $\sum_{i=1}^I \sum_{s=\tau_n}^{t-1} k_{ist} q_{ist} + \sum_{i=1}^I k_{itt} q_{itt} = b_t$.

It is clear that if $\sum_{i=1}^I \sum_{s=\tau_n}^{t-1} k_{ist} q_{ist} < b_t$, then $\sum_{i=1}^I k_{itt} q_{itt} > 0$, i.e. there will be a replenishment in period t . Suppose that there exists an optimal solution such that $\sum_{i=1}^I \sum_{s=\tau_n}^{t-1} k_{ist} q_{ist} \geq b_t$ and $\sum_{i=1}^I k_{itt} q_{itt} > 0$. The quantity shipped in period t will incur a replenishment cost of $\sum_{i=1}^I c_{itt} q_{itt}$ and an inventory holding cost of carrying the quantity for at least one time period, which is $\sum_{i=1}^I h_t k_{itt} q_{itt}$. In this one period, the quantity of $\sum_{i=1}^I k_{itt} q_{itt}$ will decrease to $\sum_{i=1}^I k_{it(t+1)} q_{itt}$. We can delay this replenishment order from period t to $t + 1$ without changing the replenishment mode in period $t + 1$. In this case, deterioration in one time period will be avoided. The replenishment costs will be the same but the holding cost will be saved. Thus, we will obtain another optimal solution with lower costs, which is a contradiction.

4.4 Special Case: Single Replenishment Mode

In this section, we consider the special case where only one replenishment mode is available. As there is a single mode with the same transportation lead time, we assume that $L_i = 0$ without loss of generality.

Hsu [46] considers the economic lot sizing model for perishable products with the availability of a single replenishment mode and fixed charge cost structure. Our model reduces to this special case if there were no cargo capacity considerations. Hsu [46] defines the following property for this model.

4.4.1 Proposition 4.1

Assume no cargo capacities and fixed charge replenishment costs. Let $1 \leq \tau_1 < \tau_2 < \dots < \tau_n \leq T$ be the indices for the N production periods in the optimal solution.

Suppose also that there are $N+1$ indices $1 \leq \gamma_1 < \gamma_2 < \dots < \gamma_{n+1} = T + 1$. For each s ($1 \leq s \leq N$), $\tau_s \leq \gamma_s$ and production in τ_s satisfies demand in periods γ_s through $\gamma_{s+1} - 1$.
(From Hsu [46])

This proposition defines Consecutive Cover Ordering (CCO) property which states that an order covers the total demand for a number of consecutive periods. Unlike the Zero Inventory Ordering property, the inventory is not required to be zero at the time of the order. However, an order that takes place when there is available inventory is not used at the same time period. It is saved until the consecutive time periods that it is targeted to replenish. Thus, there is no splitting between production and inventory for the replenishments in any time periods.

Proposition 4.1, however, does not hold when cargo capacities and associated costs are taken into consideration as the demand of a time period may be satisfied via replenishments in the same time period and/or from a number of previous time periods. We illustrate this with an example. Suppose that $\{d_1, d_2, d_3\} = \{135, 200, 509\}$, $A_1 = 80$, $s_1 = 50$, $p_1 = 2$, $C_1 = 50$, $h_t = 1$. Let $\alpha_{1,t,t} = 0$, $\alpha_{1,t,t+1} = 0.2$, $\alpha_{1,t,t+2} = 0.25$ for $1 \leq t \leq T = 3$. Then we obtain $k_{1tt} = 0$, $k_{1t(t+1)} = 0.8$, $k_{1t(t+2)} = 0.6$. The optimal solution sets $q_{111} = 135$, $q_{112} = 15$, $q_{122} = 188$, $q_{123} = 11.25$, $q_{133} = 500$, with an optimal cost of 3234.75. According to Property 4.1, each of demands in periods 2 and 3 should have been satisfied by single orders. However, $q_{112} > 0$ and $q_{122} > 0$ in the optimal solution, as well as $q_{123} > 0$ and $q_{133} > 0$. Thus, the demand of a period can be both satisfied from replenishment and inventory.

With the multiple setups cost structure, an order in an optimal solution also does not necessarily have to be a combination of replenishments for consecutive time periods. This is a result of the relationship between deterioration rates. We again illustrate this with an example. In the previous example, we assumed that $\alpha_{1,t,t} = 0$, $\alpha_{1,t,t+1} = 0.2$, $\alpha_{1,t,t+2} = 0.25$ for all values of t . However, depending on the time period t , these values may differ. For example, let $\alpha_{1,2,3} = 0.3$ and keep the remaining values same for the previous problem. Then $k_{1tt} = 1$ for all $t \leq 3$, $k_{112} = 0.8$, $k_{113} = 0.6$ and $k_{123} = 0.7$. In this case, the optimal solution sets $q_{111} = 135$, $q_{113} = 15$, $q_{122} = 200$, $q_{133} = 500$, with an optimal cost of 3237. In the solution $q_{111} > 0$ and $q_{113} > 0$ whereas $q_{112} = 0$. A sequential flow would not let q_{113} have a positive value unless $q_{112} > 0$. Thus, an optimal solution for our model can contain non-sequential flows.

The following properties hold for our model for perishable products with a single replenishment mode and a multiple setups cost structure. In our model, unit replenishment costs p_i are not a function of the time period. Thus, it complies with the nonspeculative cost structure as $p_{t+1} = p_t$. Cargo costs A_i for ($i = 1 \dots I$) are also independent of the time period. Since $i = 1$, the stationary cargo cost is equal to A in every time period. Similarly, we omit the i indices for the rest of the notation in the single mode problem. Parameters s, p and C represent the fixed setup cost, unit replenishment cost and cargo capacity respectively. q_t is the amount of replenishment in time period t , and k_{xy} represents the percentage inventory remaining at period y for a replenishment that arrives in period x . c_{xy} denotes the total replenishment and inventory cost of a replenishment arrives in period x to satisfy the demand in period y .

4.4.2 Property 4.3

Let $\tau - 1$ and γ be two consecutive regeneration points. Under a nonspeculative cost structure, if there is a LTL shipment between periods τ and γ , it occurs in the first period, τ . (Adapted from Hwang [50] and Jaruphongsa et al. [59])

Consider Case 2 in Property 4.1 as nonspeculative costs fall into this category. Let x and y ($x < y$) be two LTL shipment periods in a regeneration interval $(\tau - 1, \gamma)$. Suppose q_x and q_y are the quantities shipped by a single mode at these time periods. We can increase q_y by $\min \{ \lceil q_y/C \rceil C - q_y, q_x k_{xy}, I_x k_{(x+1)y}, I_{x+1} k_{(x+2)y}, \dots, I_{y-1} \}$ and decrease q_x by this minimum amount times $1/k_{xy}$.

1. If the first term is selected, i.e. $\min = \lceil \frac{q_y}{C} \rceil C - q_y$, then the amount of decrease in q_x is $\Delta_{xy} = (\lceil \frac{q_y}{C} \rceil C - q_y) / k_{xy}$. After this change, q_y becomes an FTL shipment whereas q_{1x} is an LTL shipment. Number of cargo containers do not change. Total inventory holding costs are decreased by $\sum_{t=x}^{y-1} h_t k_{xt} \Delta_{xy}$.
2. Selection of second term depletes q_x . With this change, setup and cargo costs at time x are avoided. Decrease in the inventory holding costs is $\sum_{t=x}^{y-1} h_t k_{xt} q_x$. In this case, q_y may be an FTL or an LTL shipment.
3. If terms with the inventory are selected, a new regeneration point is created between periods x and y . In this case, q_x and q_y become the first ordering periods of two consecutive regeneration intervals. They can both be LTL or FTL shipments. Number of containers will stay the same; however, inventory holding cost of the selected term will be saved.

In all of the cases, a solution is obtained that has a lower cost than the optimal solution, which is a contradiction to optimality. The same procedure can be applied to all possible regeneration intervals. In the optimal solution, if there has to be an LTL shipment, it will only occur in the first period of a regeneration interval.

4.4.3 Property 4.4

In an optimal solution, each FTL shipment period t between any two consecutive re-generation points $\tau - 1$ and γ satisfies $I_{t-1} < \min\{b_t, C\}$. (Adapted from Lee [64])

Let $I_{t-1} \geq \min\{b_t, C\}$ in an optimal solution for an FTL replenishment period t . Property 4.2 states that a replenishment can only take place when $I_{t-1} < b_t$. To satisfy both inequalities stated above, i.e. $\min\{b_t, C\} \leq I_{t-1} < b_t$, we should have $\min\{b_t, C\} = C$. Let x be the last replenishment period before t , ($x < t$). Suppose q_x and q_t are the replenishments in these two periods. To obtain $I_{t-1} \geq C$, we must have $I_x = (q_x + I_{x-1} - b_x) \geq C/k_{xt}$. We know that $I_{x-1} < b_x$. It follows that $q_x \geq (C/k_{xt}) + b_x - I_{x-1} > (C/k_{xt})$. In this case, we can decrease q_x by $\lceil \frac{q_x k_{xt}}{C} \rceil (C/k_{xt}) - (C/k_{xt})$ and increase q_t by $\lceil \frac{q_t}{C} \rceil C - C$. In the new solution, we will still have $q_x \geq (C/k_{xt})$ and less total costs due to decreased holding costs. This contradicts the optimality of the initial solution.

We are only interested in the solutions that satisfy Properties (4.1) - (4.4). We observed through examples that demand of a time period can be satisfied with inventory from a previous period and an FTL replenishment in the same time period. Thus, Zero Inventory Ordering property does not hold for our model. As the model is easier to solve with a Zero Inventory Ordering policy, we provide a dynamic programming algorithm using this policy in Section 4.4.4 as our first solution approach. In Section 4.4.5 we propose another a dynamic programming model that considers multiple setups cost structure which we updated from Hwang [50] to consider age-dependent perishable inventory. We analyze the error gap between these two dynamic programming algorithms and the optimal solution.

We compare the running times of both algorithms and show that a zero inventory ordering policy can provide quality solutions with small error gaps.

4.4.4 Dynamic Programming Algorithm for Zero Inventory Ordering Policy

In this section, we present a dynamic programming algorithm that works under a zero inventory ordering policy. This policy requires an order to be placed at time period t only when $I_{t-1} = 0$. Also, demand of a period cannot be supplied from both replenishment in period t and inventory from period $t - 1$.

If a replenishment schedule exists such that if period t is a replenishment period, the corresponding replenishment quantity equals $b_{t,\tau} = \sum_{\gamma=t}^{\tau-1} (b_\gamma/k_{t\gamma})$ for some $t \leq \tau \leq T+1$ where $1 \leq t \leq T$. τ represents the next replenishment period after period t . We use the dummy period $T + 1$. This period does not represent a replenishment period and there is no demand in this period. A flow from period T to $T + 1$ represents a replenishment in period T to satisfy demand in $T + 1$.

The number of cargo containers for the replenishment in period t equals $M_{t\tau} = \lceil b_{t,\tau}/C \rceil$. The cost associated with satisfying demand from period t through $\tau - 1$ is denoted by $f(t, \tau)$ and equals:

$$f(t, \tau) = s + \sum_{\gamma=t}^{\tau-1} c_{t\gamma} \frac{b_s}{k_{t\gamma}} + AM_{t\tau} \quad (4.25)$$

We create an acyclic network where each $f(t, \tau)$ represents an arc cost on the graph and we solve the shortest path problem to find the optimal solution. We create a graph G , as shown in Figure 4.4. $T + 1$ nodes are included in G ; one for each of the T time periods in addition to the dummy node $T + 1$. Each arc (t, τ) in G represents a shipment that satisfies

demands from t through $\tau - 1$. The cost of each arc (t, τ) is equal to $f(t, \tau)$. The dynamic programming algorithm finds the shortest path from node 1 to $T + 1$ in graph G .

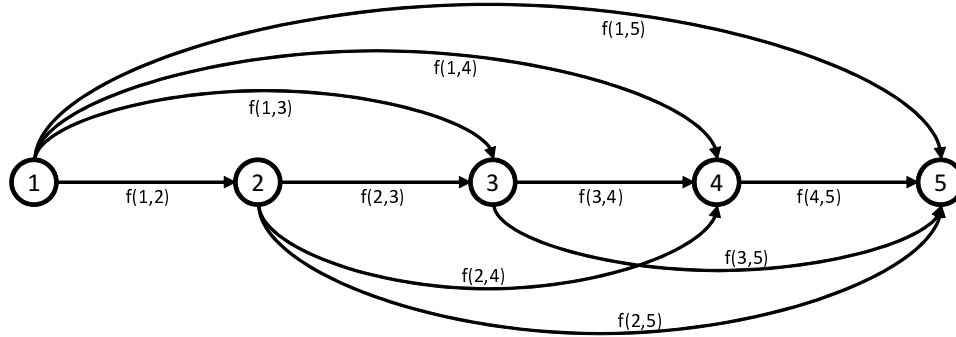


Figure 4.4

Network Representation for Dynamic Programming Algorithm ($T = 4$)

A solution under a zero ordering policy does not allow any replenishments when there is inventory available. Thus, a replenishment only takes place when the inventory level is zero and has to satisfy the demands of some consecutive demand periods. This implies that only one replenishment can take place between any two regeneration points. An optimal solution to the original problem allows FTL replenishments in a regeneration interval even if inventory level is greater than zero. So an optimal solution arranges FTL shipments to capture the tradeoffs between the cargo and inventory holding costs in every regeneration interval. However, under zero inventory ordering policy, number of containers is set depending on the total demand for every regeneration interval. Inventory holding costs and potentially cargo costs are higher since the replenishment at the beginning of the regeneration interval has to carry more than the required amounts considering the deterioration.

4.4.5 Dynamic Programming Algorithm for Multiple Setups Cost Structure

Hwang [50] proposes a dynamic programming algorithm to find the optimal solution for the problem with a single replenishment mode, stationary cargo costs and a nonspeculative cost structure. We propose a dynamic programming based heuristic by modifying this algorithm to consider age-dependent perishable inventories. The solutions found using this procedure satisfy Properties (4.1) - (4.4). We again assume $t - 1$ and $\tau - 1$ ($1 \leq t < \tau \leq T + 1$) be two consecutive regeneration points. Let the (t, τ) problem be finding the minimum cost (denoted by $f(t, \tau)$) of satisfying total demand from period t through $\tau - 1$. Once all $f(t, \tau)$ values are determined, the shortest path on Figure 4.4 finds the minimum solution to the model.

Finding $f(t, \tau)$ values are more challenging in this case, as there may be FTL shipments within the (t, τ) problem. As Property 4.3 states, if an LTL shipment exists, it can only occur in period t in a (t, τ) problem. It implies that for some m ($t < m \leq \tau$) to period τ , only FTL shipments exist. Let $g(m, \tau)$ be the minimum cost of (m, τ) problem using only FTL shipments. Thus, $f(t, \tau)$ is calculated as a function of $g(m, \tau)$. It calculates the minimum cost of satisfying the demand in (t, τ) problem with a possible LTL shipment only in period t and FTL shipments in the remaining periods. The procedure uses a backward dynamic programming approach. Thus, initially the scheduling of the FTL shipments are made in (m, τ) problem such that $g(m, \tau)$ is minimized. Then, this schedule determines the inventory that should be carried from period $m - 1$ to satisfy the total demand in the (m, τ) problem. However, due to perishability, timing of the last replenishment before period m and the level of inventory that is carried to this period affects the ordering of the

FTL shipments in any (m, τ) problem of an optimal solution. This means comparing all possible schedules of FTL shipments within any (m, τ) problem for every (t, τ) problem. However, this is a time consuming process with enumerating all solutions. Our procedure, instead, determines a minimum cost FTL replenishment schedule for every (m, τ) problem. Thus, this procedure does not capture all of the possible solutions. However, through numerical analysis, we show that it finds the optimal solution with a very high percentage.

We use the following notation to be used in the algorithm. We denote total demand in a (t, τ) problem at time period t by $b_{t,\tau} = \sum_{\gamma=t}^{\tau-1} (b_{\gamma}/k_{t\gamma})$ for some $1 \leq t < \tau \leq T + 1$. Let $\bar{u}(x) = \lceil x/C \rceil C$ represent the maximum number of items that can be shipped using total number of cargo containers required to carry x . Similarly, let $u(x) = \lfloor x/C \rfloor C$ represent the number of items that can be shipped in FTL cargo containers needed to carry x .

$h(b_{t+1,\tau})$ represents holding cost to meet the demand in periods $t + 1$ through $\tau - 1$ using a replenishment that was received in period t . Thus,

$$h(b_{t+1,\tau}) = \sum_{i=t}^{\tau-2} h_i k_{ti} \left(\sum_{j=i+1}^{\tau-1} \frac{b_j}{k_{tj}} \right) \quad (4.26)$$

Similarly, for a replenishment received in t , $h(b_{t+1,\tau} - u(b_{\gamma,\tau}))$ represents holding cost of required amount between periods $t + 1$ to γ given that there are only FTL shipments to cover the demand from periods γ through $\tau - 1$.

$$h(b_{t+1,\tau} - u(b_{\gamma,\tau})) = \sum_{i=t}^{\tau-2} h_i k_{ti} \left[\left(\sum_{j=i+1}^{\gamma-1} \frac{b_j}{k_{tj}} \right) + \left(\frac{b_{\gamma,\tau} - u(b_{\gamma,\tau})}{k_{t\gamma}} \right) \right] \quad (4.27)$$

The dynamic programming algorithm reads as follows:

$$g(m, \tau) = \min \left\{ \begin{array}{l} s + \left(\frac{A}{C} + p\right)u(b_{m,\tau}) + h(b_{m+1,\tau}), \\ \min \left\{ \begin{array}{l} s + \left(\frac{A}{C} + p\right)u\left(b_{m,\tau} - \frac{u(b_{\gamma,\tau})}{k_{m\gamma}}\right) + g(\gamma, \tau) + \\ h(b_{m+1,\tau} - u(b_{\gamma,\tau})) \quad 1 \leq m < \gamma < \tau \leq T + 1 \end{array} \right\} \end{array} \right\} \quad (4.28)$$

$$f(t, \tau) = \min \left\{ \begin{array}{l} s + \frac{A}{C}\bar{u}(b_{t,\tau}) + pb_{t,\tau} + h(b_{t+1,\tau}), \\ \min \left\{ \begin{array}{l} s + \frac{A}{C}\bar{u}\left(b_{t,\tau} - \frac{u(b_{\gamma,\tau})}{k_{t\gamma}}\right) + p\left[b_{t,\tau} - \frac{u(b_{\gamma,\tau})}{k_{t\gamma}}\right] + \\ g(\gamma, \tau) + h(b_{t+1,\tau} - u(b_{\gamma,\tau})) \\ 1 \leq t < \gamma < \tau \leq T + 1; \quad b_{\gamma,\tau} \geq C \end{array} \right\} \end{array} \right\} \quad (4.29)$$

where $g(m, \tau)$ and $f(t, \tau)$ are defined in $(1 \leq t < m \leq \tau \leq T + 1)$.

In the calculation of $g(m, \tau)$, the first term is the cost of a single FTL shipment at time period m to satisfy the demand between m and $\tau - 1$; i.e. no other FTL replenishments occur between m and $\tau - 1$. The second term finds the minimum cost of the possible replenishment schedules such that cost of an FTL shipment at time period m supported by FTL shipments in some periods γ ($m < \gamma$).

If the minimum value assigned to $g(m, \tau)$ comes from this second term, it means that another set of FTL shipments ($g(\gamma, \tau)$) start at period γ . Then, $u(b_{m,\tau})$ should be adjusted for the next iterations. It becomes: $u(b_{m,\tau}) = u\left(b_{m,\tau} - \frac{u(b_{\gamma,\tau})}{k_{m\gamma}}\right) + \frac{u(b_{\gamma,\tau})}{k_{m\gamma}}$.

A similar structure exists in the calculation of $f(t, \tau)$. The first term calculates the cost of the case where all of the demand is satisfied by an LTL shipment in the first period of the (t, τ) problem. The second term finds the minimum cost of the possible schedules such that there is an LTL shipment in the first period of the (t, τ) problem and the rest are satisfied by FTL shipments.

4.4.6 Numerical Study

In this section we compare the results of both dynamic algorithms with the optimal solutions obtained by CPLEX with respect to the error gap and the running times. For this problem, we use three demand levels for low, medium and high demand. We also capture the impact of cargo capacities, by checking a small and a large size container size. Table 4.4 presents the input data for the problems generated.

Table 4.4

Problem Parameters for Single Mode Problem

b_t	Low: U[100,300] Med:U[300,700] High: U[700,1000]
s	U[200,300]
A	U[50,75]
p	U[30,50]
C	Small: 50 Large: 100

Holding cost is $h = \$1/(\text{unit} \cdot \text{time period})$. We consider 28 problems with the number of time periods (T) and the cargo capacity of the replenishment mode as shown in Table 4.5.

We run experiments for each problem changing the demand levels and deterioration rates for each time period. We tested for deterioration rates of 0.01, 0.02 and 0.03 per time period. For each problem, we generate 10 instances and report the average running times and error gaps. In the following tables, we refer to the dynamic programming algorithm

Table 4.5

Problem Characteristics for Single Mode Problem

	Cap			Cap	
T	50	100	T	50	100
10	P1	P15	80	P8	P22
20	P2	P16	90	P9	P23
30	P3	P17	100	P10	P24
40	P4	P18	110	P11	P25
50	P5	P19	120	P12	P26
60	P6	P20	130	P13	P27
70	P7	P21	140	P14	P28

with zero inventory ordering policy as *Zero* and the algorithm with multiple setups cost structure as *MSetup*.

Table 4.6 shows the running time of the CPLEX and our two dynamic programming algorithms for Problems 1 to 14 under a low demand per time period. In this problem setting, the deterioration rate per time period is 0.01. Compared to the CPLEX running time both algorithms perform very fast. Dynamic programming algorithm for multiple setups is slower than the one with zero inventory ordering policy. The quality of the solutions obtained by both algorithms under a low demand is shown in Table 4.7. Although the error gap does not exceed 0.12% for zero inventory policy, multiple setups dynamic programming algorithm provides solutions more closer to the optimal solution.

The running times for medium and high demands are shown in Table 4.8 and Table 4.9. We only provide the results for the problems that CPLEX could find an optimal solution. For all demand levels, both of the algorithms find very close to optimal solutions in a

Table 4.6

Running times (in sec) - Low Demand - $\alpha = 0.01$

	CPLEX	Zero	MSetup
P1	0.014	0	0
P2	0.050	0	0
P3	0.299	0	0
P4	0.813	0.002	0.003
P5	2.442	0	0.005
P6	3.131	0	0.008
P7	6.375	0	0.014
P8	9.720	0.002	0.020
P9	12.620	0	0.030
P10	78.817	0	0.041
P11	146.108	0.002	0.053
P12	306.366	0.000	0.072
P13	283.019	0.003	0.089
P14	595.661	0.003	0.120

Table 4.7

Error Gaps (in %) - Low Demand - $\alpha = 0.01$

	CPLEX	Zero	MSetup
P1	0	0.089	0.013
P2	0	0.086	0.009
P3	0	0.101	0.013
P4	0	0.098	0.014
P5	0	0.106	0.011
P6	0	0.100	0.013
P7	0	0.107	0.014
P8	0	0.093	0.011
P9	0	0.087	0.012
P10	0	0.083	0.008
P11	0.0002	0.110	0.013
P12	0.0011	0.092	0.012
P13	0.0014	0.111	0.012
P14	0.0031	0.116	0.016

significantly short period of time. The quality of these solutions are provided in Table 4.10 and Table 4.11.

Table 4.8

Running times (in sec) - Med Demand - $\alpha = 0.01$

	CPLEX	Zero	MSetup
P1	0.011	0	0
P2	0.033	0	0
P3	0.091	0	0.002
P4	0.266	0	0.003
P5	1.230	0	0.005
P6	1.983	0	0.008
P7	3.523	0	0.013
P8	8.550	0	0.020
P9	4.874	0	0.028
P10	6.025	0	0.041
P11	29.411	0	0.053
P12	20.281	0.002	0.072
P13	71.134	0.003	0.091
P14	138.822	0.003	0.119

In Problems 15 to 28, we analyze the impact of large cargo capacities on the performance of the algorithms. Table 4.12 and Table 4.13 show the running times and the error gaps respectively for these problems. Both algorithms provide solutions within a maximum of 0.08% error gap within very small time frames.

Finally, we demonstrate the performance of our algorithms with respect to changes in the deterioration rate per time period in Table 4.14.

Table 4.9

Running times (in sec) - High Demand - $\alpha = 0.01$

	CPLEX	Zero	MSetup
P1	0.013	0	0
P2	0.034	0	0
P3	0.098	0	0.002
P4	0.236	0	0.003
P5	1.052	0	0.005
P6	1.594	0	0.008
P7	2.809	0	0.013
P8	7.794	0.002	0.020
P9	4.661	0.002	0.028
P10	5.894	0.002	0.039
P11	168.689	0.002	0.055
P12	26.616	0.002	0.070
P13	160.940	0.002	0.091
P14	260.642	0.003	0.119

Table 4.10

Error Gaps (in %) - Med Demand - $\alpha = 0.01$

	CPLEX	Zero	MSetup
P1	0	0.082	0
P2	0	0.070	0
P3	0	0.070	0
P4	0	0.073	0
P5	0	0.084	0
P6	0	0.073	0
P7	0	0.087	0
P8	0	0.084	0
P9	0	0.068	0
P10	0	0.063	0
P11	0	0.080	0
P12	0	0.074	0
P13	0	0.083	0
P14	0	0.088	0

Table 4.11

Error Gaps (in %) - High Demand - $\alpha = 0.01$

	CPLEX	Zero	MSetup
P1	0	0.039	0
P2	0	0.039	0
P3	0	0.041	0
P4	0	0.040	0
P5	0	0.046	0
P6	0	0.043	0
P7	0	0.048	0
P8	0	0.049	0
P9	0	0.037	0
P10	0	0.036	0
P11	0	0.048	0
P12	0	0.043	0
P13	0.00020	0.050	0.00020
P14	0.00003	0.051	0.00003

Table 4.12

Running times (in sec) - Low Demand - $\alpha = 0.01$

	CPLEX	Zero	MSetup
P15	0.016	0	0
P16	0.033	0	0
P17	0.081	0	0
P18	0.125	0	0.002
P19	0.556	0	0.005
P20	0.745	0	0.008
P21	1.542	0	0.013
P22	3.053	0.002	0.020
P23	3.277	0.002	0.027
P24	3.033	0.002	0.040
P25	7.878	0.000	0.055
P26	8.698	0.002	0.072
P27	13.470	0.002	0.094
P28	15.570	0.003	0.119

Table 4.13

Error Gaps (in %) - Low Demand - $\alpha = 0.01$

	CPLEX	Zero	MSetup
P15	0	0.053	0.010
P16	0	0.048	0.006
P17	0	0.071	0.010
P18	0	0.054	0.008
P19	0	0.063	0.009
P20	0	0.060	0.005
P21	0	0.064	0.009
P22	0	0.058	0.006
P23	0	0.054	0.007
P24	0	0.046	0.006
P25	0	0.057	0.006
P26	0	0.051	0.008
P27	0	0.063	0.006
P28	0	0.060	0.007

Table 4.14

Running times wr/t changes in α - Low Demand

	Optimal		Zero		MSetup	
	$\alpha = 0.02$	$\alpha = 0.03$	$\alpha = 0.02$	$\alpha = 0.03$	$\alpha = 0.02$	$\alpha = 0.03$
P1	0.011	0.014	0	0	0	0
P2	0.037	0.027	0	0	0	0
P3	0.088	0.064	0	0	0.0015	0.0016
P4	0.275	0.109	0	0	0.0015	0.0031
P5	1.164	0.583	0	0	0.0047	0.0047
P6	2.172	0.847	0	0	0.0062	0.0095
P7	3.564	1.778	0.0015	0	0.0125	0.0141
P8	6.294	3.333	0	0	0.0203	0.0203
P9	5.567	2.558	0.0015	0.0016	0.025	0.0297
P10	7.281	3.536	0.0015	0.0016	0.0407	0.0391
P11	19.380	8.819	0	0.0016	0.0531	0.0547
P12	59.299	9.481	0	0.0015	0.0719	0.0734
P13	206.564	20.052	0	0.0016	0.0891	0.0938
P14	200.850	84.878	0.0032	0.0015	0.1188	0.1171

Our numerical analysis show that the dynamic programming algorithms we propose perform well under varying demands, deterioration rates, and cargo capacities. They provide solutions very close to the optimal solution in short running times.

4.5 Special Case: Two Replenishment Modes

In this section, we assume that there are two transportation modes available for inventory replenishment. Let s_i, A_i, p_i, C_i represent the fixed setup costs, cargo container costs, unit replenishment costs and cargo capacities for $i = 1, 2$. We further assume that cargo capacity of one mode is a multiple of the other. Thus, $C_2 = \eta C_1$. For convenience, we assume that transportation lead time for both modes is zero ($L_i = 0$) which means that deterioration is only due to inventory storage. Similar to the single replenishment mode problem, an optimal solution can contain partial orders. Demand of a single time period can be satisfied from inventory and replenishments from mode 1 and/or mode 2. Thus, it requires a significant amount of computation to evaluate all possible combinations for the LTL and FTL shipments from both mode 1 and mode 2 for the complete time horizon. In this respect, we present a heuristic procedure to calculate an approximate solution and compare its performance to the optimal solution obtained by CPLEX. This procedure is based on solving a shortest path problem on Figure 4.4 where we determine the arc costs, $f(t, \tau)$, as described in the following.

We assume that $t - 1$ and $\tau - 1$ ($1 \leq t < \tau \leq T + 1$) are two consecutive regeneration points. For every (t, τ) problem, we solve a minimum knapsack problem to find the combination of cargo containers that would give the minimum cost of replenishment. Let

$f_i = p_i C_i + A_i$ be the cost of a cargo container for mode i . At this stage, we omit the setup costs, s_i . We define variable x_i as the number of cargo containers for mode i that is placed in the knapsack. The knapsack size (D) is determined by the demand from period t through τ . Considering the deterioration rates, $D = b_{t,\tau} = \sum_{\gamma=t}^{\tau-1} (b_\gamma/k_{1t\gamma})$ for some $t \leq \tau \leq T+1$ where $1 \leq t \leq T$. The minimum knapsack problem for each (t, τ) problem reads as follows:

$$\text{minimize } z = \sum_{i=1}^I f_i x_i \quad (4.30)$$

$$\text{Subject to } \sum_{i=1}^I C_i x_i \geq D \quad i = 1, 2, \dots, I \quad (4.31)$$

$$x_i \in Z^+ \quad i = 1, 2, \dots, I \quad (4.32)$$

The solution to this model will determine the number of cargo containers from each mode i that should be shipped at the beginning of period t to satisfy the demand through period τ . Thus, in a solution to this problem a replenishment satisfies the demand of consecutive time periods. Also, replenishments are allowed only when there is no inventory available from the previous time period. Therefore, zero inventory ordering policy is satisfied. This comes at the cost of holding inventory in the remaining time periods of the regeneration interval. As a remedy to this problem, we adjust the knapsack size if possible as follows: Let q_t be the amount replenished in a time period. In an optimal solution, an q_t can contain a number of combinations of mode 1 and mode 2. We know that the larger size mode C_2 is a multiple of C_1 and has smaller marginal costs $(p_i + A_i/C_i)$ due to economies of scale. So whenever, there is a demand in a period that is greater than C_2 ($b_\gamma \geq C_2$ for any $t \leq \gamma \leq \tau - 1$), we assume that at least $\lfloor n_t/C_2 \rfloor$ FTL mode 2 containers will be used

in that period. The rest can be supplied using mode 1 or as a part of another mode 2 replenishment. This remaining part of the demand is added into the knapsack size. Thus, we redefine $D = \sum_{\gamma=t}^{\tau-1} [(b_{\gamma} - \lfloor b_{\gamma}/C_2 \rfloor C_2) / k_{it\gamma}]$ for some $t \leq \tau \leq T + 1$ where $1 \leq t \leq T$.

We solve the knapsack model with a greedy algorithm. Let the residual capacity in the knapsack at iteration k be R_k . Also let $C_i(k) = \min\{C_i, R_k\}$. At every iteration, we select the mode i which minimizes $f_i/C_i(k)$. For the selected mode i , if $\min\{C_i, R_k\} = C_i$, we increase the value of x_i by $\lfloor R_k/C_i \rfloor$. Again, for the selected mode i , if $\min\{C_i, R_k\} = R_k$, then we increase x_i by 1 (which means that we are at the last iteration). The algorithm stops when $R_k \leq 0$.

At any iteration and for any mode i , if $\min\{C_i, R_k\} = R_k$, it implies that putting this cargo container into the knapsack will fill the knapsack and terminate the algorithm. We keep track of the total cost if this cargo were to be placed in the knapsack at that iteration. This cost may be less than the total cost that will be obtained at the end of the algorithm. We illustrate this with an example: Let $f_1 = 4, C_1 = 3$ and $f_2 = 6, C_2 = 5$ where the knapsack size is $D = 9$. In the first iteration $R_1 = 9$; $C_1(1) = \min\{3, 9\} = 3$; $C_2(1) = \min\{5, 9\} = 5$. Mode 2 is selected as $\min\{4/3, 6/5\} = 1.2$. The residual capacity after $\lfloor 9/5 \rfloor = 1$ container of mode 2 ($x_2 = 1$) is placed into the knapsack becomes $R_2 = 4$. The total cost is $z = 6$. In the second iteration, $C_1(2) = \min\{3, 4\} = 3$; $C_2(2) = \min\{5, 4\} = 4$. At this iteration, mode 1 is selected as $\min\{4/3, 6/4\} = 1.33$. As $\lfloor 4/3 \rfloor = 1$, $x_1 = 1$ and $z = 6 + 4 = 10$. In this iteration, since $C_2(2) = R_2 = 4$, we calculate the cost if mode 2 was added to the knapsack instead of mode 1: $z' = 6 + 6 = 12$. In the third iteration, $R_3 = 1$. For both modes i , $C_i(3) = 1$. Mode 1 is selected as

$\min\{4/1, 6/1\} = 4$. The total cost becomes $z = 10 + 4 = 14$. As observed, the total cost would be less ($z' = 12$) if one more container of mode 2 would be added to the solution. This simple check provides us an opportunity to lead to a better solution.

After determining the number of cargo containers for each mode i , we can calculate the $f(t, \tau)$. Total replenishment amount equals $b_{t,\tau}$. Number of setups depends on the type of containers that are selected.

4.5.1 Numerical Study

In this section we compare the running time and the error gap of the minimum knapsack based algorithm to the optimal solution. For this problem, we generate demand per period following a uniform distribution $U[250, 750]$. Holding cost is $h = \$1/(\text{unit} \cdot \text{time period})$. Table 4.15 presents the input data for the problems generated.

Table 4.15

Problem Parameters for 2 Mode Problem

	Mode 1	Mode 2
s_i	U[150,250]	U[250,350]
A_i	U[600,700]	U[900, 1100]
p_i	U[20,30]	U[25,35]
C_i	50	200

We generate 27 problems changing the number of time periods (T) and deterioration rates per time period as shown in Table 4.16. For each of the problems, we take the average

of 10 randomly generated instances and report on the running times and error gaps using their averages.

Table 4.16

Problem Characteristics for Two Mode Problem

	T		
$alpha$	10	20	30
0.00	P1	P10	P19
0.01	P2	P11	P20
0.02	P3	P12	P21
0.03	P4	P13	P22
0.04	P5	P14	P23
0.05	P6	P15	P24
0.06	P7	P16	P25
0.07	P8	P17	P26
0.08	P9	P18	P27

In Table 4.17, the running times of CPLEX to find the optimal solution for each problem is displayed. We observe that when T is large and deterioration rates are small, running times can be very large. For all of these problems, our knapsack algorithm reported a CPU time of 0 seconds. The error gaps of the solutions obtained with knapsack algorithm are shown in Table 4.18. For all of the problem instances, the error gap does not exceed 0.77%. The results indicate that our algorithm works efficiently providing good quality solutions.

4.6 General Case: Multiple Replenishment Modes

In this section, we consider the general case where there are multiple replenishment modes. We use two methods to provide solutions for this problem. In the first approach,

Table 4.17

CPLEX Running Times (in sec) for Two Mode Problem

Prob	Runtime	Prob	Runtime	Prob	Runtime
P1	0.2812	P10	4.249	P19	378.848
P2	0.5718	P11	92.234	P20	291.324
P3	0.2563	P12	6.428	P21	158.797
P4	0.3374	P13	3.559	P22	255.306
P5	0.1923	P14	3.725	P23	225.350
P6	0.1109	P15	2.095	P24	119.983
P7	0.0859	P16	2.689	P25	59.097
P8	0.0703	P17	2.202	P26	48.919
P9	0.1141	P18	6.142	P27	35.206

Table 4.18

Error gap (in %) of the Knapsack algorithm

Prob	Gap	Prob	Gap	Prob	Gap
P1	0.606	P10	0.770	P19	0.695
P2	0.618	P11	0.751	P20	0.664
P3	0.574	P12	0.753	P21	0.629
P4	0.604	P13	0.759	P22	0.613
P5	0.616	P14	0.760	P23	0.602
P6	0.635	P15	0.742	P24	0.592
P7	0.617	P16	0.709	P25	0.575
P8	0.628	P17	0.680	P26	0.562
P9	0.594	P18	0.678	P27	0.561

we extend the minimum knapsack formulation which was previously described for two modes of transportation. In the second approach, we provide a primal-dual algorithm which provides good quality solutions within a short computation time.

4.6.1 The Minimum Cost Knapsack-Based Algorithm

The knapsack formulation described for two replenishment modes can be adjusted to consider multiple replenishment modes. We assume that the adjustment in the knapsack size for C_2 in the two mode problem can only be applied to the largest capacity mode ($\max C_i, i \in I$) in this problem setting. It is not cost efficient to assign FTL shipments for demands that are greater than some C_i . Satisfying these demands by using replenishment modes that have high cargo capacities may be cheaper. In our numerical study, we analyze the problem where multiple replenishment modes are available at every time period. We compare the quality of the costs obtained from this approach to the optimal solution obtained by CPLEX.

4.6.2 A Primal - Dual Algorithm

We have shown in Section 4.2.2 that LP relaxation of our model provides tight lower bounds. Thus, the solution from solving the LP relaxation of the problem and corresponding dual are close to the optimal solution. This fact encouraged the development of a primal-dual based heuristic to find close to optimal solutions in this section. For convenience, we consider $L_i = 0$ and deterioration is only due to storage in the inventory.

The dual of problem (P) has a structure that can generate close to optimal lower bounds for this problem. Primal solutions are then generated using the dual variables. Since we are

solving the dual of the LP relaxation of problem (P), the quality of these bounds is no better than the quality of the solution from the LP relaxation of (P). However, as demonstrated in our computational analysis, the dual algorithm is much faster than CPLEX. The following is the formulation of the dual problem (D-P).

$$\text{maximize } \sum_{t=1}^T b_t v_t \quad (4.33)$$

$$\text{Subject to } \sum_{\tau=t}^T \frac{b_\tau}{k_{it\tau}} \omega_{it\tau} \leq s_i \quad i = 1, 2, \dots, I; t = 1, 2, \dots, T. \quad (4.34)$$

$$C_i \theta_{it} \leq A_i \quad i = 1, 2, \dots, I; t = 1, 2, \dots, T. \quad (4.35)$$

$$k_{it\tau} v_\tau - \omega_{it\tau} - \theta_{it} \leq c_{it\tau} \quad i = 1, 2, \dots, I; 1 \leq t \leq \tau \leq T. \quad (4.36)$$

$$\omega_{it\tau} \geq 0 \quad i = 1, 2, \dots, I; 1 \leq t \leq \tau \leq T. \quad (4.37)$$

$$\theta_{it} \geq 0 \quad i = 1, 2, \dots, I; t = 1, 2, \dots, T. \quad (4.38)$$

From (4.35) and (4.38), we have $0 \leq \theta_{it} \leq \frac{A_i}{C_i}$. Since θ_{it} are not in the objective function and appear in (4.36), when maximizing (D-P), these variables will get the maximum value they can, which is $\theta_{it} = \frac{A_i}{C_i}$ for all $t = 1, \dots, T$. Removing θ_{it} from this formulation, we obtain the following formulation (D'-P):

$$\text{maximize } \sum_{t=1}^T b_t v_t \quad (4.33)$$

$$\text{Subject to } (4.34) - (4.37)$$

$$k_{it\tau} v_\tau - \omega_{it\tau} \leq \bar{c}_{it\tau} \quad \forall I; 1 \leq t \leq \tau \leq T. \quad (4.39)$$

where, $\bar{c}_{it\tau} = c_{it\tau} + A_i/C_i$. In an optimal solution to (D'-P), $0 \leq \omega_{it\tau}$ and $k_{it\tau}v_\tau - \bar{c}_{it\tau} \leq \omega_{it\tau}$.

Since $\omega_{it\tau}$ is not in the objective function, $\omega_{it\tau}$ can be replaced with $\max(0, k_{it\tau}v_\tau - \bar{c}_{it\tau})$.

This leads to the following formulation of the dual problem (D*-P):

$$\text{maximize } \sum_{t=1}^T b_t v_t \quad (4.33)$$

$$\text{Subject to } \sum_{\tau=t}^T \frac{b_\tau}{k_{it\tau}} \max(0, k_{it\tau}v_\tau - \bar{c}_{it\tau}) \leq s_i \quad \forall i; \forall t. \quad (4.40)$$

The dual problem (D*-P) has a simple structure that allows the development of a primal-dual-based algorithm. The dual algorithm obtains near optimal lower bounds by inspection (see Figure 4.5).

Suppose that the optimal values of the first $f-1$ dual variables (v_1^*, \dots, v_{f-1}^*) of (D*-P) are known. Then to be feasible, the f^{th} dual variable (v_f) must satisfy the following:

$$\frac{b_f}{k_{itf}} \max(0, k_{itf}v_f - \bar{c}_{itf}) \leq M_{it,f-1} = s_i - \sum_{\tau=t}^{f-1} \frac{b_\tau}{k_{it\tau}} \max(0, k_{it\tau}v_\tau^* - \bar{c}_{it\tau})$$

$$i = 1, 2, \dots, I; t = 1, \dots, f. \quad (4.41)$$

To maximize the dual problem, we should assign v_f the largest value satisfying these constraints. When $b_f > 0$, this value is as follows:

$$v_f = \min_{i=1, \dots, I, t \leq f} \left\{ \frac{\bar{c}_{itf}}{k_{itf}} + \frac{M_{it,f-1}}{b_f} \right\} \quad (4.42)$$

A backward algorithm is used to find a primal feasible solution (Figure 4.6).

4.6.2.1 Complementary Slackness Conditions

Suppose that the linear programming relaxation of the formulation (P) has an optimal solution (q^*, y^*, z^*) that is integral. Let $F = \{(i, t) | y_{it} = 1, z_{it} \in Z^+\}$ and let (v^*, w^*, θ^*) denote the corresponding optimal dual solution.

```

 $M_{i\tau, \tau-1} = s_i$  for  $i = 1, \dots, I; \tau = 1, \dots, T.$ 
for  $\tau = 1$  to  $T$  do
  if  $b_\tau = 0$  then  $v_\tau = 0$ 
  else  $v_\tau = \min_{it} \{ \frac{\bar{c}_{it\tau}}{k_{it\tau}} + \frac{M_{it, \tau-1}}{b_\tau} \}, 0 \leq t \leq \tau, 0 \leq i \leq I.$ 
  for  $i = 1$  to  $I$  do
     $\theta_{i\tau} = A_i / C_i$ 
    for  $t = 1$  to  $\tau$  do
       $M_{it, \tau} = \max \{ 0, M_{it, \tau-1} - \frac{b_\tau}{k_{it\tau}} \max \{ 0, k_{it\tau} v_\tau - \bar{c}_{it\tau} \} \}$ 
    enddo
  enddo
enddo

```

Figure 4.5

Dual Algorithm

```

 $y_{it} = 0, q_{it\tau} = 0, i = 1, \dots, I; t = 1, \dots, T; t \leq \tau \leq T$ 
 $P = \{ l | b_l > 0, \text{ for } l = 1, \dots, T \}$ 
Start:  $\tau = \max l \in P$ 
Step 1: for  $i = 1, \dots, I$  do
   $t = 0$ 
  repeat  $t = t + 1$ 
    until  $M_{it\tau} = 0$  and  $\bar{c}_{it\tau} - k_{it\tau} v_\tau + \max \{ 0, k_{it\tau} v_\tau - \bar{c}_{it\tau} \} = 0$ 
     $y_{it} = 1,$  and  $i^* = i, t^* = t,$  go to Step 2
  enddo
  go to Step 3
Step 2: for  $\tau = t^*$  to  $T$  do
  if  $\bar{c}_{i^*t^*\tau} - k_{i^*t^*\tau} v_\tau + \max \{ 0, k_{i^*t^*\tau} v_\tau - \bar{c}_{i^*t^*\tau} \} = 0$ 
  then  $q_{i^*t^*\tau} = \frac{b_\tau}{k_{i^*t^*\tau}}, P = P - \{ \tau \}$ 
  enddo
Step 3: if  $P \neq \Phi$  then go to Start
else
  for  $i = 1, \dots, I$  do
    for  $t = 1, \dots, T$  do
       $z_{it} = \lceil \sum_{\tau=t}^T q_{it\tau} / C_i \rceil$ 
    enddo
  enddo

```

Figure 4.6

Primal Algorithm

$$y_{it}^* \left[s_i - \sum_{\tau=t}^T \frac{b_\tau}{k_{it\tau}} \omega_{it\tau}^* \right] = 0 \quad i = 1, \dots, I; t = 1, \dots, T \quad (4.43)$$

$$q_{it\tau}^* [c_{it\tau} - k_{it\tau} v_\tau^* + \omega_{it\tau}^* + \theta_{it}^*] = 0 \quad i = 1, \dots, I; t = 1, \dots, T, t \leq \tau \leq T \quad (4.44)$$

$$z_{it}^* [A_i - C_i \theta_{it}^*] = 0 \quad i = 1, \dots, I; t = 1, \dots, T \quad (4.45)$$

$$\omega_{it\tau}^* \left[q_{it\tau}^* - \frac{b_\tau}{k_{it\tau}} y_{it}^* \right] = 0 \quad i = 1, \dots, I; t = 1, \dots, T, t \leq \tau \leq T \quad (4.46)$$

$$v_\tau^* \left[b_\tau - \sum_{i=1}^I \sum_{t=0}^{\tau} k_{it\tau} q_{it\tau}^* \right] = 0 \quad 1 \leq t \leq \tau \leq T \quad (4.47)$$

$$\theta_{it}^* \left[C_i z_{it}^* - \sum_{\tau=t}^T q_{it\tau}^* \right] = 0 \quad i = 1, \dots, I; t = 1, \dots, T \quad (4.48)$$

4.6.2.1.1 Proposition 4.2

The solutions obtained by the primal and dual algorithms are feasible, and satisfy complementary slackness conditions (4.43), (4.44), (4.45), and (4.47).

The solutions generated by the primal and dual algorithm are feasible by construction. The dual algorithm ensures that equations (4.41) are satisfied. The dual solutions are such that $\frac{b_{\tau+1}}{k_{it(\tau+1)}} \omega_{it,\tau+1} \leq M_{it\tau}$. Therefore, if $M_{it\tau} = 0$, then $\omega_{it,\tau+1} = 0$. Consequently $M_{it,\tau+1} = M_{it,\tau+2} = \dots = M_{itT} = 0$ and $\omega_{it,\tau+1} = \omega_{it,\tau+2} = \dots = \omega_{itT} = 0$. The primal algorithm sets $y_{it} = 1$ only when $M_{it\tau} = 0$, what implies that conditions (4.43) will always be satisfied.

The algorithm sets $q_{it\tau}^* > 0$ only when $\bar{c}_{it\tau} - k_{it\tau} v_\tau^* + \omega_{it\tau}^* = 0$ where $\bar{c}_{it\tau} = c_{it\tau} + \frac{A_i}{C_i}$. That means conditions (4.44) will be satisfied. A solution generated by the dual algorithm will satisfy conditions (4.45) since the algorithm sets $\theta_{it}^* = \frac{A_i}{C_i}$.

The primal algorithm sets $q_{it\tau} = \frac{b_\tau}{k_{it\tau}}$ when $\bar{c}_{it\tau} - k_{it\tau}v_\tau + \max\{0, k_{it\tau}v_\tau - \bar{c}_{it\tau}\} = 0$. This condition is equal to zero when $v_\tau > 0$ (assuming $\bar{c}_{it\tau} > 0$). Therefore, conditions (4.47) are satisfied.

The algorithm sets $q_{it\tau}^* = \frac{b_\tau}{k_{it\tau}}$ when $\omega_{it\tau}^* = 0$. The algorithm assumes that demand in a period is satisfied by a single replenishment mode. However, based on Jaruphongsra et al. [59] in an optimal solution to our problem demand in a time period can be satisfied by more than one replenishment mode. Such a solution would not satisfy conditions (4.46). The algorithm will not always satisfy conditions (4.48) since the primal algorithm sets $z_{it}^* = \left\lceil \frac{\sum_{\tau=t}^T q_{it\tau}^*}{C_i} \right\rceil$ and $\theta_{it}^* = \frac{A_i}{C_i} > 0$. That implies, conditions (4.48) will be satisfied only in the case that the optimal solution consists of full truck shipments. The running time of the primal-dual algorithm is $O(IT^2)$.

4.6.3 Numerical Study

In this section, we solve a multiple replenishment mode problem with CPLEX for an optimal solution. We compare the performances of our minimum knapsack based algorithm and primal dual algorithm with respect to the running times and error gaps. We generate demand per period following a uniform distribution $U[500, 1000]$. Holding cost is $h = \$1/(\text{unit} \cdot \text{time period})$. We assume that there are three types of transportation modes with the costs presented in Table 4.19.

We generate 12 problems by changing the number of time periods (T) and the number of replenishment modes (I). We assume equal number of different transportation modes

Table 4.19

Problem Parameters for Multiple Mode Problem

	Mode 1	Mode 2	Mode 3
s_i	U[150,250]	U[250,350]	U[200,300]
A_i	U[600,700]	U[900, 1100]	U[750, 850]
p_i	U[20,30]	U[25,35]	U[23,33]
C_i	50	200	150

for every I . For example, an $I = 3$ uses one of each type of transportation modes, whereas $I = 15$ uses five of each. For each problem, we report on 10 randomly generated instances.

Table 4.20 shows the characteristics of the problems generated.

Table 4.20

Problem Characteristics for Multiple Mode Problem

Prob	I	T	Prob	I	T	Prob	I	T
1	3	5	5	6	5	9	15	5
2	3	10	6	6	10	10	15	10
3	3	15	7	6	15	11	15	15
4	3	20	8	6	20	12	15	20

Table 4.21 and Table 4.22 show the running times and error gaps of the algorithms respectively. The first column in Table 4.21 shows the running time of CPLEX for an optimal solution. Both primal-dual and the knapsack algorithms run in 0 sec CPU time. The error gaps for the primal dual algorithm do not exceed 1.5%. The knapsack algorithm works less efficiently than the primal-dual algorithm. As the problem size increases, the error gap climbs up to 6.5%.

Table 4.21

Running Times (in sec) for Multiple Mode Problem

Problem	Optimal	Knapsack	Prim-Dual
1	0.053	0	0
2	1.027	0	0
3	0.900	0.0015	0
4	17.567	0	0
5	0.083	0	0
6	1.063	0.0016	0
7	18.572	0	0
8	80.836	0	0
9	0.169	0.0015	0
10	3.569	0	0
11	16.463	0	0
12	177.372	0	0

Table 4.22

Error gap (in %) of Algorithms

Problem	Knapsack	Dual	Primal
1	0.823	0.463	1.369
2	0.959	0.328	1.147
3	0.929	0.396	1.369
4	0.745	0.351	1.228
5	2.344	0.521	1.397
6	2.527	0.383	1.221
7	2.682	0.379	1.335
8	2.883	0.354	1.458
9	7.282	0.467	1.343
10	6.375	0.387	1.118
11	6.576	0.367	1.309
12	6.744	0.370	1.254

4.7 Conclusions

In this chapter, we analyze an extension of the ELS model that considers replenishment of age-dependent perishable products via multiple replenishment modes. We assume a multiple setups cost structure for replenishment costs. We analyze the performance of our formulation by comparing it to another formulation with a different network structure proposed in the literature. We show that LP relaxation of our formulation provides higher lower bounds. We analyze the properties of an optimal solution. We consider two special cases which allow use of a single and two replenishment modes respectively. For the single replenishment mode problem, we first propose a dynamic programming algorithm which works under a zero inventory ordering policy. Secondly, we propose a dynamic programming algorithm that takes multiple setups cost structure into consideration. For the two replenishment mode problem, we present a minimum knapsack based algorithm. For both special cases, we show that our algorithms provide good quality solutions within a short running times. For the general problem with multiple replenishment modes, we extend the minimum knapsack based algorithm and also present a primal dual algorithm. We show that both algorithms outperform the CPLEX running time. The quality of the solutions obtained by the primal dual algorithm are better than the minimum knapsack based algorithm.

CHAPTER 5
BI-OBJECTIVE MODELS FOR GREEN SUPPLY CHAIN MANAGEMENT OF
PERISHABLE PRODUCTS

5.1 Introduction

In this chapter we extend our mathematical models for the replenishment decisions of deteriorating products to include multiple objectives of minimizing costs and carbon emissions. Inventory decisions are impacted by tradeoffs that exist between replenishment and inventory holding costs, and also by the lead time and remaining shelf life of perishable products. Using refrigerated trucks and storage areas can increase the remaining shelf life of a perishable product. These activities increase energy consumption and consequently carbon emissions. We live in an environment with an increased public concern about the effects of carbon emissions on the quality of our lives. Many countries and governments have accepted that there is an urgent need to put policies into action that set reduction targets for total emissions. For example, through its European Climate Change Program, the European Union aims to reduce its carbon emissions by at least 20% by 2020 as compared to 1990 levels [34]. As a consequence, many companies are required to take actions by revising their operations and updating their technologies. Other companies are readily committed to going green since green initiatives not only benefit the environment, but also increase customer goodwill and loyalty and guarantee sustainable operations. Thus, the

companies are faced with replenishment decisions which are not easy to make. The goal of this chapter is to provide tools that can be used by companies in order to make cost efficient and environmentally conscious inventory replenishment decisions for perishable products. The objective of our models is to minimize a combination of costs and the environmental impacts associated with replenishment-related decisions.

The model we propose is a multi-objective, mixed-integer linear programming model which minimizes costs and environmental impacts due to supply chain activities including transportation and inventory. The cost objective of this model minimizes the total inventory replenishment costs which consist of transportation, inventory, purchase and fixed order costs. The environmental objective minimizes greenhouse gas (GHG) emissions due to transportation and inventory. In addition to the tradeoffs mentioned before, this model also captures the tradeoffs that exist between costs and emissions in the supply chain. For example, using refrigerated trucks and refrigerated storage areas for dairy products increases products' shelf life. Longer product shelf life reduces the fixed inventory replenishment costs since less frequent replenishments are necessary. On one side, using refrigerated trucks and storage areas increases energy consumption and, as a consequence, GHG emissions. Reducing the number of replenishments saves transportation-related energy.

We propose two solution approaches for the multi-objective models. These solution approaches include (a) weighted sum method, and (b) ϵ -constraint method. The methods also help the reader gain insights about the carbon regulatory mechanisms of carbon tax and carbon cap respectively. Using numerical analysis, we make important observations with respect to the tradeoffs that exist between costs and emissions and identify the mech-

anism that has the greatest impact on GHG emission reductions on the supply chain. Environmentally conscious companies can use these models and the corresponding solution algorithms as sub-modules within their MRP systems to account for requirements planning when multiple modes, perishable products, and multi-supplier replenishment options exist.

5.2 Multi Objective Model Formulation

In this section, we formulate a multi-objective model to replenish perishable products with multiple transportation modes with the aim of minimizing the total costs and environmental impacts. We use the same variables and parameters as described in Section 4.2.1). Defining $c_{it\tau} = p_i + \sum_{s=t}^{\tau-1} h_s k_{its}$, the total cost (TC) objective of our problem reads as follows:

$$TC(q, y, z) = \sum_{i=1}^I \sum_{t=1}^T \left[\sum_{\tau=t}^T c_{it\tau} q_{it\tau} + s_i y_{it} + A_i z_{it} \right] \quad (5.1)$$

The environmental objective minimizes emissions due to inventory and transportation. In this study we consider only CO_2 emissions since this accounts for about 90% of the total GHG emissions. Carbon emissions due to loading and unloading of one cargo container are considered fixed, and denoted by \hat{A}_{it} . Variable emissions, denoted by \hat{c}_{it} , are due to transportation. Both types of emissions depend on the transportation mode used and the price of fuel in period t . Variable emissions also depend on the distance traveled. Emissions due to holding one unit of inventory in period t are denoted by \hat{h}_t . We define $\hat{c}_{it\tau} = \hat{c}_{it} + \sum_{s=t}^{\tau-1} \hat{h}_s k_{its}$. The following is the total emissions (TE) objective of our problem.

$$TE(q, z) = \sum_{i=1}^I \sum_{t=1}^T \left[\sum_{\tau=t}^T \hat{c}_{it\tau} q_{it\tau} + \hat{A}_{it} z_{it} \right] \quad (5.2)$$

The following is a multi-objective, mixed integer linear programming (MILP) formulation for this inventory replenishment problem.

$$\text{minimize}_{q,y,z} \quad (TC(q, y, z), TE(q, z)) \quad (5.3)$$

$$\text{Subject to} \quad \sum_{i=1}^I \sum_{t=1}^{\tau} k_{i,t,\tau} q_{it\tau} = b_{\tau} \quad 1 \leq \tau \leq T \quad (5.4)$$

$$q_{it\tau} - \frac{b_{\tau}}{k_{i,t,\tau}} y_{it} \leq 0 \quad i = 1, 2, \dots, I; 1 \leq t \leq \tau \leq T \quad (5.5)$$

$$\sum_{\tau=t}^T q_{it\tau} - C_i z_{it} \leq 0 \quad i = 1, 2, \dots, I; t = 1, 2, \dots, T \quad (5.6)$$

$$y_{it} \in \{0, 1\} \quad i = 1, 2, \dots, I; t = 1, 2, \dots, T \quad (5.7)$$

$$z_{it} \in Z^+ \quad i = 1, 2, \dots, I; t = 1, 2, \dots, T \quad (5.8)$$

$$q_{it\tau} \geq 0 \quad i = 1, 2, \dots, I; 1 \leq t \leq \tau \leq T \quad (5.9)$$

5.3 Solution Approaches

MOP models are used when optimal decisions need to be taken in the presence of tradeoffs between two or more conflicting objectives. Typically, there does not exist a single solution that simultaneously optimizes each objective. Thus, solving an MOP deals with approximating or computing all or a representative set of Pareto optimal solutions. We describe two approaches to calculate the Pareto set of solutions for this bi-objective optimization problem which are the weighted sum and ϵ -constraint methods.

The weighted sum method is a traditional, popular method which transforms a bi-objective problem into a series of single-objective problems. This method generates a number of single-objective problems by changing the weights assigned to each objective function. The solutions to these problems approximate the Pareto frontier for the bi-objective

problem [111]. The ϵ -constraint method minimizes one individual objective function with an upper level constraint imposed on the other objective function [68]. The Pareto frontier is approximated by solving this single-objective problem for different values of the upper bound imposed on the other objective function.

5.3.1 Weighted sum method

The weighted sum method minimizes a weighted sum of the two objectives $\lambda_1 TC + \lambda_2 TE$. Typically, the values of λ_1 and λ_2 are selected such that $\lambda_1 + \lambda_2 = 1$ and $\lambda_1, \lambda_2 \geq 0$. The Pareto frontier is then created by solving the single-objective problem for different values of λ_1 and λ_2 .

The following is the objective function of the single-optimization problem under the weighted sum approach.

$$Z(q, y, z) = \sum_{i=1}^I \sum_{t=1}^T \left(\lambda_1 \left[\sum_{\tau=t}^T c_{it\tau} q_{it\tau} + s_i y_{it} + A_i z_{it} \right] + \lambda_2 \left[\sum_{\tau=t}^T \hat{c}_{it\tau} q_{it\tau} + \hat{A}_{it} z_{it} \right] \right) \quad (5.10)$$

In this study, the sum of λ_1 and λ_2 is not equal to 1. We set the value of $\lambda_1 = 1$ and change the value of λ_2 . One can think of the values of λ_2 as the cost of per unit of CO₂ emissions. In this case, the objective function calculates the total costs due to replenishment and emissions in the supply chain. This approach helps us test for changes in the total costs by increasing in the relative importance of λ_2 to λ_1 . λ_2 could as well be considered as the tax a facility would pay per unit of emission under a carbon tax mechanism. Carbon regulatory mechanisms, such as carbon cap, carbon tax, carbon cap-and-trade, and carbon offset do not exist at the federal level. However, a few actions have

already been enacted. For example, policies articulated by executive order in California set statewide GHG emission reduction targets for 2010, 2020, and 2050.

5.3.2 ϵ -constraint method

The ϵ -constraint method approximates the set of Pareto solutions by solving a series of instances of the following single-objective problem (R) for different values of the parameter ϵ .

$$\min TC(q, y, z) \quad (5.1)$$

Subject to (4.5) to (4.10)

$$TE(q, z) \leq \epsilon \quad (5.11)$$

$$\underline{\epsilon} \leq \epsilon \leq \bar{\epsilon} \quad (5.12)$$

Model (R) identifies an inventory replenishment schedule which minimizes total costs, subject to, carbon emission constraints. One can think of ϵ as an emission cap imposed on the facility under the scenario that a carbon cap policy is used.

The lower and upper limits within which the ϵ parameter must fall in are obtained from the optimization of each separate objective function as follows:

$$\min TE(q, z) \quad (5.2)$$

Subject to (4.5) to (4.10)

Let $(\underline{q}, \underline{y}, \underline{z})$, be the solution to this problem. Then, $\underline{\epsilon} = TE(\underline{q}, \underline{z})$ represents the minimum level of carbon emissions required to meet demand, without any considerations of costs.

$$\min TC(q, y, z) \quad (5.1)$$

Subject to (4.5) to (4.10)

Let $(\bar{q}, \bar{y}, \bar{z})$, be a solution to this problem. Then, $\bar{\epsilon} = TE(\bar{q}, \bar{z})$ represents the emission levels for the cost-optimal solution to the problem.

5.4 Results

This section summarizes the results of the computational experiments performed. We solved our model using the ILOG/CPLEX commercial solver. We consider the following example. Suppose that a retailer replenishes its inventories for a perishable product using 3 suppliers. Supplier 1 is a local supplier who uses a less-than-truckload (LTL) service provider. Delivery lead time for shipments from this supplier is 1 day since the LTL service provider, in order to minimize its costs, serves a number of customers in each route. The lead time from supplier 2 is 2 days. This supplier is a wholesaler who provides the product at a discount price. This supplier sends shipments using dedicated, non-refrigerated trucks. The third supplier is also a wholesaler who uses dedicated, refrigerated trucks for delivery. The delivery time for this supplier is 3 days. We assume that products do not perish during delivery time if shipped by refrigerated trucks. Replenishment costs from this supplier are higher than supplier 2 due to using a refrigerated truck, but smaller than the local supplier. Order set-up and processing costs are the same for each supplier. Cargo container

costs, which represent loading and unloading costs, are zero for the LTL service provider since he simply charges a fixed dollar amount per ton of product shipped. The dedicated trucks have a fixed capacity of 25 tons. Unit emissions are higher for shipments that use refrigerated trucks since additional energy is consumed for refrigeration. We consider a time horizon $T = 10$ days, and a time period equal to 1 day. We assume that inventory holding costs equal $\$1/(\text{ton} \cdot \text{day})$ and inventory holding emissions are $0.5 \text{ kg}/(\text{ton} \cdot \text{day})$. Inventory holding emissions are due to using air conditioning in the storage area. Table 5.1 summarizes the input data.

We test the performance of this retailer considering different daily demands which vary from low demand levels ($b_t \sim [2, 4]$ tons), to medium ($b_t \sim [4, 6]$ tons) and high ($b_t \sim [14, 16]$ tons). The daily deterioration rates vary from 0 to 19%. Since deterioration increases with a product's age, we consider the increment to be constant at 1% daily. Deterioration rate during refrigeration is assumed zero.

Table 5.1

Problem Parameters

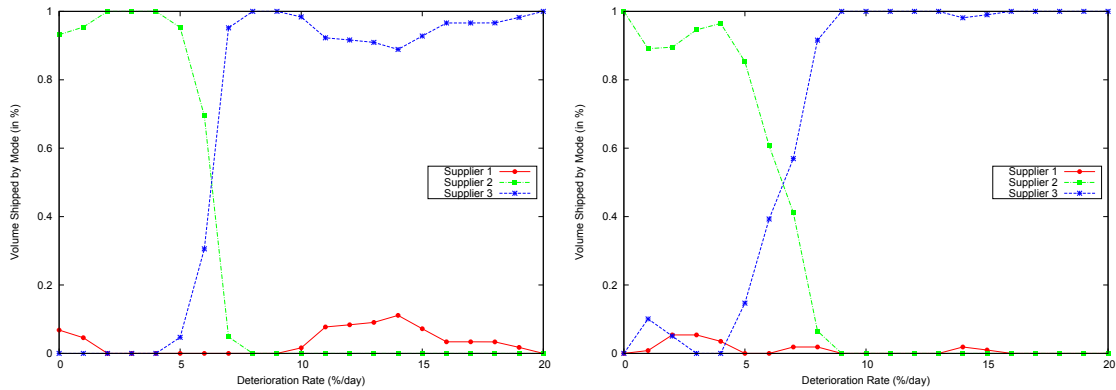
Supplier	s_i	A_i	p_i	C_i	\hat{A}_i	\hat{p}_i	L_i
1	50	0	15		30	1	1
2	50	U[45,55]	10	25	50	1	2
3	50	U[45,55]	12	25	50	1.5	3

In order to generate the results presented in Figure 5.1 to Figure 5.3 we used the ϵ -constraint method and set the value of $\bar{\epsilon}$ equal to 325 kg. This is the same as solving

the problem by considering the cost objective only. The purpose of these experiments is to observe the impact of perishability on replenishment decisions. Each point in a graph represents the average results from solving 10 different randomly generated problem instances.

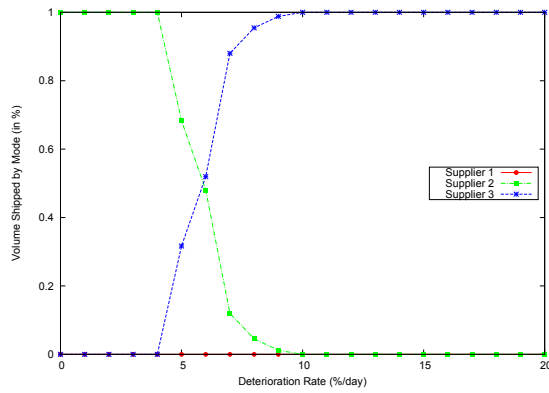
Figure 5.1 presents the relationship between supplier selection decisions and the product's deterioration rate for different levels of customer demand. We make two major observations from these graphs. First, as demand increases, the volume shipped from a local supplier decreases. This finding makes sense since high demand levels justify the use of full truckloads. Therefore, the retailer makes use of wholesalers who provide discounted prices. Second, as the deterioration rate increases, the volume shipped using refrigerated trucks increases (supplier 3). When daily deterioration rate is 8% or higher, supplier 2 is not used, despite the fact that supplier 2 provides a smaller unit replenishment cost as compared to supplier 3. This is because the lead time from this supplier is 2 days, and therefore, the remaining shelf life for the product delivered decreases dramatically.

Figure 5.2 helps understand the relationship that exists between deterioration rate and (a) replenishment and inventory holding costs ($\sum_{i,t,\tau} C_{it\tau} q_{it\tau}$); (b) order costs ($\sum_{i,t} S_i y_{it}$); and (c) cargo costs ($\sum_{i,t} A_i z_{it}$) for different levels of demand. As the deterioration rate increases, replenishment costs increase due to the fact that the volume shipped using supplier 2 (refrigerated trucks) increases. This supplier is relatively more expensive. As the deterioration rate increases the shelf life of products decreases, and therefore, the retailer chooses orders of smaller size. To satisfy demand, orders are initiated more frequently resulting in higher order costs. Similarly, as the deterioration rate increases, the facility moves away



(a) Low demand

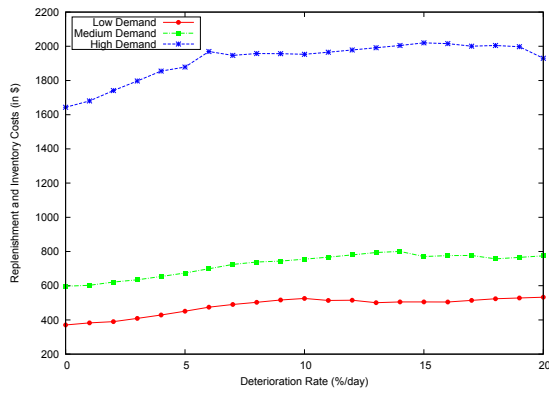
(b) Medium demand



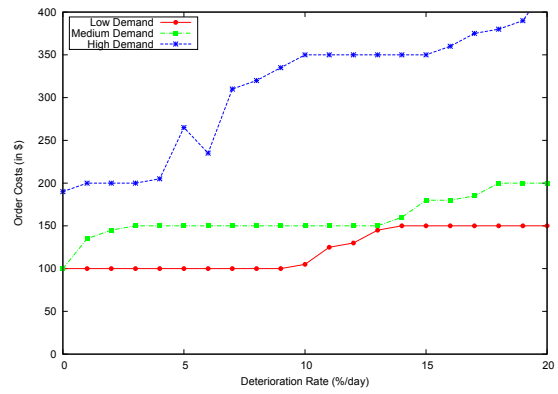
(c) High demand

Figure 5.1

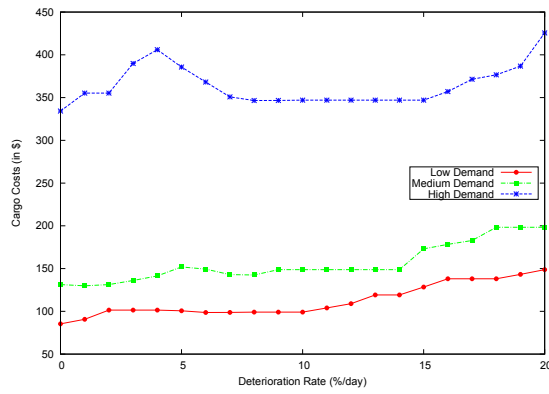
Transportation Mode Selection



(a) Replenishment and Inventory Costs



(b) Order Costs



(c) Cargo Costs

Figure 5.2

Total Cost Distribution

from using the local supplier who sends LTL shipments that do not incur cargo container costs. As a consequence, cargo costs increase with the deterioration rate. The increase in costs (due to increasing deterioration rate) becomes greater as the demand for the product increases.

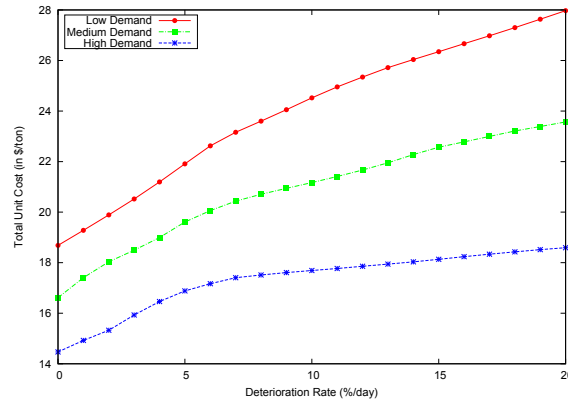


Figure 5.3

Total Unit Costs

Figure 5.3 presents the total unit cost versus deterioration rates for low, medium and high demand. We make two observations here. First, as demand increases, the total unit cost decreases. This decrease is due to the economies of scale achieved from using full truckload shipments. Second, as the deterioration rate increases, the total unit cost increases. As deterioration costs increase (see Figure 5.2), the volume shipped from supplier 3 increases. The increase in costs is due to the higher replenishment costs of supplier 3.

Figure 5.4 displays the set of Pareto solutions (costs versus emissions) for the bi-objective optimization problem. The three Pareto frontiers presented are generated for

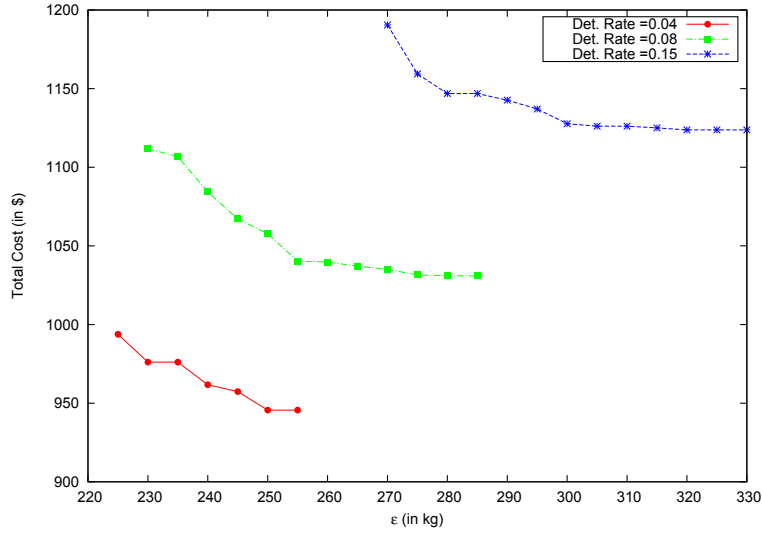


Figure 5.4

Emissions versus Costs

low, medium and high deterioration rates. We make the following observations from the graphs. First, as the deterioration rate increases, both costs and emissions required to satisfy demand increase. The increase in costs is due to using refrigerated trucks and due to increasing the number of orders required because of the limited shelf life of these products. The increase in emissions is due to increasing the volume shipped by refrigerated trucks. Second, decreasing emissions in this two-stage supply chain comes at a cost. For example, when the deterioration rate is 4% and $\bar{\epsilon} = 260\text{kg}$, a decrease in emissions from 260 to 225 increases costs from \$960 to \$993. In other words, a 13.5% improvement in emissions comes at a 3.3% increase in costs. For this particular problem, experimental results indicate that great reductions in emissions can be achieved in a supply chain with minimum impact on costs.

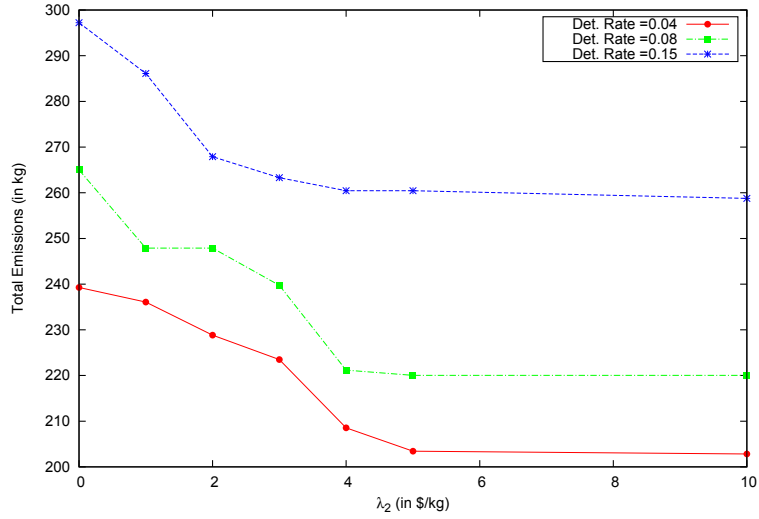


Figure 5.5

Total Emissions versus λ_2

We use the weighted sum method to generate Figure 5.5 which presents emissions versus λ_2 for different deterioration rates. The amount of CO_2 emitted decreases as the value of λ_2 increases. This is understandable since, when the model is solved using the weighted sum method, each unit of CO_2 emitted is penalized by an amount λ_2 . Total emissions also increase with deterioration rate due to the increase in the volume shipped by refrigerated trucks.

In our problem setting, we have considered different lead times (1 to 3 days long) for each supplier. In order to observe the effects of lead time on costs and emissions, we re-ran the experiments for different values of lead time. To simplify the experiments and observe the impact of lead time only on costs and emissions, we assume that each supplier has exactly the same lead time. Figure 5.6 and Figure 5.7 summarize the results. As deterioration rate and lead time increase, both costs and emissions in this supply chain initially increase.

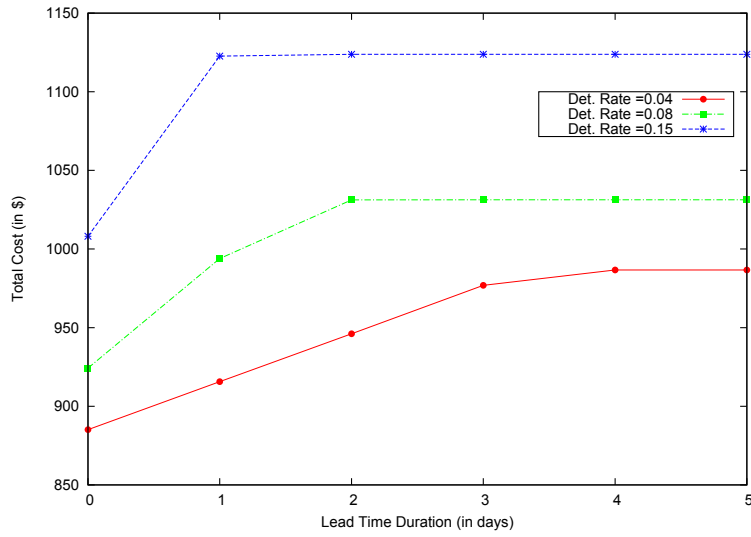


Figure 5.6

Lead Time Costs

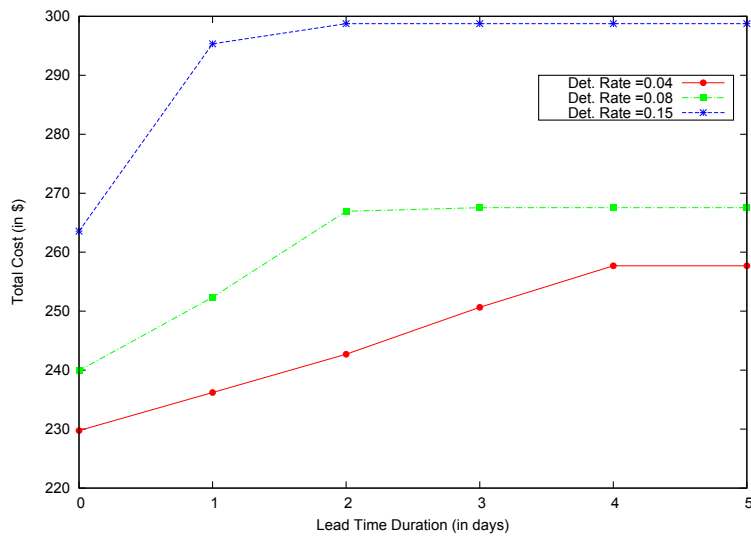


Figure 5.7

Lead Time Emissions

After some point, the lines remain flat and do not change with lead time. Recall that products shipped using refrigerated trucks do not deteriorate during delivery. Therefore, the breakpoint where the lines become flat corresponds to using only refrigerated trucks for inventory replenishment.

This breakpoint of lead times decreases as the deterioration rate increases. For example, a rate of 4% requires 4 days of lead time for the costs to remain constant whereas 15% can only afford 1 day of lead time. Figure 5.7 shows the level of emissions for increasing lead times. Emissions keep increasing up to the breakpoint in lead times and stay constant with the usage of refrigerated trucks.

5.5 Conclusions

This paper proposes a bi-objective mathematical model that aids inventory replenishment decisions for perishable products, such as agricultural and dairy products, human blood, photographic film, etc. This is a mixed-integer linear programming model which minimizes costs and environmental impacts due to supply chain activities such as transportation and inventory. The cost objective of this model minimizes the total inventory replenishment costs, including transportation, inventory, purchase and fixed order costs. The environmental objective minimizes greenhouse gas (GHG) emissions due to transportation and inventory.

We propose two solution procedures to solve this problem, a weighted sum method and a ϵ -constraint method. The weighted sum method minimizes a series of single-objective problems. The objective function represents the total supply chain costs as well as penalties

due to CO₂ emissions necessary to maintain supply chain operations. The ϵ -constraint method minimizes one individual objective function with an upper level constraint imposed on the other objective function. The Pareto frontier is approximated by solving this single objective problem for different values of the upper bound imposed on the other objective function. The single-objective problems are solved using CPLEX.

We ran a number of experiments in order to observe the relationships that exist between costs and emissions in the supply chain. The following are some important observations we made. (a) An increasing deterioration rate impacts supplier selection decisions in the supply chain. Suppliers that have shorter lead times are preferred since shorter lead times for perishable products imply longer shelf life. (b) An increasing deterioration rate increases inventory replenishment costs since often suppliers that have shorter lead times (such as local suppliers) do not necessarily provide the least expensive products. (c) As the deterioration rate increases and shelf life of a product decreases, inventories are replenished in smaller quantities. This increases the frequency of shipments and consequently, the fixed order replenishment costs. (d) An increasing deterioration rate increases emissions due to using refrigerated trucks, and increasing the frequency of shipments. (e) Decreasing emissions in the supply chain comes at a cost. There are a number of operational changes (such as supplier selection, or transportation mode selection) which result in great emission reductions and result in relatively small increases in costs.

CHAPTER 6

CONCLUDING REMARKS

This dissertation studies extensions of ELS models to consider multiple objectives of cost and emission minimization for contemporary supply chain problems. It also provides applications of the models proposed in biomass and perishable product supply chains. These products have special characteristics due to their nature. Thus, replenishment decisions are subject to a variety of tradeoffs between costs and emissions.

In particular a facility with access to multiple replenishment modes is considered. The objective is to satisfy the demand of the facility over the time horizon using a set of these replenishment modes such that the total costs and total emissions of the supply chain are minimized. Chapter 3 provides an extension of the ELS model with fixed charge replenishment costs and multiple replenishment modes. Carbon costs and emissions are then integrated into this model to gain insights about potential carbon regulatory mechanisms. Through numerical analysis on a biomass supply chain, the study provides a better understanding of the tradeoffs between costs and emissions and how the replenishment decisions are impacted by carbon mechanisms.

Chapters 4 and 5 discuss models for perishable products. Chapter 4 provides the ELS model with perishable products with multiple setups cost structure which gives a more

realistic representation of replenishment costs. This section only considers the cost minimization objective. The properties of an optimal solution are presented followed by algorithms to solve cases where one, two or multiple replenishment modes are available. For a single mode of replenishment, two dynamic programming algorithms are presented: (1) assuming zero inventory ordering policy, and (2) considering multiple setups cost structure. For two modes of replenishment, a minimum knapsack based algorithm is proposed. For multiple modes of replenishment, an extension of the minimum knapsack based algorithm is presented in addition to a primal dual algorithm for this problem. It is shown that these algorithms work in short running times and provide good quality solutions.

Chapter 5 extends the model with multiple setups cost structure and perishable products to consider multiple objectives of cost and emission minimization. Two solution methods are proposed which are ϵ -constraint and weighted sum methods. These methods provide insights about carbon cap and carbon tax mechanisms respectively.

Overall, this research provides models to satisfy the demand of a facility for a single type of product using multiple replenishment modes in order to minimize costs and emissions. Variations include two different replenishment cost structures (fixed and multiple-setups) and product types (non-perishable and age-dependent perishable products). A possible extension to this research is considering perishable products with fixed shelf lives. These type of products do not lose their value depending on their age; however, they have to be discarded at their expiration dates. Examples include pharmaceuticals and packaged and canned foods. Thus, this extension can potentially find an application area in the sustainable healthcare supply chains and/or food supply chains.

Another extension can consider the joint replenishment of different products types using same replenishment modes. In this case, replenishment decisions should address additional tradeoffs that exist between replenishment costs, required delivery time and shelf life of multiple products and lead time of each replenishment mode. Consolidating different products may lead to fewer replenishments but may increase total inventory holding costs. Depending on the perishability of the products, replenishments can require refrigeration which increases total emissions. Thus, this problem requires an extended analysis to understand the impact of joint replenishment decisions on the total costs and emissions.

REFERENCES

- [1] N. Absi, S. Dauzère-Pérès, S. Kedad-Sidhoum, B. Penz, and C. Rapine. Lot sizing with carbon emission constraints. *European Journal of Operational Research*, 227: 55–61, 2013.
- [2] Agricultural Marketing Services. Grain transportation quarterly updates. <http://www.ams.usda.gov/AMSV1.0/getfile?dDocName=STELPRDC5100281>, 2012.
- [3] R. Ahuja, W. Huang, H. Romeijn, and D. Morales. A heuristic approach to the multi-period single-sourcing problem with production and inventory capacities and perishability constraints. *INFORMS Journal on Computing Winter*, 19(1):14–26, 2007.
- [4] O. Akgul, A. Zamboni, F. Bezzo, N. Shah, and L. Papageorgiou. Optimization-based approaches for bioethanol supply chains. *Industrial and Engineering Chemistry Research*, 50:4927–4938, 2011.
- [5] H. An, W. Wilhelm, and S. Searcy. Biofuel and petroleum-based fuel supply chain research: A literature review. *Biomass and Bioenergy*, 35:3763–3774, 2011.
- [6] M. Arslan and M. Turkey. EOQ revisited with sustainability considerations. http://home.ku.edu.tr/~mturkey/pub/EOQ_Sustainability.pdf, 2010.
- [7] A. Balakrishnan and J. Geunes. Requirements planning with substitutions: Exploiting bill-of-materials flexibility in production planning. *Manufacturing & Service Operations Management*, 2(2):166–185, 2000.
- [8] I. Barany, J. van Roy, and L. Wolsey. Strong formulations for multi-item capacitated lot sizing. *Management Science*, 30:1255–1261, 1984.
- [9] J. Bauer, T. Bektas, and T. Crainic. Minimizing greenhouse gas emissions in intermodal freight transport: An application to rail service design. <https://www.cirrelt.ca/documentstravail/cirrelt-2009-44.pdf>, 2009.
- [10] S. Benjaafar, Y. Li, and M. Daskin. Carbon footprint and the management of supply chains: Insights from simple models. *IEEE Transactions on Automation Science and Engineering*, 10:99–116, 2013.

- [11] G. Bitran and H. Yanasse. Computational complexity of the capacitated lot size problem. *Management Science*, 28:1174–1186, 1982.
- [12] M. Bonney and M. Jaber. Environmentally responsible inventory models: Non-classical models for a non-classical era. *International Journal of Production Economics*, 133:43–53, 2011.
- [13] M. Cadarso, L. López, N. Gómez, and M. Tobarra. CO₂ emissions of international freight transport and offshoring: Measurement and allocation. *Ecological Economics*, 69:1682–1694, 2010.
- [14] Center for Climate and Energy Solutions. Cellulosic ethanol. <http://www.c2es.org/technology/factsheet/CellulosicEthanol>, 2009.
- [15] A. Chaabane, A. Ramudhin, and M. Paquet. Design of sustainable supply chains under the emission trading scheme. *International Journal of Production Economics*, 135:37–49, 2012.
- [16] X. Chen, S. Benjaafar, and A. Elomri. The carbon-constrained EOQ. <http://www.isye.umn.edu/faculty/pdf/cbe-2011.pdf>, 2011.
- [17] S. Chopra and P. Meindl. *Supply Chain Management: Strategy, Planning & Operations*. Pearson Education, Inc., Upper Saddle River, New Jersey, USA, 2007.
- [18] L. E. Clarke, J. A. Edmonds, H. D. Jacoby, H. M. Pitcher, J. M. Reilly, and R. G. Richels. Scenarios of greenhouse gas emissions and atmospheric concentrations. http://globalchange.mit.edu/files/document/CCSP_SAP2-1a-FullReport.pdf, 2007.
- [19] R. Covert and G. Philip. An eoq model for items with weibull distribution. *IIE Transactions*, 5(4):323–326, 1972.
- [20] M. Dal Mas, S. Giarola, A. Zamboni, and F. Bezzo. Capacity planning and financial optimisation of the bioethanol supply chain under price uncertainty. *20th European Symposium on Computer Aided Process Engineering*, 28:97–102, 2010.
- [21] S. Davis, S. Diegel, and R. Boundy. Transportation energy data book: Edition 31. http://cta.ornl.gov/data/tedb31/Edition31_Full_Doc.pdf, 2012.
- [22] R. De Mol, M. Jogems, P. V. Beek, and J. Gigler. Simulation and optimization of the logistics of biomass fuel collection. *Netherlands Journal of Agricultural Science*, 45: 219–228, 1997.

- [23] R. Dekker, J. Bloemhof, and I. Mallidis. Operations research for green logistics: An overview of aspects, issues, contributions and challenges. *European Journal of Operational Research*, 219:671–679, 2012.
- [24] Department of Transportation. Transportation’s role in reducing U.S. greenhouse gas emissions. http://ntl.bts.gov/lib/32000/32700/32779/DOT_Climate_Change_Report_-_April_2010_-_Volume_1_and_2.pdf, 2010.
- [25] S. Du, F. Ma, Z. Fu, L. Zhu, and J. Zhang. Game-theoretic analysis for an emission-dependent supply chain in a cap-and-trade system. *Annals of Operations Research*, 2011. doi: 10.1007/s10479-011-0964-6.
- [26] A. Dunnett, C. Adjiman, and N. Shah. Biomass to heat supply chains: Applications of process optimisation. *Process Safety and Environmental Protection*, 85:419–429, 2007.
- [27] A. J. Dunnett, C. S. Adjiman, and N. Shah. A spatially explicit whole-system model of the lignocellulosic bioethanol supply chain: an assessment of decentralised processing potential. *Biotechnology for Biofuels*, 1, 2008. doi: 10.1186/1754-6834-1-13.
- [28] S. Eksioglu. A primal-dual algorithm for the economic lot-sizing problem with multi-mode replenishment. *European Journal of Operational Research*, 197:93–101, 2009.
- [29] S. Eksioglu and M. Jin. Cross-facility production and transportation planning problem with perishable inventory. *Lecture Notes in Computer Science*, 3982:708–717, 2006.
- [30] S. Eksioglu, A. Acharya, L. Leightley, and S. Arora. Analyzing the design and management of biomass-to-biorefinery supply chain. *Computers & Industrial Engineering*, 57:1342–1352, 2009.
- [31] S. Eksioglu, S. Li, S. Zhang, S. Sokhansanj, and D. Petrolia. Analyzing impact of intermodal facilities on design and management of biofuel supply chain. *Transportation Research Record: Journal of the Transportation Research Board*, 2191:144–151, 2010.
- [32] Environmental Protection Agency. Greenhouse gas emissions from the U.S. transportation sector 1990–2003. <http://www.epa.gov/otaq/climate/420r06003.pdf>, 2006.
- [33] Environmental Protection Agency. Inventory of U.S. greenhouse gas emissions and sinks:1990–2010. <http://www.epa.gov/climatechange/Downloads/ghgemissions/US-GHG-Inventory-2012-Main-Text.pdf>, 2012.

- [34] European Commission. EU action against climate change: Leading global action to 2020 and beyond. http://ec.europa.eu/clima/sites/campaign/pdf/post_2012_en.pdf, 2008.
- [35] A. Federgruen and M. Tzur. A simple forward algorithm to solve general dynamic lot sizing models with n periods in $O(n \log n)$ or $O(n)$ time. *Management Science*, 37: 909–925, 1991.
- [36] M. Florian and M. Klein. Deterministic production planning with concave costs and capacity constraints. *Management Science*, 18(1):12–20, 1971.
- [37] P. Ghare and G. Schrader. A model for exponentially decaying inventories. *Journal of Industrial Engineering*, 14:238–243, 1963.
- [38] S. Goyal and B. Giri. Recent trends in modeling of deteriorating inventory. *European Journal of Operational Research*, 134(1):1–16, 2001.
- [39] D. Greene, H. Baker, and S. Plotkin. Reducing greenhouse gas emissions from U.S. transportation. <http://www.c2es.org/docUploads/reducing-transportation-ghg.pdf>, 2011.
- [40] H. Gunnarsson, M. Rönnqvist, and J. Lundgren. Supply chain modelling of forest fuel. *European Journal of Operational Research*, 158:103–123, 2004.
- [41] M. Helmrich, R. Jans, W. van den Heuvel, and A. Wagelmans. The economic lot-sizing problem with an emission constraint. <http://repub.eur.nl/res/pub/37650/EI2012-41.pdf>, 2012.
- [42] J. R. Hess, C. T. Wright, K. L. Kenney, and E. M. Searchy. Uniform-format solid feedstock supply system: A commodity-scale desing to produce an infrastructure-compatible bulk solid from lignocellulosic biomass. https://inlportal.inl.gov/portal/server.pt/gateway/PTARGS_0_1829_37189_0_0_18/Executive_Summary_Final_w_cover.pdf, 2009.
- [43] K. Hoen, T. Tan, J. Fransoo, and G. van Houtum. Effect of carbon emission regulations on transport mode selection in supply chains. <http://alexandria.tue.nl/repository/books/672727.pdf>, 2010.
- [44] K. Hoen, T. Tan, J. Fransoo, and G. van Houtum. Effect of carbon emission regulations on transport mode selection under stochastic demand. *Flexible Services and Manufacturing Journal*, 2012. doi: 10.1007/s10696-012-9151-6.
- [45] W. Hoffman. Who’s carbon free? *Traffic World*, 271(42):15, 2007.

- [46] V. Hsu. Dynamic economic lot size model with perishable inventory. *Management Science*, 46(8):1159–1169, 2000.
- [47] V. Hsu. An economic lot size model for perishable products with age-dependent inventory and backorder costs. *IIE Transactions*, 35(8):775–780, 2003.
- [48] G. Hua, T. Cheng, and S. Wang. Managing carbon footprints in inventory management. *International Journal of Production Economics*, 132:178–185, 2011.
- [49] Y. Huang, C. Chen, and Y. Fan. Multistage optimization of the supply chains of biofuels. *Transportation Research Part E*, 46:820–830, 2010.
- [50] H. Hwang. Economic lot-sizing for integrated production and transportation. *Operations Research*, 58:428–444, 2010.
- [51] E. Iakovou, A. Karagiannidis, D. Vlachos, A. Toka, and A. Malamakis. Waste biomass-to-energy supply chain management: A critical synthesis. *Waste Management*, 30:1860–1870, 2010.
- [52] K. Ileleji. Transportation logistics of biomass for industrial fuel and energy enterprises, 2007. Presented at 7th annual conference on renewable energy from organics recycling, Indianapolis, IN.
- [53] International Energy Agency. Transport, energy and CO₂: Moving toward sustainability. <http://www.iea.org/textbase/nppdf/free/2009/transport2009.pdf>, 2009.
- [54] International Energy Agency. Transport energy efficiency. http://www.iea.org/papers/2010/transport_energy_efficiency.pdf, 2010.
- [55] International Transport Forum. Greenhouse gas reduction strategies in the transport sector: Preliminary report. <http://www.internationaltransportforum.org/pub/pdf/08ghg.pdf>, 2008.
- [56] International Transport Forum. Reducing transport ghg emissions opportunities and costs: Preliminary findings. <http://www.internationaltransportforum.org/Pub/pdf/09GHGsum.pdf>, 2009.
- [57] International Transport Forum. Reducing transport greenhouse gas emissions: Trends&data 2010. <http://www.internationaltransportforum.org/Pub/pdf/10GHGTrends.pdf>, 2010.
- [58] IOWA Department Of Transportation. Compare... <http://www.iowadot.gov/compare.pdf>, 2012.

- [59] W. Jaruphongsa, S. Çetinkaya, and C. Lee. A dynamic lot-sizing model with multi-mode replenishments: polynomial algorithms for special cases with dual and multiple modes. *IIE Transactions*, 37:453–467, 2005.
- [60] P. Kaminsky and D. Simchi-Levi. Production and distribution lot sizing in a two stage supply chain. *IIE Transactions*, 35:1065–1075, 2003.
- [61] J. Kim, M. Realff, and J. Lee. Simultaneous design and operation decisions for biorefinery supply chain networks: Centralized vs. distributed system. In *Proceedings of the 9th International Symposium on Dynamics and Control of Process Systems*, pages 73–78, 2010.
- [62] N. Kim, M. Janic, and B. van Wee. Trade-off between carbon dioxide emissions and logistics costs based on multiobjective optimization. *Transportation Research Record: Journal of the Transportation Research Board*, 2139:107–116, 2009.
- [63] Kior. Production facilities. <http://kior.com/content/?s=6&s2=56&p=56&t=Production-Facilities>, 2012.
- [64] C. Lee. Inventory replenishment model: lot sizing versus just-in-time delivery. *Operations Research Letters*, 32:581–590, 2004.
- [65] M. Mahmoudi, T. Sowlati, and S. Sokhansanj. Logistics of supplying biomass from a mountain pine beetle-infested forest to a power plant in British Columbia. *Scandinavian Journal of Forest Research*, 24:76–86, 2009.
- [66] A. Manne. Programming of economic lot sizes. *Management Science*, 4:115–135, 1958.
- [67] B. Mansoornejad, V. Chambost, and P. Stuart. Integrating product portfolio design and supply chain design for the forest biorefinery. *Computers and Chemical Engineering*, 34:1497–1506, 2010.
- [68] S. Marglin. MIT Press, Cambridge, MA, USA, 1967.
- [69] W. Marvin, L. Schmidt, S. Benjaafar, D. Tiffany, and P. Daoutidis. Economic optimization of a lignocellulosic biomass-to-ethanol supply chain. *Chemical Engineering Science*, 67:68–79, 2012.
- [70] McKinsey & Company. Pathways to a low carbon economy. <https://solutions.mckinsey.com/ClimateDesk/default.aspx>, 2009.

- [71] McKinsey & Company. Impact of the financial crisis on carbon economics. https://solutions.mckinsey.com/climatedesk/default/en-us/Files/wp211154643/ImpactOfTheFinancialCrisisOnCarbonEconomics_GHGcostcurveV2.1.pdf, 2010.
- [72] J. McNeel, J. Wang, J. Wu, and T. Goff. Woody biomass sustainability for bioenergy production in West Virginia. <http://www.ncfap.org/documents/BEADII/WVU-BiomassGChallengeBEADII.pdf>, 2008.
- [73] B. Mooij. Finding a lagrangean lower bound on the emission lot-sizing problem. <http://oathesis.eur.nl/ir/repub/asset/10135/10135-Mooij.pdf>, 2011.
- [74] W. Morrow, W. Griffin, and H. Matthews. Modeling switchgrass derived cellulosic ethanol distribution in the United States. *Environmental Science and Technology*, 40: 2877–2886, 2006.
- [75] W. Mtalaa, R. Aggoune, and J. Schaefers. CO₂ emission calculation models for green supply chain management. In *POMS 20th Annual Conference Proceedings*, number 011-0590, 2009.
- [76] S. Nahmias. Perishable inventory theory: A review. *Operations Research*, 30:680–708, 1982.
- [77] J. Neto, G. Waltherb, J. Bloemhofa, J. van Nunena, and T. Spenglerb. A methodology for assessing eco-efficiency in logistics networks. *European Journal of Operational Research*, 193(3):670–682, 2009.
- [78] M. Onal. *Extensions to the Economic Lot Sizing Problem*. PhD thesis, University of Florida, Gainesville, FL, 2009.
- [79] S. Pan, E. Ballot, and F. Fontane. The reduction of greenhouse gas emissions from freight transport by pooling supply chains. *International Journal of Production Economics*, 2010. ISSN 0925-5273. doi: 10.1016/j.ijpe.2010.10.023.
- [80] N. Parker, P.Tittmann, Q. Hart, R. Nelson, K. Skog, A. Schmidt, E. Gray, and B. Jenkins. Development of a biorefinery optimized biofuel supply curve for the western United States. *Biomass and Bioenergy*, 34:1597–1607, 2010.
- [81] M. Piecyk and A. McKinnon. Forecasting the carbon footprint of road freight transport in 2020. *International Journal of Production Economics*, 128:31–42, 2010.
- [82] T. Ranta and S. Rinne. The profitability of transporting uncomminuted raw materials in Finland. *Biomass and Bioenergy*, 30:231–237, 2006.

- [83] P. Ravula, R. Grisso, and J. Cudiff. Cotton logistics as a model for a biomass transportation system. *Biomass and Bioenergy*, 32:314325, 2008.
- [84] Renewable Fuels Association. Cellulosic ethanol production delayed, but coming. <http://www.ethanolrfa.org/news/entry/cellulosic-ethanol-production-delayed-but-coming>, 2012.
- [85] H. Rogner, D. Zhou, R. Bradley, P. Crabbé, O. Edenhofer, B. Hare (Australia), L. Kuijpers, and M. Yamaguchi. Introduction. In B. Metz, O. Davidson, P. Bosch, R. Dave, and L. Meyer, editors, *Climate Change 2007: Mitigation. Contribution of Working Group III to the Fourth Assessment Report of the Intergovernmental Panel on Climate Change*, pages 95–116. Cambridge University Press, Cambridge, United Kingdom and New York, NY, USA, 2007.
- [86] H. Rosič. *The economic and environmental sustainability of dual sourcing*. PhD thesis, Vienna University of Economics and Business, 2011.
- [87] D. Simchi-Levi, P. Kaminsky, and E. Simchi-Levi. *Designing & Managing the Supply Chain*. McGraw-Hill/Irwin, Boston, MA, USA, 2000.
- [88] S. Sokhansanj, A. Kumar, and A. Turhollow. Development and implementation of integrated biomass supply analysis and logistics model (IBSAL). *Biomass and Bioenergy*, 30:838–847, 2006.
- [89] S. Solomon, D. Qin, M. Manning, Z. Chen, M. Marquis, K. Averyt, M. Tignor, and H. Miller. *Climate Change 2007: The Physical Science Basis. Contribution of Working Group I to the Fourth Assessment Report of the Intergovernmental Panel on Climate Change*. Cambridge University Press, Cambridge, United Kingdom and New York, NY, USA, 2007.
- [90] S. K. Srivastava. Green supply-chain management: A state-of-the-art literature review. *International Journal of Management Reviews*, 9:53–80, 2007.
- [91] R. Steuer. John Wiley & Sons, New York, NY, USA, 1985.
- [92] B. Sundarakani, R. de Souza, M. Goh, S. Wagner, and S. Manikandan. Modeling carbon footprints across the supply chain. *International Journal of Production Economics*, 128:43–50, 2010.
- [93] I. Tatsiopoulos and A. Tolis. Economic aspects of the cotton-stalk biomass logistics and comparison of supply chain methods. *Biomass and Bioenergy*, 24:199–214, 2003.

- [94] G. Tembo, F. Epplin, and R. Huhnke. Integrative investment appraisal of a lignocellulosic biomass-to-ethanol industry. *Journal of Agricultural and Resource Economics*, 28:611–633, 2003.
- [95] N. Ty. A variable neighborhood search based heuristic for the lot sizing problem with an emission constraint. <http://oathesis.eur.nl/ir/repub/asset/10134/10134-Ty.pdf>, 2011.
- [96] United Nations Framework Convention on Climate Change. Report of the in-depth review of the fourth national communication of the United States of America. <http://unfccc.int/resource/docs/2009/idr/usa04.pdf>, 2009.
- [97] United Nations Framework Convention on Climate Change. Kyoto protocol. http://unfccc.int/kyoto_protocol/items/2830.php, 2013.
- [98] US Department of Energy. DOE to award \$187 million to improve car and truck fuel efficiency. http://apps1.eere.energy.gov/news/news_detail.cfm/news_id=15725, 2010.
- [99] US Department of Energy - Energy Efficiency and Renewable Energy. U.S. Billion-Ton Update. http://www1.eere.energy.gov/biomass/pdfs/billion_ton_update.pdf, 2011.
- [100] US Department of Energy - Energy Efficiency and Renewable Energy. Blue-Fire Fulton Renewable Energy Project. http://www1.eere.energy.gov/biomass/pdfs/ibr_commercial_bluefire.pdf, 2012.
- [101] US Government Accountability Office. Carbon offsets: The U.S. voluntary market is growing, but quality assurance poses challenges for market participants. <http://www.gao.gov/new.items/d081048.pdf>, 2008.
- [102] W. van den Heuvel, H. Romeijn, D. R. Morales, R. Jans, and A. Wagelmans. Multi-objective economic lot-sizing models. Working Paper, 2012.
- [103] A. Wagelmans, S. van Hoesel, and A. Kolen. Economic lot sizing: An $O(n \log n)$ algorithm that runs in linear time in the Wagner-Whitin case. *Operations Research*, 40(1):145–156, 1992.
- [104] H. Wagner and T. Whitin. Dynamic version of the economic lot size model. *Management Science*, 5:89–96, 1958.
- [105] M. Wahab, S. Mamun, and P. Ongkunaruk. EOQ models for a coordinated two-level international supply chain considering imperfect items and environmental impact. *International Journal of Production Economics*, 134:151–158, 2011.

- [106] F. Wang, X. Lai, and N. Shi. A multi-objective optimization for green supply chain network design. *Decision Support Systems*, 51(2):262–269, 2011.
- [107] F. Wang, X. Lai, and N. Shi. A multi-objective optimization for green supply chain network design. *Decision Support Systems*, 51:262–269, 2011.
- [108] M. Wihersaari. Evaluation of greenhouse gas emission risks from storage of wood residue. *Biomass and Bioenergy*, 28:444–453, 2005.
- [109] J. Winebrake, J. Corbett, A. Falzarano, J. Hawker, K. Korfmacher, S. Ketha, and S. Zilora. Assessing energy, environmental, and economic tradeoffs in intermodal freight transportation. *Journal of the Air & Waste Management Association*, 58:1004–1013, 2008.
- [110] Y. Yu, J. Bartle, C. Li, and H. Wu. Mallee biomass as a key bioenergy source in western Australia: Importance of biomass supply chain. *Energy & Fuels*, 23:3290–3299, 2009.
- [111] L. Zadeh. Optimality and non-scalar-valued performance criteria. *IEEE Transactions in Automation Control*, 8:59–60, 1963.
- [112] A. Zamboni, N. Shah, and F. Bezzo. Spatially explicit static model for the strategic design of future bioethanol production systems. 1. cost minimization. *Energy Fuels*, 23: 5121–5133, 2009.
- [113] S. Zhang and S. Eksioglu. Economic lot-sizing problem with multimode replenishment and perishable inventory. In *Proceedings of the 2009 IIE Annual Conference*, Miami, FL, USA, 2009.